

The Dissertation Committee for Chun-Hung Liu
certifies that this is the approved version of the following dissertation:

**Fundamentals of Distributed Transmission in Wireless
Networks: A Transmission-Capacity Perspective**

Committee:

Jeffrey G. Andrews, Supervisor

Ari Arapostathis

David Morton

Sanjay Shakkottai

Sriram Vishwanath

**Fundamentals of Distributed Transmission in Wireless
Networks: A Transmission-Capacity Perspective**

by

Chun-Hung Liu, B.S.E.; M.S., M.S.

DISSERTATION

Presented to the Faculty of the Graduate School of

The University of Texas at Austin

in Partial Fulfillment

of the Requirements

for the Degree of

DOCTOR OF PHILOSOPHY

THE UNIVERSITY OF TEXAS AT AUSTIN

May 2011

Dedicated to my family.

Acknowledgments

First, I would like to thank Professor Jeffrey G. Andrews for recruiting me to join his research project funded by the DARPA IT-MANET program and his advising and supporting of my Ph.D. study. I benefitted a lot by not only his great skill in presenting research works but also his keenness in new research directions. Second, I would like to thank Professor Ari Arapostathis for his mentorship during the early years of my Ph.D., which significantly enhanced my mathematical level. Also, I would like to thank Professors David Morton, Sanjay Shakkottai and Sriram Vishwanath for serving on my thesis committee and providing valuable suggestions and comments on my research works.

I had a very pleasant time doing research in WNCG and in Professor Andrews' group. For this, I would like to thank my colleagues, Ping Xia, Jiaming Xu, Yuxin Chen, Radha K. Ganti, Tom Novlan, Jaeweon Kim, Behrang Nosrati-Makouei, Beiyu Rong for their helpful discussions and support. Finally, I would like to thank my parents and brother for their endless assistance and encouragement, and thank my wife Mei-Feng Chang for her long-standing support and care.

Fundamentals of Distributed Transmission in Wireless Networks: A Transmission-Capacity Perspective

Publication No. _____

Chun-Hung Liu, Ph.D.

The University of Texas at Austin, 2011

Supervisor: Jeffrey G. Andrews

Interference is a defining feature of a wireless network. How to optimally deal with it is one of the most critical and least understood aspects of decentralized multiuser communication. This dissertation focuses on distributed transmission strategies that a transmitter can follow to achieve reliability while reducing the impact of interference. The problem is investigated from three directions : distributed opportunistic scheduling, multicast outage and transmission capacity, and ergodic transmission capacity, which study distributed transmission in different scenarios from a transmission-capacity perspective. Transmission capacity is spatial throughput metric in a large-scale wireless network with outage constraints. To understand the fundamental limits of distributed transmission, these three directions are investigated from the underlying tradeoffs in different transmission scenarios.

All analytic results regarding the three directions are rigorously derived and proved under the framework of transmission capacity. For the first direction,

three distributed opportunistic scheduling schemes – distributed channel-aware, interferer-aware and interferer-channel-aware scheduling are proposed. The main idea of the three schemes is to avoid transmitting in a deep fading and/or severe interfering context. Theoretical analysis and simulations show that the three schemes are able to achieve high transmission capacity and reliability. The second direction focuses on the study of the transmission capacity problem in a distributed multicast transmission scenario. Multicast transmission, wherein the same packet must be delivered to multiple receivers, has several distinctive traits as opposed to more commonly studied unicast transmission. The general expression for the scaling law of multicast transmission capacity is found and it can provide some insight on how to do distributed single-hop and multi-hop retransmissions. In the third direction, the transmission capacity problem is investigated for Markovian fading channels with temporal and spatial ergodicity. The scaling law of the ergodic transmission capacity is derived and it can indicate a long-term distributed transmission and interference management policy for enhancing transmission capacity.

Table of Contents

Acknowledgments	iv
Abstract	v
List of Tables	xi
List of Figures	xii
Chapter 1. Introduction	1
1.1 Network Model	3
1.1.1 Node Distribution Model	4
1.1.2 Interference Model	5
1.2 Capacity Metrics of Wireless Networks	7
1.2.1 Spatial Throughput	8
1.2.2 Transport Capacity	8
1.2.3 Transmission Capacity	9
1.3 Summary of Main Results and Contributions	11
1.3.1 Distributed Opportunistic Scheduling	11
1.3.2 Multicast Outage and Transmission Capacity	12
1.3.3 Ergodic Transmission Capacity	13
1.4 Organization	14
Chapter 2. Distributed Opportunistic Scheduling	16
2.1 Literature Review and Motivation	17
2.2 Overview of the Three Proposed DOS Schemes	20
2.3 Contributions	21
2.4 Network Model and Preliminaries	24
2.4.1 The Network Model	24
2.4.2 Definitions	28

2.5	Distributed Channel-Aware Scheduling (DCAS)	29
2.5.1	Transmission Capacity achieved by DCAS	29
2.5.2	Discussion and Numerical Results	33
2.6	Distributed Interferer-Aware Scheduling (DIAS)	36
2.6.1	Is reducing the interference at the nearest unintended receiver sufficient?	37
2.6.2	Transmission Capacity achieved by DIAS	39
2.7	Distributed Interferer-Channel-Aware Scheduling (DICAS)	43
2.7.1	Transmission Capacity achieved by DICAS	44
2.7.2	A Geometric Interpretation for the DICAS Scheme	47
2.7.3	DICAS with Geometry-based Interference Cancellation	48
2.8	Appendix I : Useful Propositions	54
2.8.1	The Conservation Property of a Homogeneous PPP	54
2.8.2	The Mean Lebesgue Measure of the Δ -level Dominant Interferer Coverage of a Receiver	55
2.9	Appendix II : Proofs of Lemmas and Theorems	57
2.9.1	Proof of Theorem 2.4.1	57
2.9.2	Proof of Theorem 2.5.1	59
2.9.3	Proof of Lemma 2.6.1	59
2.9.4	Proof of Theorem 2.6.2	60
2.9.5	Proof of Theorem 2.7.1	63
2.9.6	Proof of Theorem 2.7.3	65
Chapter 3. Multicast Outage and Transmission Capacity		68
3.1	Motivation and Related Work	70
3.2	Main Contributions and Chapter Organization	73
3.3	Network Model and Preliminaries	75
3.3.1	Clustered Network Model for Multicast Transmission	75
3.3.2	Multicast Transmission Outage	79
3.3.3	Definitions of Multicast Transmission Capacity, Largeness and Denseness of Networks	81
3.3.4	Multicast Transmission Methods – Single-hop and Multihop	83
3.4	Multicast Transmission Capacity with Single-Hop Multicast	83
3.4.1	The Receiver-Connected Process	84

3.4.2	Single-hop Multicast Transmission Capacity	86
3.5	Multicast Transmission Capacity with Multihop Multicast	91
3.5.1	Multicast over Multihop	93
3.5.2	Capacity Gain Achieved by Multihop Multicast	97
3.6	Appendix I : Useful Propositions	99
3.6.1	Moment Generating Functional of Stationary Independent PPPs	99
3.6.2	The Duality between PCP and PPP	102
3.7	Appendix II : Proofs of Lemmas and Theorems	103
3.7.1	Proof of Lemma 3.4.1	103
3.7.2	Proof of Theorem 3.4.3	106
3.7.3	Proof of Lemma 3.4.5	107
3.7.4	Proof of Theorem 3.5.1	108
Chapter 4.	Ergodic Transmission Capacity	112
4.1	Motivation and Related Work	113
4.2	Contributions	114
4.3	Network Model and Definitions	116
4.3.1	The Network Model	116
4.3.2	Definitions	120
4.4	General Results on Ergodic Transmission Capacity	122
4.4.1	Bounds on the Outage Probability	123
4.4.2	Ergodic Transmission Capacity	126
4.4.3	Observations and Discussion	129
4.5	Ergodic Transmission Capacity with Interference Management	133
4.5.1	Interference Management – A Stochastic Geometry Perspec- tive	134
4.5.2	Bounds on Outage Probability with Interference Management	136
4.5.3	ETC with Interference Management	138
4.6	Appendix : Proofs of Lemmas and Theorems	141
4.6.1	Proof of Theorem 4.4.1	141
4.6.2	Proof of Theorem 4.4.2	145
4.6.3	Proof of Theorem 4.5.1	146
4.6.4	Proof of Corollary 4.5.2	148

Chapter 5. Conclusions	149
5.1 Summary of Main Results	149
5.1.1 Distributed Opportunistic Scheduling	149
5.1.2 Multicast Outage Probability and Transmission Capacity .	150
5.1.3 Ergodic Transmission Capacity	151
5.2 Future Work	151
5.2.1 Distributed Physical Layer Security	152
5.2.2 Distributed Opportunistic Relaying	153
Bibliography	156
Vita	169

List of Tables

2.1	Notation of Main Variables, Processes and Functions in Chapter 2 . . .	25
3.1	Notation of Main Variables, Processes and Functions in Chapter 3 . . .	72
3.2	Summary of Main Results in Chapter 3	74
4.1	Summary of Main Mathematical Notation in Chapter 4	121

List of Figures

1.1	A wireless ad hoc network model in which there are many TX-RX pairs. The red triangles are the active transmitters and black triangles denote the idle transmitters.	4
2.1	The network model: All transmitters form a homogeneous PPP with certain intensity. Red and black triangles represent active transmitters and idle transmitters, respectively. Communication and interference channels are represented by solid and dashed arrows, respectively. Receiver Y_0 located at the origin is called reference receiver and its transmitter is called reference transmitter. In addition, the network is interference-limited and uses slotted-ALOHA protocol.	18
2.2	A schematic explanation for the three proposed DOS schemes: The communication channel of the $X_0 - Y_0$ pair is the solid arrow and its fading channel gain is denoted by $H_0 D_0^{-\alpha}$. All other dashed arrows stand for interference channels, and $\tilde{H}_* \tilde{D}_*^{-\alpha}$ represents the channel gain of the interference channel from transmitter X_0 to its nearest unintended receiver.	21
2.3	The simulation results of TC for the DCAS scheme with different $\Delta_c(\lambda_c)$. The network parameters for simulation are: $\alpha = 4$, $\beta = 2$, $\Delta_c = \lambda_c^\gamma$ and $D = 8m$	35
2.4	The simulation results of TC for the DIAS scheme with different $\Delta_i(\lambda_i)$. The network parameters for simulation are: $\alpha = 4$, $\beta = 2$ and $D_0 = 8m$	41
2.5	The simulation results of TC for the DCAS, DIAS and DICAS schemes. The network parameters for simulation are: $\alpha = 4$, $\beta = 2$, $D_0 = 8m$, $\Delta_c(\lambda_{ic}) = \lambda_{ic}$ and $\Delta_i(\lambda_{ic}) = \lambda_{ic}^{0.6}$	46
3.1	Multicast transmission model in a planar wireless ad hoc network: The transmitters in the network form a stationary PPP of intensity λ_t . Each transmitter (triangle) has an intended multicast area of radius s , where all the intended receivers (small circles) also form a stationary PPP of intensity λ_r . A transmitter and its corresponding intended receivers are indicated by the same color in a cluster.	69
3.2	The simulated MTC of a large network with Rayleigh fading for $\epsilon = 0.1$, $\beta = 2$, $\alpha = 3$ and $\lambda_r = 0.1$	87
3.3	The simulated MTC of a large dense network with Rayleigh fading for $\epsilon = 0.1$, $\beta = 2$ and $\alpha = 3$	90

3.4	Each multicast cluster in a planar network is tessellated into 6 smaller multicast regions of equal area. The arrows in each cluster show an example path of delivering a packet over the tessellated regions by the multihop multicast method.	94
3.5	The simulated MTC achieved by multihop multicast in a large network with Rayleigh fading for $\epsilon = 0.1$, $\beta = 2$, $\alpha = 3$, $\tau = 20$ and $\lambda_r = 0.2$. . .	95
3.6	The simulated MTC achieved by multihop multicast in a large dense network with Rayleigh fading for $\epsilon = 0.1$, $\beta = 2$, $\alpha = 3$ and $\tau = 20$. . .	96
4.1	The gap between the upper and lower bounds on $q_k(\lambda)$. Channel fading is modeled by a Markov chain with 2 states. The network parameters for simulation are: $d = 5m$, $\lambda = 0.01$, $\alpha = 3$, $\beta = 2$, $s_1 = 0.5$, $s_2 = 2$ and $\phi_1 = \phi_2 = 0.5$	125
4.2	The Gilbert-Elliott channel model and its corresponding geometric presentation of C_E , where $\{p_{ij}\}$ are the state transition probabilities for the FSMC model and $\tilde{s}_k = \frac{\epsilon^{\frac{\alpha}{2}} s_k}{\left(\nu - \pi s_k^{\frac{2}{\alpha}}\right)^{\frac{\alpha}{2}}}$	130
4.3	A geometric example of illustrating why DCAS does not always benefit ETC.	132
4.4	Numerical results for ETC with and without DCAS. The network parameters for simulation are : $d = 10m$, $\beta = 2$, $\alpha = 3$, $\delta = 1.5$, $s_1 = 0.5$, $s_2 = 2$, $\phi_1 = 0.8$, $\phi_2 = 0.2$ and $\lambda = 0.01$	133
4.5	Numerical results for ETC with and without interference management. The network parameters for simulation are : $d = 10m$, $\beta = 2$, $\alpha = 3$, $\delta = 2$, $s_1 = 0.5$, $s_2 = 2$, $\phi_1 = \phi_2 = 0.5$, $\gamma_1 = \gamma_2 = 0.6$ and $\lambda = 0.02$. . .	140
4.6	The geometric representation of the ETC for an FSMC with 2 states. \mathbf{s}_ϵ^* is the optimal vector that \mathbf{s}_ϵ can achieve by interference management. By using interference management, vertices \mathbf{a} and \mathbf{c} can be optimally moved to \mathbf{f} and \mathbf{h} , respectively. The projection points of vertices \mathbf{b} and \mathbf{g} on Φ are \mathbf{d} and \mathbf{i} , respectively.	142

Chapter 1

Introduction

A wireless ad hoc network is a decentralized wireless network lacking the preexisting infrastructure that usually helps manage and control information flows between source and destination nodes. Each transmitting node in the network has to decide how to deliver its packets based on local limited information. Efficiently sending packets between two nodes (usually over multiple hops) is much more challenging than an infrastructure-based network, especially when those packets have quality-of-service (QoS) constraints such as guaranteed throughput and delay. In addition to the issues introduced by decentralization, the broadcast nature of wireless communication causes physical layer interference between nodes, which increases the failure probability of delivering packets.

According to the Shannon channel capacity [1] [2], signal-to-noise (plus interference) ratio characterizes the upper bound of how much information can be reliably carried by a communication link. So if many transmission activities occur in a wireless network at the same time, the end-to-end throughput between two nodes would be significantly reduced since the quality of communication links is degraded. For example, consider an n -hop transmission from node A to node B. Let C_i denote by the link capacity at the i th hop. The end-to-end link capacity

from node A to node B, C_{AB} , can be shown to be [3]

$$C_{AB} = \left(\sum_{i=1}^n C_i^{-1} \right)^{-1}. \quad (1.1)$$

Equation (1.1) indicates that the end-to-end throughput will be dominated by the minimum link capacity, i.e. the weakest link. That means if there are multiple relaying paths from node A to node B, one would ideally avoid the path with a poor link quality. Increasing transmit power to overcome bad link conditions is often self-defeating because of the large amount of interference generated. As a result, analysis of the fundamental limits of wireless networks is very complex, and the capacity of a wireless network is a well-known open problem [4]. For instance, the Shannon capacity region of a wireless network with 3 fully connected nodes is still not known in full generality [5–10].

Due to transmission conflicts in uncoordinated wireless networks, how to allocate resources and schedule transmissions in order to alleviate interference is a crucial issue. First, transmission scheduling must be done in a decentralized fashion, which means a transmitter has to determine when to transmit by using local information. Therefore, a fundamental question arises: How does each potential transmitting node choose to transmit in order to maximize its transmission reliability as well as the network throughput (capacity) as a whole? Before answering this question, let us revisit how to evaluate the capacity of a wireless ad hoc network. Putting aside the dream of quantifying the network capacity via the Shannon link-capacity approach, a fairly intuitive notion is the *transport capacity*, which was proposed in [11] more than ten years ago. The transport capacity has become a very popular metric for quantifying network capacity, and it

involves calculating the sum of the distance-weighted maximum achievable rates of all successful communication links in the network. An excellent review for the transport capacity work can be found in [12] and the references therein. Another more recent network-capacity metric is the *transmission capacity* coined in [13]. Transmission capacity is defined as the supportable data rate per link times the maximum allowable spatial intensity (density) of successful transmissions under a given outage constraint.

In this dissertation, we aim at finding good distributed transmission strategies for each transmitter from a transmission-capacity perspective. Such strategies are able to provide some insights on how to do scheduling from a network-level performance metric so that advantages gained by one node do not come at the expense of overall network performance. In the following subsections, we first discuss the network models proposed in the literature. Then the “capacity”¹ metrics developed under those models are briefly introduced. Afterwards, we summarize our main results and contributions.

1.1 Network Model

The model of a wireless ad hoc network as used in this dissertation consists of two parts. One is the model of how nodes are distributed in the network and the other is the interference model for a given transmitter-receiver (TX-RX) pair. Figure 1.1 shows an ad hoc network model in which there are many TX-RX

¹The “capacity” word is loosely used here since it does not mean the strict upper bound of a network capacity in a Shannon-limit sense.

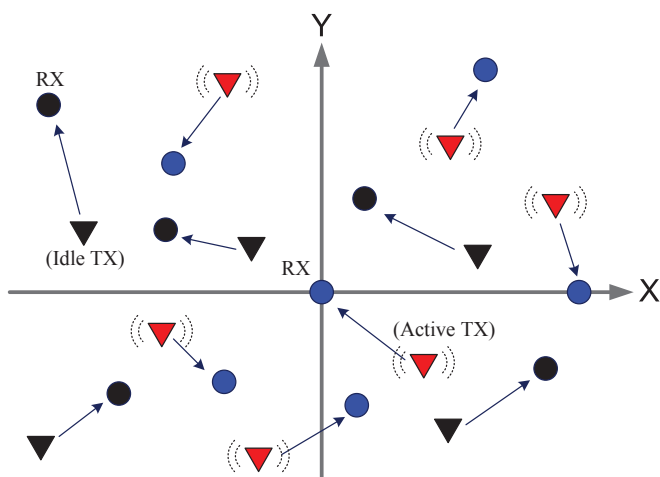


Figure 1.1: A wireless ad hoc network model in which there are many TX-RX pairs. The red triangles are the active transmitters and black triangles denote the idle transmitters.

pairs. In order to investigate network capacity, the node distribution model and interference model are both needed to determine prior to theoretical analysis.

1.1.1 Node Distribution Model

Generally speaking, there are two main node distribution models that are commonly used to analyze network-wise performance such as outage probability, delay and throughput. One model assumes that there are a certain number of nodes uniformly distributed in an area of fixed size. This uniformly distributed model is suitable for a wireless network with limited size and nodes appearing in the network do not have any location preference. For example, the seminal work on transport capacity by Gupta and Kumar [11] was built using this model.

The other model assumes that all nodes are randomly (and independently) distributed in a wireless network with certain intensity. This model is usually applied in the context that the exact number of nodes and network size are unknown; therefore, an infinitely large network with known intensity can be perfectly specified by this model. In recent years, some point processes from stochastic geometry, such as the Poisson point process (PPP) and Poisson cluster process (PCP), have been successfully applied in describing the random locations of nodes in this model [13–18]. Using the Poisson point process (PPP) to model the random distribution of nodes in a wireless ad hoc network is appropriate, especially for a large network. In addition, the PPP model for terminal positions is well-accepted in such a scenario and has been proven very accurate for CDMA cellular networks amongst others [14]. Thus, the node distribution specified by a PPP is a more general model compared to the aforementioned uniform distribution model. In fact, the uniform distribution model will coverage to the PPP model if its network size goes to infinity. Throughout this dissertation, we will use PPP and/or PCP to model the spatial randomness of all nodes in a wireless ad hoc network.

1.1.2 Interference Model

When many mutually interfering transmitters are sending each other information, how does each of their intended receivers claim that it successfully receives its intended information? This problem requires an appropriate interference model. There are two popular interference models used in most of the literature: the “protocol” model and signal-to-interference and noise ratio (SINR)-based “physical” model.

Protocol model: This model was first introduced in [11] and is a geometry-based model. Using this model, a receiver can only receive the information from its intended transmitter provided that there are no other transmitters in its receiving range (sometimes called a guard zone) which is a circular area with a large enough radius. In other words, a transmission will fail if a transmitter has an unintended receiver and the distance between them is less than a designated threshold that is larger than the distance between the transmitter and its intended receiver. The protocol model is simple and analytically tractable, and thus much work is based on this model such as [19–25]. Although the analysis for the protocol model is straight-forward, it has some nonrealistic assumptions. First, it assumes that transmissions are *always* successful if and only if some necessary geometry constraints are satisfied. Second, the uncertainty and unreliability of wireless transmission are completely ignored in this model. Also, it is unable to capture the fact that a receiver is able to receive at a low rate even under high interference.

SINR-based physical model: This model uses the received SINR to judge if a transmission is successful between a TX-RX pair. To successfully decode received signals, the SINR_i at receiver Y_i has to be greater than or equal to some threshold as shown in the following:

$$\text{SINR}_i \triangleq \frac{P_i \ell(|X_i - Y_i|)}{\sum_{X_j \in \Pi \setminus X_i} P_j \ell(|X_j - Y_i|) + n_i} \geq \beta, \quad (1.2)$$

where $|X_i - Y_i|$ represents the distance between transmitter X_i and its receiver Y_i , $\ell(\cdot)$ is the path loss model accounting for power loss due to propagation², P

²The most popular propagation model for $\ell(|X_i - Y_i|)$ is $|X_i - Y_i|^{-\alpha}$ where α is the path loss

denotes transmit power, Π is the set of all transmitters, n_i is the noise power at receiver Y_i and β is the SINR threshold for successful decoding³. Equation (1.2) means that transmitter X_i can send at a specific data rate to receiver Y_i as long as the condition $\text{SINR}_i \geq \beta$ is satisfied. The physical model is more realistic than the protocol model; however, the analysis based on this model is much more complex than that on the protocol model because in general interference is hard to calculate due to the random locations of all interferers.

1.2 Capacity Metrics of Wireless Networks

As we have mentioned in the previous section, the Shannon limit for network capacity is difficult to even characterize, much less find. So we should instead look for other metrics to “measure” the capacity of a wireless ad hoc network. There have been proposed several capacity metrics in the literature such as throughput capacity [11, 20, 21], end-to-end throughput (per node), transport capacity, spatial throughput and transmission capacity. Here we merely briefly review the definitions of spatial throughput, transport capacity and transmission capacity because these three metrics are very related to our following work in this dissertation.

exponent. Although it becomes unbounded when the distance between two nodes is close to zero, the transmission distance of a transmitting node is usually larger than one at most of time and thus much of work still uses this model due to its simplicity and traceability [13, 26–31].

³Note that we do not consider channel fading in (1.2).

1.2.1 Spatial Throughput

Spatial throughput is defined according to how many successful transmissions can coexist in a wireless network at the same time. Assuming there are n transmitting nodes in the network, the spatial throughput can be formally given by

$$c_t \triangleq \mathbb{E} \left[\sum_{i=1}^n b_i \mathbf{1}(\text{SINR}_i \geq \beta) \right] = \sum_{i=1}^n b_i \mathbb{P}[\text{SINR}_i \geq \beta], \quad (1.3)$$

where b_i is the constant transmission rate from transmitter X_i to its receiver Y_i and $\mathbf{1}(\mathcal{E})$ is an indicator function which is one if event \mathcal{E} is true and 0, otherwise. If all transmission rates are the same, spatial throughput is characterized by the number of transmitting nodes without outage. If transmitting nodes in a wireless network form a PPP of intensity λ , the spatial throughput (per unit area) can be defined as

$$c_t \triangleq b \lambda \mathbb{P}[\text{SINR}(\lambda) \geq \beta], \quad (1.4)$$

where b is the supportable transmission rate for each link (e.g. $b = \log_2(1 + \beta)$). Equation (1.4) can be interpreted as a metric of area spectral efficiency. Note that $\text{SINR}(\lambda)$ means SINR is a function of intensity λ .

1.2.2 Transport Capacity

Transport capacity originally proposed by Gupta and Kumar in [11] has become a popular capacity metric. It is defined based on the data rate that can be transported over a communication link of some distance. Combining this notion with the idea of spatial throughput yields the formal definition of transport capacity [11, 12, 32, 33]: The transport capacity of a specific network is defined

as the maximum bit-meters per second the network can achieve in aggregate. If there are n nodes in the network, then transport capacity can be explicitly expressed in the following equation:

$$T_c \triangleq \sup_{i,j} \sum_{i \neq j} b_{ij} |X_i - X_j|, \quad i, j \in [1, 2, \dots, n], \quad (1.5)$$

where b_{ij} is the supportable transmission rate (bits per second, bps) for the link from node X_i to node X_j . Hence, we can say that T_c captures the physical difficulty in carrying data to some distance away.

A main result of the transport capacity on the protocol and physical models is summarized as follows. Assuming there are n nodes in the network that are distributed in a region of area A . The transport capacity cannot grow faster than $\Theta(\sqrt{An})$. The importance of this result is that the per-node transport capacity scales like $\Theta(1/\sqrt{n})$ when area A is fixed.

1.2.3 Transmission Capacity

Transmission capacity originally proposed in [13] is defined based on the idea of area spectral efficiency (in a Poisson field of transmitters). Suppose the transmitters in a wireless ad hoc network form a PPP of intensity λ and the outage probability of each transmitter cannot be greater than $\epsilon \in (0, 1)$. The transmission capacity is defined as

$$c_\epsilon \triangleq b \bar{\lambda}_\epsilon (1 - \epsilon), \quad (1.6)$$

where b is the supportable transmission rate and $\bar{\lambda}_\epsilon$ is the maximum contention intensity given by

$$\bar{\lambda}_\epsilon = \sup_{\lambda} \{\lambda > 0 : \mathbb{P}[\text{SINR} < \beta] \leq \epsilon\}.$$

So c_ϵ is defined as the area spectral efficiency of the successful transmissions resulting from the optimal contention intensity. Actually, transmission capacity is a special case of spatial throughput in (1.4), and thus it can be viewed as a QoS-constrained spatial throughput. It is a good capacity metric in the context that a wireless network has an upper limit requirement for outage probability. It is also often computable in close-form.

The basic result of transmission capacity c_ϵ shows that $\bar{\lambda}_\epsilon = \Theta(\epsilon/\beta^{2/\alpha}d^2)$ for $\epsilon \ll 1$ if using path loss model $\ell(x) = x^{-\alpha}$ where $\alpha > 2$ is the path loss exponent⁴. If each receiver is able to increase the received power by M -fold, then $c_\epsilon = \Theta(M^{2/\alpha}\epsilon/d^2\beta^{2/\alpha})$. For example, a DS-CDMA network with spreading gain M can achieve this transmission capacity. However, $c_\epsilon = \Theta(M\epsilon/d^2\beta^{2/\alpha})$ if the transmitter intensity is reduced by M -fold. This capacity can be achieved in a FH-CDMA network with M available channels. From this basic result, we know that interference avoidance is more efficient in increasing transmission capacity than interference suppression in an ad hoc network. Also, transmission capacity has a close relationship with transport capacity. Since we know the transmission distance d in a network with intensity λ is $\Theta(1/\sqrt{\lambda})$, the transport capacity dependence obtained from transmission capacity is $\Theta(d\bar{\lambda}_\epsilon) = \Theta(\sqrt{\bar{\lambda}_\epsilon})$, which coincides with the transport capacity result in the previous subsection.

⁴The closed form of $\bar{\lambda}_\epsilon$ can be found for some particular fading model such as Rayleigh.

1.3 Summary of Main Results and Contributions

In this dissertation, we investigate fundamental issues regarding distributed transmission in a wireless ad hoc network with spatial randomness. Specifically, we consider three related directions. First, the problem of how to do distributed opportunistic scheduling to increase transmission capacity based on local information, such as channel state, transmitter intensity, and the dominant interferer coverage area. The distributed transmission methods in this work all aspire to generate as little interference as possible, while transmitting as much information as possible. Next, we consider the multicast scenario where each transmitter has to communicate with multiple receivers, and we wish to know the best transmission policy to satisfy delay and outage requirements. Finally, we investigate the transmission capacity problem in a long-term sense, assuming all fading channels are a finite-state Markov chain. The results we obtain show how to do long-term distributed transmissions and interference management such that high *ergodic* transmission capacity can be achieved. The following is a summary of main results and contributions of each direction, which then follow in distinct chapters.

1.3.1 Distributed Opportunistic Scheduling

It is well known that opportunistic scheduling and routing can be significantly leveraged in decentralized wireless networks to improve the reliability of communication. However, complex opportunistic schemes incur a large overhead in terms of required channel state information leading to an overall degradation of the effective throughput. We propose three distributed opportunistic schedul-

ing (DOS) schemes that have very little overhead and are easy to implement. We consider transmission capacity (TC) as the metric and provide analysis of the proposed schemes inclusive of the spatial statistics and the interference. In the distributed channel-aware scheduling (DCAS) scheme, a transmission is scheduled by comparing the *quality* of the channel between a transmitter and its associated receiver to a threshold. We show that it is critical to choose the threshold as a function of the intensity of network transmissions and we quantify the gain using the TC framework. In the distributed interferer-aware scheduling (DIAS) scheme, the scheduling explicitly reduces the interference at the nearest unintended receiver thereby improving the average signal-to-interference ratio (SIR) of the entire network. Distributed interferer-channel-aware scheduling (DICAS) scheme is a combination of DCAS and DIAS schemes that schedules links with a good channel state that have a minimal interference footprint. Our main results show that all the three schemes can significantly increase the TC and DICAS provides the greatest gain. In addition, we show that the outage probabilities of the three schemes can be further reduced by using a geometry-based interference cancellation approach, which provides a fundamental view of how much outage probability can be improved by receivers.

1.3.2 Multicast Outage and Transmission Capacity

Multicast transmission, wherein the same packet must be delivered to multiple receivers, is an important aspect of sensor and tactical networks and has several distinctive traits as opposed to more commonly studied unicast networks. Specially, these include (i) identical packets must be delivered successfully to

several nodes, (ii) outage at any receiver requires the packet to be retransmitted at least to that receiver, and (iii) the multicast rate is dominated by the receiver with the weakest link in order to minimize outage and retransmission. A first contribution in this topic is the development of a tractable multicast model and throughput metric that captures each of these key traits in a multicast wireless network. We utilize a Poisson cluster process (PCP) consisting of a distinct Poisson point process (PPP) for the transmitters and receivers, and then define the multicast transmission capacity (MTC) as the maximum achievable multicast rate per transmission attempt times the maximum intensity of multicast clusters under decoding delay and multicast outage constraints. A multicast cluster is a contiguous area over which a packet is multicasted, and to reduce outage it can be tessellated into v smaller regions of multicast. The second contribution in this topic is the analysis of several key aspects of this model, for which we develop the following main result. Assuming τ/v transmission attempts are allowed for each tessellated region in a multicast cluster, we show that the MTC is $\Theta(\rho k^x \log(k)v^y)$ where ρ , x and y are functions of τ and v depending on the network size and intensity, and k is the average number of the intended receivers in a cluster. We derive $\{\rho, x, y\}$ for a number of regimes of interest, and also show that an appropriate number of retransmissions can significantly enhance the MTC.

1.3.3 Ergodic Transmission Capacity

Most work on wireless network throughput ignores the temporal correlation inherent to wireless channels because it degrades tractability. To better model and quantify the temporal variations of wireless network throughput, we

introduce a metric termed ergodic transmission capacity (ETC), which includes spatial and temporal ergodicity. All transmitters in the network form a stationary Poisson point process and all channels are modeled by a finite state Markov chain. The bounds on outage probability and ETC are characterized, and their scaling behaviors for a sparse and dense network are discussed. From these results, we show that the ETC can be characterized by the inner product of the channel-state related vector and the invariant probability vector of the Markov chain. This indicates that distributed channel-aware opportunistic scheduling (DCAS) does not always increase ETC. Finally, we look at outage probability with interference management from a stochastic geometry point of view. The improved bounds on outage probability and ETC due to interference management are characterized and they provide some useful insights on how to effectively manage interference in sparse and dense networks.

1.4 Organization

The rest of the dissertation is organized as follows. Chapter 2 studies the first direction that how a transmitter should opportunistically schedule its transmissions with limited system information such that transmission capacity can be enhanced. The second direction regarding the problem of multicast outage and transmission capacity is investigated in Chapter 3 and a multihop multicast transmission method is proposed to increase multicast transmission capacity. Chapter 4 focuses on the third direction, i.e. ergodic transmission capacity without and with interference management. In this chapter, how to achieve a high ergodic

transmission capacity through distributed transmission and interference management is discussed. Finally, conclusions are provided in Chapter 5.

Chapter 2

Distributed Opportunistic Scheduling

Opportunistic scheduling exploits channel variations to schedule transmission and improve the overall performance of the network. In a point-to-point link, the small scale fading can be opportunistically exploited by changing the modulation rate/power depending on the channel quality. Opportunism is particularly attractive in a multiuser setting, where in the channel fluctuations between users (spatial variations over different channels) can be exploited to improve the diversity and rate. The network throughput can be significantly improved by a high-priority scheduling of users with good channels [34] [35]. It is easy to devise optimal centralized opportunistic scheduling when the global channel state information of the entire network is known. For example, in a cellular network, base stations can use the global state information to opportunistically schedule mobile users and improve network coverage and capacity [36–39]. However, in decentralized ad hoc networks, the absence of global state knowledge makes it difficult to implement *optimal* scheduling strategies. In such networks, opportunistic scheduling should be distributed and depend only on the local information rather than the global state of the network.

Because of the distributed nature of an ad hoc network, interference is

a main performance limiting factor. So in a decentralized network, a good opportunistic schedule should consider interference when scheduling transmitters. In this chapter, we introduce three simple distributed opportunistic scheduling (DOS) strategies of increasing complexity that reduce interference while maximizing the *network performance*. We use transmission capacity as the network-wise performance metric. Transmission capacity (TC) was introduced in [13] [40] and measures the area spectral efficiency with outage constraints. This metric is well suited for analyzing opportunistic scheduling techniques in an ad hoc network since it penalizes selfish strategies that maximize a single-link rate at the expense of increasing interference in the network. We model the nodes as a homogeneous Poisson point process (PPP) on the plane and obtain and compare the transmission capacity of the proposed schemes. A schematic example of the network model considered in this chapter is shown in Figure 2.1.

2.1 Literature Review and Motivation

In most of the literature, distributed opportunistic scheduling usually refers to opportunistic routing and scheduling. Changes in topology and the channel make opportunistic routing extremely challenging. The core idea of distributed opportunistic routing [41–45], is to exploit the multitude of paths available between the source and the destination, in effect leading to “multi-path diversity”. This leads to a significant reduction of end-to-end outage probability. For practical implementation, intermediate routers require channel state information of their *neighboring* receivers resulting in a large transmission overhead

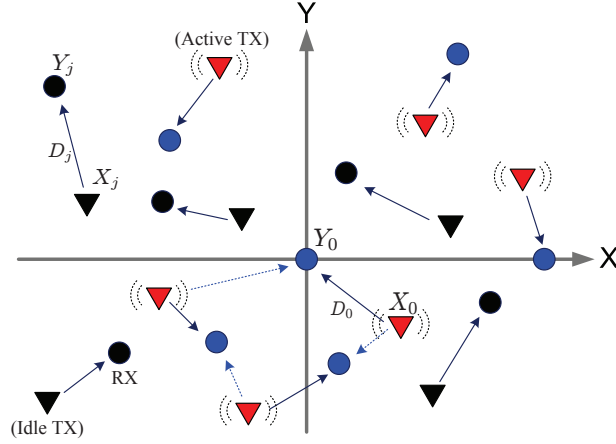


Figure 2.1: The network model: All transmitters form a homogeneous PPP with certain intensity. Red and black triangles represent active transmitters and idle transmitters, respectively. Communication and interference channels are represented by solid and dashed arrows, respectively. Receiver Y_0 located at the origin is called reference receiver and its transmitter is called reference transmitter. In addition, the network is interference-limited and uses slotted-ALOHA protocol.

especially when the network is dense. Also while it is clear that opportunistic routing increases the reliability of a single path, its impact on the entire network throughput is not clear. This is because developing a distributed routing algorithm based on network-wise performance metrics is complex and thus intractable in analysis, especially in a large-scale random network.

The current literature of distributed opportunistic scheduling focuses on channel access by joint channel probing and distributed scheduling [46–50]. The idea is to exploit multi-user diversity by favoring the transmitter-receiver pair with a good channel status to access the channel. Game-theoretic formulation is

commonly used to design and analyze such schemes, particularly when scheduling decisions of neighboring transmitters are correlated [46] [47]. These correlations introduced because of scheduling makes the analysis intractable. In addition, the current opportunistic scheduling schemes have two main drawbacks. First, they induce a serious communication overhead problem in a large (dense) network because a large amount of channel state information is required. Second, these schemes are not devised from a spatial throughput point of view. In general, only one transmit-receiver pair can access the channel at a time. This leads to conservative throughput since links which do not significantly interfere each other are prohibited from sharing the same channel. Moreover, it is not very clear that the gain in the network throughput achieved by these schemes. In [47], a cooperative (team) game approach was introduced for scheduling and throughput analysis of the entire network. However, as mentioned before, the complexity of these schemes for increasing the maximal throughput is extremely high in a large and dense networks.

In summary, current distributed opportunistic scheduling schemes are inappropriate for a large-scale random network because of their high implementation complexity and communication overhead. Most importantly, the overall network throughput achieved by those schemes is unknown and the analysis is extremely difficult. This motivates us to develop simple and low-complexity DOS schemes in a large-scale wireless ad hoc network with spatial randomness.

2.2 Overview of the Three Proposed DOS Schemes

In this chapter, three DOS schemes – distributed channel-aware scheduling (DCAS), distributed interferer-aware scheduling (DIAS) and distributed interferer-channel aware scheduling (DICAS), are proposed. They will be analyzed and discussed in the following three sections, respectively. Here we briefly introduce each of them and explain the main ideas behind them. The DCAS scheme adopts the communication channel information to help a transmitter decide when to schedule a transmission. It has a transmission threshold and transmitters are allowed to transmit whenever their communication channel gain is no less than the threshold. In Figure 2.2, for example, transmitter X_0 is allowed to transmit if its communication channel gain $H_0 D_0^{-\alpha}$ is greater than or equal to the threshold. DCAS with a properly designed threshold can avoid transmitting when communication channels are weak and interfering is severe, and thus it can enhance SIR by increasing received power and decreasing interference at the same time.

The idea of DIAS is to exclude transmissions from the transmitters that seriously interfere their unintended receivers. To make DIAS simple, it only uses the fading status of the interference channel from a transmitter to its nearest unintended receiver¹. So if transmitter X_0 in Figure 2.2 uses the DIAS scheme, it schedules a transmission whenever its interference channel gain $\tilde{H}_* \tilde{D}_*^{-\alpha}$ is smaller than some threshold. This scheme uses an indirect method to avoid all receivers to be seriously interfered and thus it can only reduce interference and cannot avoid transmissions in deep fading. DIAS is suitable for the scenario that transmitters

¹DIAS is actually implementable by using the status of any interference channels

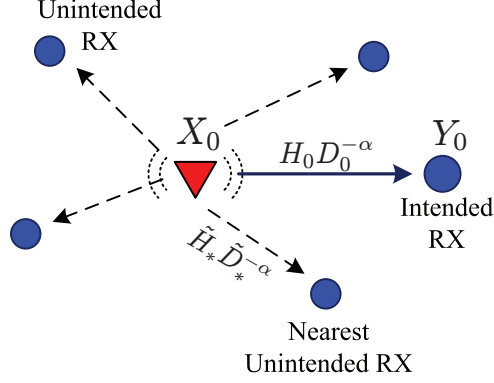


Figure 2.2: A schematic explanation for the three proposed DOS schemes: The communication channel of the $X_0 - Y_0$ pair is the solid arrow and its fading channel gain is denoted by $H_0 D_0^{-\alpha}$. All other dashed arrows stand for interference channels, and $\tilde{H}_* \tilde{D}_*^{-\alpha}$ represents the channel gain of the interference channel from transmitter X_0 to its nearest unintended receiver.

are unable to acquire their channel state information, but can occasionally know the channel state information of their nearby unintended receivers. DICAS, the combined scheme of DCAS and DIAS, can be shown to be the best scheme among the three because DCAS and DIAS can compensate their drawbacks and thus benefit each other. In Figure 2.2, if transmitter X_0 uses the DICAS scheme, it can schedule a transmission only when $H_0 D_0^{-\alpha}$ and $\tilde{H}_* \tilde{D}_*^{-\alpha}$ both satisfy their transmission threshold constraints.

2.3 Contributions

Our first contribution is to investigate distributed opportunistic scheduling in a large-scale random network from a spatial throughput point of view. This

is a new approach to developing distributed opportunistic scheduling based on a network-wise throughput metric. Our second contribution is proposing the three aforementioned DOS schemes which are inspired by the definition of transmission capacity. The three schemes use *adaptive* transmission thresholds that capture transmitting activities of the network. Most importantly, the proposed schemes are easily implementable because of their low overhead and complexity.

DCAS is a more general scheme than threshold scheduling proposed in [51] which bases transmission decision on a fixed threshold. The fixed threshold scheduling fails to capture the transmission activities in the network and hence do not fully exploit the possible spatial reuse. Instead, DCAS threshold depends on the intensity of concurrent transmitters thus leading to increased spatial reuse, and hence TC. The DIAS scheme schedules transmitters by limiting the interference at the nearest unintended receiver to a predetermined threshold. Although DIAS only considers to control the interference generated at the nearest unintended receiver of a transmitter, we show that this is sufficient in most cases. DICAS is a combination of DCAS and DIAS, and provides the best performance.

We provide bounds on the outage probability for these three schemes. These bounds are used to characterize the transmission capacity of the schemes. Our results show that DCAS can significantly increase TC and outperform the constant threshold scheduling scheme. Tight bounds on TC can be obtained for any path loss exponent for a class of threshold functions. For DIAS, bounds on TC can be obtained in closed-form for some special cases of the transmission threshold and we theoretically show that it can increase TC significantly, especially when the network is dense. Bounds on TC for the DICAS scheme can be

very tight if two transmission thresholds for DCAS and DIAS are jointly and properly designed. They also indicate that DICAS is the most efficient scheme to significantly improve TC. In addition, the asymptotic tightness of the bounds on TC for each scheme is found as well and they can provide some insights on how to devise the transmission threshold for each scheme in sparse and dense networks.

This third contribution in this work is that a geometric interpretation of the bounds on the outage probability for the three DOS schemes is provided. We found that the three schemes can efficiently reduce the average number of the interferers in their *dominant interferer coverage*. Using the notion of the dominant interfere coverage, a geometric perspective of canceling interference for the three DOS schemes is also introduced and it provides a fundamental understanding of how much outage probability can be reduced by canceling interference at a receiver. The *interference cancellation coverage* of each scheme is defined and its mean Lebesgue measure is able to characterize the average number of the cancelable interferers in the coverage of the scheme. Bounds on the outage probability of the three DOS schemes with interference cancellation are obtained, and they can provide us a good insight on how to design transmission thresholds to make interference cancellation be efficiently utilized for those schemes.

2.4 Network Model and Preliminaries

2.4.1 The Network Model

In this chapter, we consider an infinitely large wireless ad hoc network in which there are many transmitter-receiver pairs and they are independently and randomly distributed. Specifically, a random access protocol in the style of slotted Aloha without power control is operated in the network and all transmitting nodes are assumed to form a marked homogeneous Poisson point process (PPP) on the plane \mathbb{R}^2 denoted by

$$\Pi_t \triangleq \{(X_j, T_j, D_j, H_j) : X_j \in \mathbb{R}^2, T_j \in \{0, 1\}, D_j \geq 1, H_j \in \mathbb{R}_+\}, \quad (2.1)$$

where X_j denotes the transmitter of pair j and its location, T_j represents the transmission status of a transmitter (If $T_j = 1$, the transmitter is allowed to transmit; otherwise $T_j = 0$), D_j represents the distance between the transmitter and the intended receiver of pair j , and H_j denotes the fading channel gain between the transmitter and the receiver of pair j . The spatial intensity of this PPP is denoted by λ_t , which gives the average number of transmitting nodes per unit area. All transmission distances $\{D_j\}$ are assumed to be i.i.d. random variables, and all fading channel gains are i.i.d. exponential random variables with unit mean and variance. The notation of main network parameters, processes and functions are listed in Table 3.1.

All transmitted signals undergo path loss and fading before they reach their intended receivers and all transmitters have the same unit transmit power. Let pair 0 be the reference pair whose receiver (called reference receiver) is located

Table 2.1: Notation of Main Variables, Processes and Functions in Chapter 2

Symbol	Definition
Π_t	Homogeneous PPP of transmitters
$\Pi_c(\Pi_i, \Pi_{ic})$	PPP of transmitters using DCAS (DIAS, DICAS)
$\lambda_c(\lambda_i, \lambda_{ic})$	Intensity of $\Pi_c(\Pi_i, \Pi_{ic})$
$\underline{\lambda}(\bar{\lambda})$	Lower (upper) bound on λ
$\bar{\lambda}_\epsilon$	Maximum contention intensity
β	SIR threshold
α	Path loss exponent ($\alpha > 2$)
ϵ	Upper bound of outage probability
$X_j(Y_j)$	Transmitter (Receiver) of pair j
D_j	$ X_j - Y_j $, Random transmission distance of pair j
$\Delta_c, \Delta_i, \Delta_{ic}$	Transmission threshold for DCAS, DIAS, DICAS
$p_c(\cdot), p_i(\cdot), p_{ic}(\cdot)$	Transmission probability for DCAS, DIAS, DICAS
$q(\lambda_c), q(\lambda_i), q(\lambda_{ic})$	Outage probabilities for DCAS, DIAS, DICAS
$\underline{q}(\cdot)(\bar{q}(\cdot))$	Lower (upper) bound on outage probability $q(\cdot)$
\mathcal{C}_Δ	Δ -level dominant interferer coverage
$\mathcal{C}_c^c(\mathcal{C}_i^c, \mathcal{C}_{ic}^c)$	Interference cancellation coverage for DCAS (DIAS, DICAS)
$\mu(\mathcal{A})$	(Mean) Lebesgue measure of a bounded set \mathcal{A}
$f_Z(\cdot), F_Z(\cdot), F_Z^c(\cdot)$	PDF, CDF, CCDF of random variable Z

at the origin. So the desired signal power is $H_0 D_0^{-\alpha}$ and its received interference can be written as a Poisson shot noise process [52–56],

$$I_0 = \sum_{X_j \in \Pi_t \setminus X_0} \tilde{H}_j |X_j|^{-\alpha}, \quad (2.2)$$

where $\alpha > 2$ is the path loss exponent², $|X_j|$ denotes the Euclidean distance between transmitter X_j and the origin and \tilde{H}_j is the fading channel gain from the transmitter of pair j to the reference receiver. Since the PPP Π_t is homogeneous, according to Slivnyak's theorem the statistics of signal reception seen by the reference receiver is the same as that seen by any other receivers of all other pairs [57] [17]. Our following analysis is based on the reference pair. The performance measured at the origin is often referred to the Palm measure and according to [57] conditioning on the event of a node lying at the origin does not affect the statistics of the rest of the process. Hence, without loss of ambiguity, the the probability and expectation of functionals conditioned at the origin are just denoted by \mathbb{P} and \mathbb{E} , respectively.

Since the network in this chapter is assumed to be interference-limited, noise power is not considered in (4.7). The received signal-to-interference ratio (SIR) can be expressed as

$$\text{SIR}(\lambda_t) = \frac{H_0 D_0^{-\alpha}}{I_0}. \quad (2.3)$$

The typical receiver can successfully decode the information when $\text{SIR} > \beta$ and is in outage otherwise. The outage probability is given by

$$q(\lambda_t) \triangleq \mathbb{P}[\text{SIR}(\lambda_t) < \beta] = \mathbb{P}\left[\frac{H_0 D_0^{-\alpha}}{I_0} < \beta\right]. \quad (2.4)$$

The above outage probability for the case of Rayleigh fading is well known and can be found exactly [15]. For most other cases, it is difficult to find because of

²For a planar wireless network, α has to be greater than 2 in order to obtain a bounded interference almost surely (a.s.), i.e. $I_0 < \infty$ a.s. if $\alpha > 2$ [18].

the complex distribution of random variable I_0 . However, bounds on the CCDF of I_0 are able to be found as shown in the following lemma, and they are very useful while finding the bounds on the outage probability for the three DOS schemes.

Theorem 2.4.1 (Bounds on the CCDF of the shot-noise process of a nonhomogeneous PPP). *Suppose $\Pi_n = \{(X_j, \tilde{H}_j) : X_j \in \mathbb{R}^2, \tilde{H}_j \in \mathbb{R}_+, \forall j \in \mathbb{N}_+\}$ is a marked nonhomogeneous PPP and $\{\tilde{H}_j\}$ are i.i.d. exponential random variables with unit mean and variance. The intensity of Π_n at location X is denoted by $\lambda_n(|X|)$. Let I_n be the shot-noise process generated by Π_n and it is defined as $I_n = \sum_{X_j \in \Pi_n} \tilde{H}_j |X_j|^{-\alpha}$ where $\alpha > 2$. Then the CCDF of I_n can be bounded as*

$$1 - e^{-A(x)} \leq F_{I_n}^c(x) \leq 1 - \left(1 - \frac{(\alpha - 1)A(x)}{[(\alpha - 1) - A(x)]^2}\right)^+ e^{-A(x)}, \quad (2.5)$$

where $A(x) = \frac{2\pi}{\alpha} x^{-\frac{2}{\alpha}} \int_0^\infty \lambda_n\left(\sqrt[{\alpha}]{u/x}\right) u^{\frac{2}{\alpha}-1} e^{-u} du$ and $(y)^+ \triangleq \max(y, 0)$. In addition, if Π_n is homogeneous, then $A(x)$ reduces to $\pi x^{-\frac{2}{\alpha}} \Gamma(1 + \frac{2}{\alpha}) \lambda_n$ where $\Gamma(x) \triangleq \int_0^\infty t^{x-1} e^{-t} dt$ is the Gamma function.

Proof. The proof is given in Appendix 2.9.1 and it is similar to the technique used in [51]. □

Remark 2.4.2. *If λ_n approaches to zero (infinity), then $A(x)$ approaches to zero (infinity) so that the gap between the upper and lower bounds in (2.5) becomes tight since it scales with $A(x)e^{-A(x)}$ ($e^{-A(x)}/A(x)$). That means, using the upper or lower bound in (2.5) to evaluate $F_{I_n}^c(x)$ in a sparse (dense) network is sufficient³.*

³See Definition 2.4.4 in Section 2.4.2 for the spatial sparseness and denseness of a Poisson-

2.4.2 Definitions

Our main objective in this chapter is to study when is a good transmission opportunity for each transmitter so that the outage probability can be suppressed. Suppressing outage probability is not only to maintain reliable transmission but also to increase the throughput of the network. The throughput metric used in this paper is called *transmission capacity*, as defined in the following.

Definition 2.4.3 (Transmission Capacity). *Transmission capacity (TC) c_ϵ originally proposed in [13] gives units of area spectral efficiency and has an outage probability constraint $\epsilon \in (0, 1)$. It is defined as*

$$c_\epsilon \triangleq b \bar{\lambda}_\epsilon (1 - \epsilon), \quad (2.6)$$

where b denotes the supportable transmission rate for every link (e.g. $\log_2(1 + \beta)$) and $\bar{\lambda}_\epsilon \triangleq \sup_\lambda \{\lambda > 0 : \mathbb{P}[\text{SIR}(\lambda) < \beta] \leq \epsilon\}$ is called *maximum contention intensity*.

In other words, TC characterizes how many successful transmissions of rate b per unit area can coexist. The following definition of network sparseness and denseness is helpful for characterizing the asymptotic behaviors of transmission capacity for the three DOS schemes.

Definition 2.4.4 (Spatial sparseness and denseness of a network). *Let Π_s be the PPP for transmission scheme s and the transmission coverage of a transmitter in Π_s be the circular area with radius as its transmission distance D_0 .*

distributed network.

Suppose λ_s is the intensity of Π_s and $\pi\lambda_s\mathbb{E}[D_0^2]$ is the average number of nodes in the transmission coverage of the transmitter. The network is called “dense” if $\lambda_s\pi\mathbb{E}[D_0^2]$ is sufficiently large (i.e. $\lambda_s\pi\mathbb{E}[D_0^2] \gg 1$). On the contrary, the network is call “sparse”, then it means $\lambda_s\pi\mathbb{E}[D_0^2]$ is sufficiently small (i.e. $\lambda_s\pi\mathbb{E}[D_0^2] \ll 1$).

2.5 Distributed Channel-Aware Scheduling (DCAS)

The DCAS scheme uses the channel state information between a transmitter and its intended receiver to schedule transmissions. In this section, we obtain bounds on the outage probability and the transmission capacity of this scheme, and some observations and numerical results are provided as well.

2.5.1 Transmission Capacity achieved by DCAS

If a transmitter knows the channel state information to its receiver, it can avoid transmitting when the channel is in a deep fade. Prohibiting the transmissions with a bad channel reduces interference and hence the outage probability. A fixed threshold-based scheduling is proposed in [51] and was shown to improve the transmission capacity. Using a fixed threshold to decide when to transmit has a drawback – it only captures the fading condition of a channel and fails to capture transmitting activities of interfering transmitters in the network. So a better approach is to change the threshold adaptively with the intensity of transmitters so as to capture the interference level in the network.

Since a transmitter $X_j \in \Pi_t$ can schedule a transmission if $H_j D_j^{-\alpha} \geq \Delta_c(\lambda_c)$ and the transmission decision of every transmitter is independent of other

transmitters, it follows that the final transmission set

$$\Pi_c = \{X_j \in \Pi_t : T_j = \mathbf{1}(H_j D_j^{-\alpha} \geq \Delta_c(\lambda_c)), \forall j \in \mathbb{N}_+\}, \quad (2.7)$$

is again a homogeneous PPP with intensity λ_c that is given by

$$\lambda_c = \lambda_t \mathbb{P}[H_0 D_0^{-\alpha} \geq \Delta_c(\lambda_c)] = \lambda_t p_c(\lambda_c), \quad (2.8)$$

where $p_c(\lambda_c)$ is the transmission probability for a transmitter using the DCAS scheme. Hence, given the distribution of D_0 and the function $\Delta_c(\lambda_c)$, the final intensity λ_c can numerically be obtained. For example, when all link distances are a constant d , i.e. $D_j = d$, it follows from the exponential distribution of H_0 that

$$\lambda_c = \lambda_t \exp(-d^\alpha \Delta_c(\lambda_c)).$$

The following theorem characterizes the outage probability of the DCAS scheme.

Theorem 2.5.1. *Let $\Delta_c(x)$ be a nondecreasing function of $x \in \mathbb{R}_+$. The upper bound $\bar{q}(\lambda_c)$ and lower bound $\underline{q}(\lambda_c)$ on the outage probability $q_k(\lambda_c)$ in the DCAS scheme are*

$$\underline{q}(\lambda_c) = (1 - e^{-A_c})(1 - B_c), \quad (2.9a)$$

$$\bar{q}(\lambda_c) = \left[1 - \left(1 - \frac{(\alpha - 1)A_c}{[(\alpha - 1) - A_c]^2} \right)^+ e^{-A_c} \right] (1 - B_c), \quad (2.9b)$$

where $A_c = \pi \Gamma(1 + \frac{2}{\alpha}) \lambda_c \beta^{\frac{2}{\alpha}} [\Delta_c(\lambda_c)]^{-\frac{2}{\alpha}}$, $B_c = \mathbb{E}[\exp(-\lambda_c \beta^{\frac{2}{\alpha}} \psi D_0^2)]$, and $\psi = \pi \Gamma(1 + \frac{2}{\alpha}) \Gamma(1 - \frac{2}{\alpha})$.

Proof. See Appendix 2.9.2. □

Remark 2.5.2. Note that the threshold $\Delta_c(\lambda_c)$ should depend on the final intensity of transmitters λ_c and not λ_t . This is because the final interference scales with λ_c rather than λ_t . Denote the upper and lower bounds on the maximum contention intensity achieved by DCAS by $\underline{\lambda}_c$ and $\bar{\lambda}_c$ respectively. More precisely, $\bar{\lambda}_c = \sup\{\lambda_c : \underline{q}(\lambda_c) \leq \epsilon\}$ and $\underline{\lambda}_c = \sup\{\lambda_c : \bar{q}(\lambda_c) \leq \epsilon\}$ and these two bounds can be obtained numerically using the bounds on the outage probability.

Remark 2.5.3. Bounds on the outage probability both reduce to $1 - B_c$ if no DCAS is used (i.e. $\Delta_c = 0$). In this case, we can have the exact result of TC once the distribution of transmission distance D_0 is specified. For example, if $D_0 = d$ is a constant and $\Delta_c = 0$, then $\underline{q}(\lambda_c) = \bar{q}(\lambda_c) = 1 - \exp(-d^2 \beta^{\frac{2}{\alpha}} \psi \lambda_c)$ and thus $\bar{\lambda}_\epsilon = \frac{-b \ln(1-\epsilon)}{d^2 \beta^{\frac{2}{\alpha}} \psi} = \frac{b\epsilon}{d^2 \beta^{\frac{2}{\alpha}} \psi} + O(\epsilon^2)$ same as [13].

Upper bound $\underline{q}(\lambda_c)$ in (2.9a) and lower bound $\bar{q}(\lambda_c)$ in (2.9b) are consisting of two probabilities. The first term in the lower bound (2.9a) is obtained as a lower bound to the probability $\mathbb{P}[I_0 \geq \Delta_c(\lambda_c)/\beta]$, i.e.,

$$\mathbb{P}[I_0 \geq \Delta_c(\lambda_c)/\beta] \geq 1 - e^{-A_c} = 1 - \exp\left(-\lambda_c \pi \left(\sqrt{\frac{A_c}{\lambda_c \pi}}\right)^2\right). \quad (2.10)$$

Since Π_c is a PPP, $1 - \exp\left(-\lambda_c \pi \left(\sqrt{\frac{A_c}{\lambda_c \pi}}\right)^2\right)$ equals the probability that a disc of radius $\sqrt{\frac{A_c}{\lambda_c \pi}}$ is nonempty. So A_c/λ_c can be viewed as the area in which any single interferer can generate the interference greater than or equal to $\Delta_c(\lambda_c)/\beta$. Setting $\Delta_c = 0$, we observe that the term $1 - B_c$ equals the outage probability in a homogeneous PPP network without DCAS. When the transmission distance D_0 is a constant, $-\ln(B_c)/\lambda_c$ can also be viewed as the area in which any single interferer is able to cause outage at the (reference) receiver.

We now provide heuristics for choosing an appropriate threshold function for $\Delta_c(\lambda_c)$:

1. It is very clear that the interference increases with increasing λ_c . As the interference is high, it is good to only schedule transmitters that have a “good” channel quality as compared to the ambient interference. Hence the threshold $\Delta_c(\lambda_c)$ should increase with λ_c .
2. Using the conservation property (see Proposition 2.8.1 in Appendix 2.8.1), it follows that

$$I_0 = \sum_{X_j \in \Pi_c \setminus X_0} \tilde{H}_j |X_j|^{-\alpha} = \lambda_c^{\frac{2}{\alpha}} \sum_{X_k \in \Pi'_c \setminus X_0} \tilde{H}_k |X_k|^{-\alpha}, \quad (2.11)$$

where Π'_c is a homogeneous PPP with unit intensity. Note that I_0 depends on λ_c here because Π_c is the PPP of active transmitters. So we have

$$\mathbb{P}[I_0 \geq \Delta_c(\lambda_c)/\beta] = \mathbb{P} \left[\lambda_c^{\frac{2}{\alpha}} \sum_{X_k \in \Pi'_c \setminus X_0} \tilde{H}_k |X_k|^{-\alpha} \geq \frac{\Delta_c(\lambda_c)}{\beta} \right].$$

Hence, in order to capture a reasonable level of interference I_0 , it follows that $\Delta_c(\lambda_c)$ should be designed to (linearly) scale with $\lambda_c^{\frac{2}{\alpha}}$.

The above arguments both suggest that $\Delta_c(\lambda_c) \in \Theta(\lambda_c^\gamma)$ with $\gamma \in \mathbb{R}_+^4$, i.e. $\Delta_c(\lambda_c)$ is a nondecreasing function of λ_c .

⁴Throughout this chapter, we use the asymptotic tightness notation $f(n) \in \Theta(g(n))$ to also represent the case that $k_1|g(n)| \leq |f(n)| \leq k_2|g(n)|$ holds for any $n > 0$ where k_1 and k_2 are positive constants. Namely, n is not necessary to be large for holding the inequality.

2.5.2 Discussion and Numerical Results

There are several interesting observations that can be perceived from the results in Theorem 2.5.1. We specify them in the following, respectively.

Bounds on outage probability: As mentioned earlier, $1 - B_c$ represents the outage probability without DCAS. From Theorem 2.5.1 and since $\left[1 - \left(1 - \frac{(\alpha-1)A_c}{[(\alpha-1)-A_c]^2}\right)^+ e^{-A_c}\right] < 1$, it follows that the outage probability is lower with DCAS than without it. If the threshold $\Delta_c(\lambda_c)$ is chosen to be a constant (instead of a function of λ_c), i.e. $\Delta_c(\lambda_c) \equiv \rho$, then there does not exist a non-trivial optimal value of ρ that maximizes the TC. This is because $\underline{q}(\lambda_c)$ and $\bar{q}(\lambda_c)$ both approach to 0 when ρ goes to infinity and to $1 - B_c$ as ρ goes to zero. However, there does exist an optimal transmission threshold for maximizing TC if some power control methods are applied, such as channel inversion power control [51].

Spatial reuse with adaptive threshold $\Delta_c(\lambda_c)$: As we have mentioned, threshold scheduling proposed in [51] does not take into account the transmitting activities of transmitters. It fails to capture an interference effect such that transmitters whose receivers have a satisfactory SIR may not be allowed to transmit. We can use a spatial reuse point of view to explain why using an adaptive threshold is better. Using the similar definition of the spatial reuse factor in [15], the spatial reuse factor under the DCAS scheme is defined as the average transmission distance divided by the average distance from a receiver to its nearest unintended transmitter when the maximum contention intensity is achieved, i.e. $2\mathbb{E}[D_0]\sqrt{\bar{\lambda}_c}$. *A better transmission scheduling scheme can have a larger spatial reuse factor.* Now consider $\Delta_c(\lambda_c) = \rho\lambda_c^\gamma$ where $\rho > 0$ and the network is sparse.

In this case, the spatial reuse factor can be approximated by $\frac{2\sqrt{\epsilon}\mathbb{E}[D_0]}{\sqrt{[1-e^{-A_c(\bar{\lambda}_\epsilon)]\beta^{\frac{2}{\alpha}}\psi\mathbb{E}[D_0^2]}}$. If Δ_c is a constant, $1 - e^{-A_c(\bar{\lambda}_\epsilon)}$ increases as $\bar{\lambda}_\epsilon$ increases. That means the spatial reuse factor decreases with intensity λ_c for threshold scheduling. So if γ is chosen properly so that $1 - e^{-A_c}$ does not depend on λ_c or decreases with λ_c , then DCAS has better spatial reuse than threshold scheduling. A better spatial reuse means a larger TC achieved. A simulation example of TC for the DCAS scheme with different thresholds is shown in Figure 2.3. As you can see, the DCAS scheme with a properly designed $\Delta_c(\lambda_c)$ can significantly outperform the schemes of threshold scheduling and No DCAS⁵. So using a well-designed adaptive threshold really can achieve a (much) higher TC.

Asymptotic tightness of bounds on TC: We can conclude the following asymptotic results for the bounds on TC in a sparse and dense network.

Lemma 2.5.4. *Suppose $\Delta_c(\lambda_c) \in \Theta(\lambda_c^\gamma)$ where $\gamma \in \mathbb{R}_+$. If the network is sparse, then we have the following asymptotic result:*

$$\lim_{\lambda_t \rightarrow 0} \frac{\bar{\lambda}_c}{\underline{\lambda}_c} = \begin{cases} \left(\frac{\alpha}{\alpha-1}\right)^{\frac{1}{2-2\gamma/\alpha}}, & \text{for } \gamma \in (0, \frac{\alpha}{2}) \\ 1, & \text{otherwise} \end{cases}. \quad (2.12)$$

If the network is dense, different asymptotic results are shown in the following

$$\lim_{\lambda_t \rightarrow \infty} \frac{\bar{\lambda}_c}{\underline{\lambda}_c} = \begin{cases} 1, & \text{otherwise} \\ \left(\frac{\alpha}{\alpha-1}\right)^{\frac{\alpha}{2\gamma-\alpha}}, & \text{for } \gamma \in [\frac{\alpha}{2}, \infty) \end{cases}. \quad (2.13)$$

⁵No DCAS means the transmitting nodes which use slotted Aloha to randomly access the shared link has the original intensity λ_t .

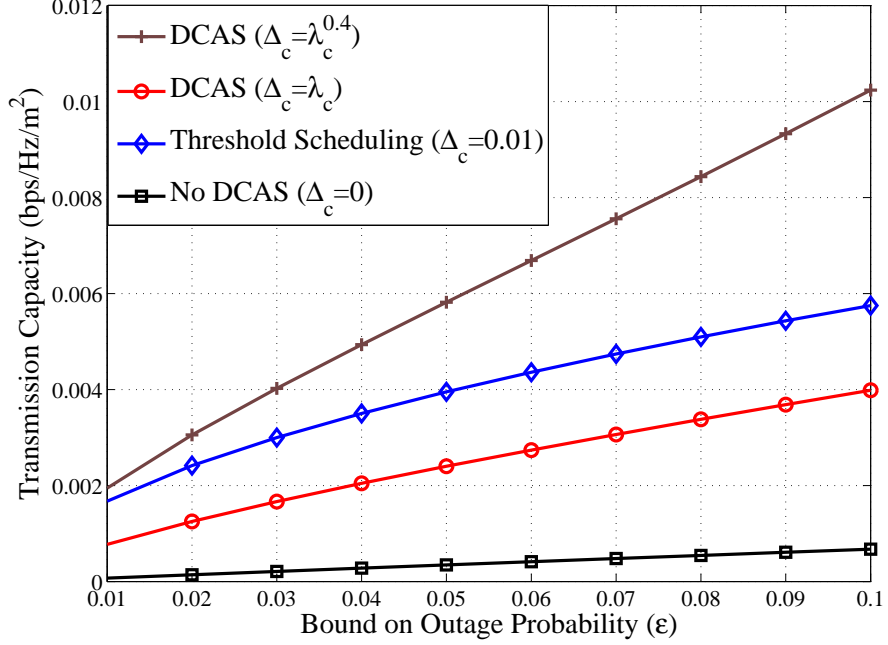


Figure 2.3: The simulation results of TC for the DCAS scheme with different $\Delta_c(\lambda_c)$. The network parameters for simulation are: $\alpha = 4$, $\beta = 2$, $\Delta_c = \lambda_c^\gamma$ and $D = 8m$.

Proof. Here we only prove the case of a sparse network since the proofs for other cases are similar. First, we have to notice that “ $\lambda_t \rightarrow 0$ ” and “ $\lambda_t \rightarrow \infty$ ” respectively correspond to “ $\lambda_c \rightarrow 0$ ” (a sparse network) and “ $\lambda_c \rightarrow \infty$ ” (a dense network) because $\lambda_c = \lambda_t \mathbb{P}[H_0 D_0^{-\alpha} \geq \Delta_c(\lambda_c)]$ and $\Delta_c(\lambda_c)$ is a nondecreasing function. When $\lambda_c \rightarrow 0$, observe that the network is sparse since $\pi \mathbb{E}[D_0^2] \lambda_c \ll 1$. So for $\gamma \leq \frac{\alpha}{2}$ and $\lambda_c \rightarrow 0$, we have $\Delta_c(\lambda_c) \rightarrow 0$ and thus $\underline{q}(\lambda_c) = \pi \beta^{\frac{4}{\alpha}} \Gamma(1 + \frac{2}{\alpha}) \psi \mathbb{E}[D_0^2] \lambda_c^{2 - \frac{2\gamma}{\alpha}} + O(\lambda_c^{3 - \frac{2\gamma}{\alpha}})$, and thus $\bar{\lambda}_c = \Theta(\epsilon^{\frac{1}{2 - 2\gamma/\alpha}})$. Similarly, we can show that $\bar{q}(\lambda_c) = \frac{\alpha \pi \beta^{\frac{4}{\alpha}}}{\alpha - 1} \Gamma(1 + \frac{2}{\alpha}) \psi \mathbb{E}[D_0^2] \lambda_c^{2 - \frac{2\gamma}{\alpha}} + O(\lambda_c^{3 - \frac{2\gamma}{\alpha}})$ and $\underline{\lambda}_c = \Theta((\frac{\alpha - 1}{\alpha} \epsilon)^{\frac{1}{2 - 2\gamma/\alpha}})$. Therefore, it follows that $\lim_{\lambda_t \rightarrow 0} \frac{\bar{\lambda}_c}{\underline{\lambda}_c} = (\frac{\alpha}{\alpha - 1})^{\frac{1}{2 - 2\gamma/\alpha}}$. When

$\gamma > \frac{\alpha}{2}$ and $\lambda_c \rightarrow 0$, $\underline{q}(\lambda_c)$ and $\bar{q}(\lambda_c)$ both can be simplified as $\pi\beta^{\frac{2}{\alpha}}\psi\mathbb{E}[D_0^2]\lambda_c + O(\lambda_c^2)$ so that $\frac{\bar{\lambda}_c}{\underline{\lambda}_c} \rightarrow 1$ as $\lambda_c \rightarrow 0$, which completes the proof. \square

Lemma 2.5.4 indicates that the ratio of $\bar{\lambda}_c$ to $\underline{\lambda}_c$ depends on path loss exponent α in a sparse (dense) network if $\gamma < \frac{\alpha}{2}$ ($\gamma \geq \frac{\alpha}{2}$). For large α , $\alpha/(\alpha - 1) \approx 1$ and hence the bounds on the TC are asymptotically tight in all regimes. However, if $\gamma \geq \frac{\alpha}{2}$ ($\gamma < \frac{\alpha}{2}$), bounds on TC are very tight for all α in the sparse (dense) network. That is better than the case of using fixed threshold because we have the following results if threshold Δ_c is a constant (i.e. $\gamma = 0$):

$$\lim_{\lambda_c \rightarrow 0} \frac{\bar{\lambda}_c}{\underline{\lambda}_c} = \sqrt{\frac{\alpha}{\alpha - 1}} \quad \text{and} \quad \lim_{\lambda_c \rightarrow \infty} \frac{\bar{\lambda}_c}{\underline{\lambda}_c} = 1. \quad (2.14)$$

So designing $\Delta_c(\lambda_c)$ properly can make TC be accurately approximated by its upper or lower bound no matter if α is large or not.

2.6 Distributed Interferer-Aware Scheduling (DIAS)

The previous distributed strategy (DCAS) depended only on the channel between the transmitter and the receiver and the average intensity of the network. DCAS is essentially a *selfish* opportunistic scheduling scheme since a nodes decision to transmit does not consider its effects on *unintended* receivers. However, if a transmitter has knowledge about other receivers, it can use this information to make a better scheduling decision. In the distributed interferer-aware scheduling (DIAS) scheme, a transmitter schedules a transmission only when it generates an acceptable interference level at its unintended receivers. Although DIAS does not

directly benefit SIR of a receiver, each receiver can avoid significant interfering from its unintended transmitters.

2.6.1 Is reducing the interference at the nearest unintended receiver sufficient?

So what information do we need to determine the transmission threshold of DIAS? Ideally, a transmitter should design its transmission threshold by considering the interference generated by its transmission at all the receivers in its network. However, this requires prohibitively large amounts of channel state information which is not feasible in practice. So in the proposed DIAS scheme, a potential transmitter only considers its impact on the nearest unintended receiver and schedules a transmission only when the interference generated at its nearest unintended receiver is lower than a threshold. Let \tilde{H}_* be the fading channel gain from a transmitter to its nearest unintended receiver and thus transmission probability for DIAS is $p_i(\lambda_i) = \mathbb{P}[\tilde{H}_* \tilde{D}_*^{-\alpha} \leq \Delta_i(\lambda_i)]$ where $\Delta_i(\lambda_i) > 0$ is the transmission threshold. Since p_i only depends on intensity λ_i , the transmitter set resulting from DIAS is a thinning of Π_t . More precisely,

$$\Pi_i = \{X_j \in \Pi_t : T_j = \mathbf{1}(\tilde{H}_{j*}|X_j - Y_{j*}|^{-\alpha} \leq \Delta_i(\lambda_i)), \forall j \in \mathbb{N}_+\}, \quad (2.15)$$

where Y_{j*} is the nearest unintended receiver of transmitter X_j and \tilde{H}_{j*} is the fading channel gain from X_j to Y_{j*} . Thus, the intensity of Π_i is $\lambda_i = \lambda_t p_i(\lambda_i)$. Since all active receivers also form a homogeneous PPP of intensity λ_i , let \tilde{D}_* be the (random) distance from an active transmitter to its nearest unintended

active receiver and the CDF of \tilde{D}_* is

$$F_{\tilde{D}_*}(x) = 1 - \exp(-\pi\lambda_t x^2) = 1 - \exp(-\pi\lambda_i x^2/p_i). \quad (2.16)$$

Using (2.16), $p_i(\lambda_i)$ can be explicitly expressed as

$$\begin{aligned} p_i(\lambda_i) &= 1 - 2\pi\lambda_t \int_0^\infty x e^{-(\Delta_i(\lambda_i)x^\alpha + \pi\lambda_t x^2)} dx \\ &= 1 - \int_0^\infty \exp\left(-\left[\frac{p_i(\lambda_i)u}{\pi\lambda_i}\right]^{\frac{2}{\alpha}} \Delta_i(\lambda_i) - u\right) du. \quad (\text{using } \lambda_t = \lambda_i/p_i(2\lambda_t)) \end{aligned}$$

Due to fading, for each transmitter, its nearest unintended receiver may not be the unintended receiver that receives the largest interference. However, the interference generated by a transmitter at its nearest unintended receiver dominates those at its other unintended receivers *in probability* because $\tilde{D}_* \leq |X_j - Y_k|$ almost surely for any $X_j \in \Pi_t$ and its unintended receiver Y_k . Since \tilde{H}_{j*} and \tilde{H}_{jk} are i.i.d., it follows that

$$\mathbb{P}[\tilde{H}_{j*}\tilde{D}_*^{-\alpha} \geq \Delta_i(\lambda_i)] \geq \mathbb{P}[\tilde{H}_{jk}|X_j - Y_k|^{-\alpha} \geq \Delta_i(\lambda_i)],$$

which means $1 - p_i(\lambda_i) \geq \mathbb{P}[\tilde{H}_{jk}|X_j - Y_k|^{-\alpha} \geq \Delta_i(\lambda_i)]$. Hence carefully choosing $p_i(\lambda_i)$, would limit interference in the network. In addition, the following lemma provides an analytical explanation why limiting the interference generated at the nearest unintended receiver of a transmitter is sufficient.

Lemma 2.6.1. *Let \tilde{H}_* and \tilde{D}_* denote the fading channel gain and distance from reference transmitter X_0 to its nearest unintended receiver. Suppose Y_j is one of the non-nearest unintended receivers of X_0 and ρ_* is a positive constant. Then, we have*

$$\lim_{\rho_* \rightarrow 0} \mathbb{P}[\tilde{H}_j\tilde{D}_j^{-\alpha} \leq \rho_* | \tilde{H}_*\tilde{D}_*^{-\alpha} \leq \rho_*] = 1, \quad (2.18)$$

where $\tilde{D}_j = |X_0 - Y_j|$.

Proof. See Appendix 2.9.3. □

Lemma 2.6.1 reveals a very interesting phenomenon, that is, if the channel from a transmitter to its nearest unintended receiver is in deep fading, then the channels from the transmitter to other unintended receivers are also in deep fading with *high probability*. So using the channel condition of the nearest unintended receiver is an effective means to judge if the interference generated by a transmitter is under a reasonable level. The threshold $\Delta_i(\lambda_i)$ has a significant impact on the performance of DIAS, and should be appropriately designed to adaptively capture the transmission activities in the network.

2.6.2 Transmission Capacity achieved by DIAS

Bounds on the outage probability and the maximum contention intensity for DIAS with transmission threshold $\Delta_i(\lambda_i)$ are given in the following theorem.

Theorem 2.6.2. *Suppose each transmitter uses DIAS to determine when to transmit. That is, a transmitter transmits whenever the interference channel gain at its nearest unintended receiver is less than threshold $\Delta_i(\lambda_i) > 0$ where $\Delta_i(\lambda_i)$ is a function of λ_i . Bounds on the outage probability with DIAS can be shown as*

$$\underline{q}(\lambda_i) = 1 - \exp\left(-\lambda_i \beta^{\frac{2}{\alpha}} \psi \mathbb{E}[D_0^2] p_i(\lambda_i)\right), \quad (2.19)$$

$$\bar{q}(\lambda_i) = 1 - \exp\left(-2\lambda_i \beta^{\frac{2}{\alpha}} \psi \mathbb{E}[D_0^2] p_i(\lambda_i)\right). \quad (2.20)$$

Let $\underline{\lambda}_i \leq \bar{\lambda}_\epsilon \leq \bar{\lambda}_i$ where $\underline{\lambda}_i = \sup_{\lambda_i} \{\lambda_i : \bar{q}(\lambda_i) \leq \epsilon\}$ and $\bar{\lambda}_i = \sup_{\lambda_i} \{\lambda_i : \underline{q}(\lambda_i) \leq \epsilon\}$. $\underline{\lambda}_i$ and $\bar{\lambda}_i$ can be found by solving the following

$$\bar{\lambda}_i p_i(\bar{\lambda}_i) = \frac{-\ln(1-\epsilon)}{\beta^{\frac{2}{\alpha}} \psi \mathbb{E}[D_0^2]} \quad \text{and} \quad \underline{\lambda}_i p_i(\underline{\lambda}_i) = \frac{-\ln(1-\epsilon)}{2\beta^{\frac{2}{\alpha}} \psi \mathbb{E}[D_0^2]}. \quad (2.21)$$

Specifically, suppose $\Delta_i(\lambda_i) = \rho \lambda_i^{\frac{2}{\alpha}}$, $\rho > 0$. Then there exists a sufficiently small ρ such that $p_i(\lambda_i) > \frac{1}{2}$ and thus

$$\bar{\lambda}_\epsilon > \frac{-\ln(1-\epsilon)}{\beta^{\frac{2}{\alpha}} \psi \mathbb{E}[D_0^2]}. \quad (2.22)$$

Proof. See Appendix 2.9.4. □

Remark 2.6.3. *The right hand side in (2.22) is the maximum contention intensity without DIAS. The result in (2.22) indicates that if a proper ρ is chosen then DIAS can achieve a TC which is (much) larger than the TC without DIAS no matter if the network is dense or not.*

The results in Theorem 2.6.2 indicate that DIAS can increase TC since $p_i(\lambda_i) < 1$. From (2.17), it follows that $p_i(\lambda_i) \approx 0$ when $\Delta_i(\lambda_i)/\lambda_i^{\frac{2}{\alpha}}$ is close to zero. Hence, in this case each transmitting node generates very limited interference at its nearest unintended receiver. Thus from (2.21), $\bar{\lambda}_\epsilon \gg \frac{-\ln(1-\epsilon)}{\beta^{\frac{2}{\alpha}} \mathbb{E}[D_0^2] \psi}$ due to small $p_i(\lambda_i)$. On the other hand, when transmitters hardly use DIAS, i.e. the case of $\Delta_i(\lambda_i)/\lambda_i^{\frac{2}{\alpha}} \gg 1$, we know $p_i(\lambda_i) \approx 1$ and thus $\bar{\lambda}_\epsilon = \Theta\left(\frac{-\ln(1-\epsilon)}{\mathbb{E}[D_0^2] \psi \beta^{\frac{2}{\alpha}}}\right)$. Intuitively, it is good to design $\Delta_i(\lambda_i)$ as a non-increasing function of λ_i in order to avoid transmitting in a heavy traffic context. For example, in a dense network, $\Delta_i(\lambda_i)$ should be designed as a monotonically decreasing function of λ_i such that $\lambda_i p_i(\lambda_i)$ decreases as λ_i increases since this improves the TC with increasing λ_i . In Figure

2.4, we present the TC of the DIAS scheme for different $\Delta_i(\lambda_i)$. As mentioned earlier, we observe that DIAS ($\Delta_i(\lambda_i) \neq 0$) outperforms No DIAS⁶. Also, $\Delta_i(\lambda_i) = 0.015\lambda_i^{-0.01}$ (a monotonically decreasing function of λ_i) results in a better TC as compared to a monotonically increasing $\Delta_i(\lambda_i)$. This is because $\Delta_i(\lambda_i) = 0.015\lambda_i^{-0.01}$ restricts the number of transmissions with increasing λ_i .

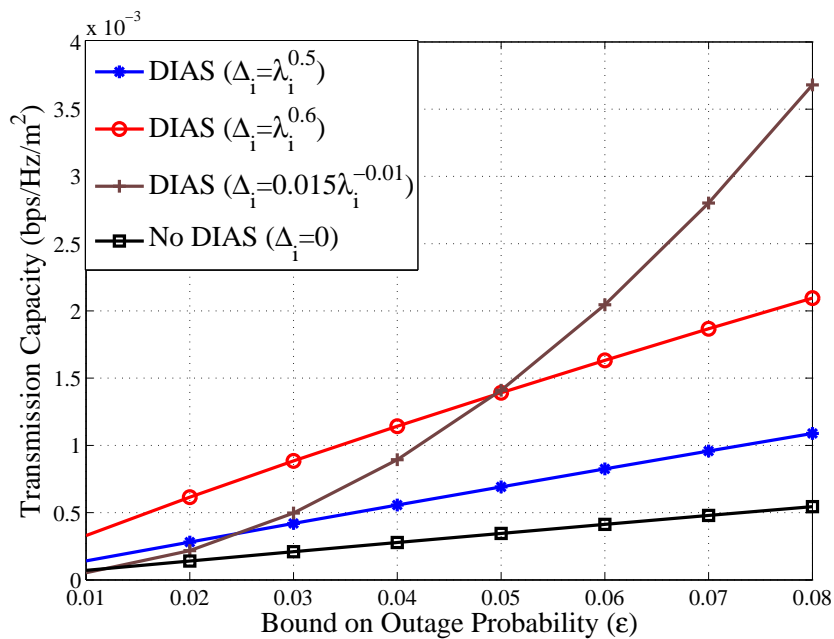


Figure 2.4: The simulation results of TC for the DIAS scheme with different $\Delta_i(\lambda_i)$.

The network parameters for simulation are: $\alpha = 4$, $\beta = 2$ and $D_0 = 8m$.

The above discussions indicate that threshold $\Delta_i(\lambda_i)$ can be designed as a function like $\Theta(\lambda_i^\delta)$ where $\delta \in \mathbb{R}$. Nonetheless, the following lemma shows that the

⁶No DIAS is the case that all transmitting nodes only use slotted Aloha to randomly access the shared link and thus their intensity still remain λ_t

upper and lower bounds on the maximum contention intensity are asymptotically tight for certain positive δ in sparse and dense networks.

Lemma 2.6.4. *If $\Delta_i(\lambda_i) = \Theta(\lambda_i^\delta)$ and $\delta \in \mathbb{R}$, then the asymptotic tightness of the bounds on TC in a sparse network can be summarized as follows*

$$\lim_{\lambda_t \rightarrow 0} \frac{\bar{\lambda}_i}{\underline{\lambda}_i} = \begin{cases} 2^{\frac{\alpha-2}{\alpha(\delta+1)-4}}, & \text{for } \delta \in (\frac{2}{\alpha}, \infty) \\ 2, & \text{otherwise} \end{cases}. \quad (2.23)$$

Nevertheless, if the network is dense, then the asymptotic tightness of the bounds on TC becomes

$$\lim_{\lambda_t \rightarrow \infty} \frac{\bar{\lambda}_i}{\underline{\lambda}_i} = \begin{cases} 2^{\frac{\alpha-2}{\alpha(\delta+1)-4}}, & \text{for } \delta \in (-\infty, \frac{2}{\alpha}) \\ 2, & \text{otherwise} \end{cases}. \quad (2.24)$$

Proof. We provide the proof for a sparse network. The other case follows in a similar way. Let $\delta \in (\frac{2}{\alpha}, \infty)$ which implies $\Delta_i(\lambda_i)/\lambda_i^{\frac{2}{\alpha}} \rightarrow 0$ as follow as $\lambda_i \rightarrow 0$. Note that $\lambda_t \rightarrow 0$ means $\lambda_i \rightarrow 0$. So transmission probability $p_i(\lambda_i)$ in (2.17) can be simplified as

$$p_i(\lambda_i) = \kappa [p_i(\lambda_i)]^{\frac{2}{\alpha}} \lambda_i^{\delta - \frac{2}{\alpha}} + O\left(p_i^{\frac{4}{\alpha}} \lambda_i^{2\delta - \frac{4}{\alpha}}\right) \text{ as } \lambda_t, \lambda_i \rightarrow 0,$$

where κ is a positive constant. It can be further simplified as

$$[p_i(\lambda_i)]^{1 - \frac{2}{\alpha}} = \kappa \lambda_i^{\delta - \frac{2}{\alpha}} + O\left(p_i^{\frac{2}{\alpha}} \lambda_i^{2\delta - \frac{4}{\alpha}}\right) \Rightarrow p_i(\lambda_i) = \Theta\left(\lambda_i^{\frac{\delta - 2/\alpha}{1 - 2/\alpha}}\right).$$

So it follows that $p_i(\lambda_i) \rightarrow 0$ as $\lambda_i \rightarrow 0$ since $\delta \in (\frac{2}{\alpha}, \infty)$. Substituting the above result into $\underline{q}(\lambda_i)$, then we have $\underline{q}(\lambda_i) = \beta^{\frac{2}{\alpha}} \psi \mathbb{E}[D_0^2] \lambda_i p_i(\lambda_i) + O(\lambda_i^2 p_i^2)$ and the upper bound on $\bar{\lambda}_\epsilon$ can be shown to be

$$\bar{\lambda}_i p_i(\bar{\lambda}_i) = \Theta\left(\frac{\epsilon}{\beta^{\frac{2}{\alpha}} \psi \mathbb{E}[D_0^2]}\right) \Rightarrow \bar{\lambda}_i = \Theta\left(\epsilon^{\frac{\alpha-2}{\alpha(\delta+1)-4}}\right).$$

Similarly, we can find $\underline{\lambda}_i$ as $\lambda_i \rightarrow 0$ and show that $(\bar{\lambda}_i/\underline{\lambda}_i) \rightarrow 2^{\frac{\alpha-2}{\alpha(\delta+1)-4}}$ as $\lambda_i \rightarrow 0$. When $\delta \leq \frac{2}{\alpha}$ and $\lambda_i \rightarrow 0$, $p_i(\lambda_i)$ approaches to a constant. Therefore, $(\bar{\lambda}_i/\underline{\lambda}_i) \rightarrow 2$ as $\lambda_i \rightarrow 0$. \square

Finally, there is one point that needs to be clarified. That is, although the DIAS scheme only eliminates some interference and does not avoid transmitting in deep fading, it does not follow that the TC achieved by DIAS is less than that achieved by DCAS. DIAS is particularly advantageous in dense networks since the interference to the unintended receivers can be better managed and thus efficiently increasing the TC.

2.7 Distributed Interferer-Channel-Aware Scheduling (DICAS)

DCAS schedules links that have good received signal power, while DIAS schedules link that cause minimal interference. Now consider the DICAS scheme that combines both the DIAS and the DCAS schemes. We first study the TC achieved by the DICAS scheme and a geometry-based perspective for DICAS without and with interference cancellation is provided.

2.7.1 Transmission Capacity achieved by DICAS

Transmitters in Π_t using the DICAS scheme form a thinning PPP Π_{ic} given by

$$\Pi_{ic} = \{X_j \in \Pi_t : T_j = \mathbf{1}(H_j D_j^{-\alpha} \geq \Delta_c(\lambda_{ic}), \tilde{H}_{j*} \tilde{D}_{j*}^{-\alpha} \leq \Delta_i(\lambda_{ic})), \forall j \in \mathbb{N}_+\}. \quad (2.25)$$

So the intensity of Π_{ic} is $\lambda_{ic} = \lambda_t p_{ic}(\lambda_{ic})$ where $p_{ic}(\lambda_{ic}) = p_c(\lambda_{ic}) p_i(\lambda_{ic})$. Bounds on the outage probability and TC are shown in the following theorem.

Theorem 2.7.1. *Let $\bar{q}(\lambda_{ic})$ and $\underline{q}(\lambda_{ic})$ denote the upper and lower bounds on the outage probability when DICAS scheme is used. Also let $\Delta_c(\lambda_{ic}) \in \mathbb{R}_+$ be a nondecreasing function of λ_{ic} , and $\Delta_i(\lambda_{ic}) \in \mathbb{R}_+$ a function of λ_{ic} . Then*

$$\underline{q}(\lambda_{ic}) = (1 - e^{-A_{ic}}) (1 - B_{ic}), \quad (2.26a)$$

$$\bar{q}(\lambda_{ic}) = \left[1 - \left(1 - \frac{(\alpha - 1)A_{ic}}{[(\alpha - 1) - A_{ic}]^2} \right)^+ e^{-A_{ic}} \right] (1 - B_{ic}), \quad (2.26b)$$

where $A_{ic} = \pi \lambda_{ic} \Gamma(1 + \frac{2}{\alpha}) \beta^{\frac{2}{\alpha}} [\Delta_c(\lambda_{ic})]^{-\frac{2}{\alpha}} p_i(\lambda_{ic}) = A_c(\lambda_{ic}) p_i(\lambda_{ic})$ and $B_{ic} = \mathbb{E}[\exp(-\lambda_{ic} \psi \beta^{\frac{2}{\alpha}} D_0^2 p_i(\lambda_{ic}))]$. Bounds on the maximum contention intensity for DICAS are given by

$$\underline{\lambda}_{ic} \leq \bar{\lambda}_\epsilon \leq \bar{\lambda}_{ic}, \quad (2.27)$$

where $\bar{\lambda}_{ic} = \sup\{\lambda_{ic} : \underline{q}(\lambda_{ic}) \leq \epsilon\}$, $\underline{\lambda}_{ic} = \sup\{\lambda_{ic} : \bar{q}(\lambda_{ic}) \leq \epsilon\}$.

Proof. See Appendix 2.9.5. □

The results in (2.26a) and (2.26b) should not surprise us since they look like the superimposed results of Theorems 2.5.1 and 2.6.2. The TC achieved by

DICAS is larger than that merely achieved by DCAS or DIAS. Since the two transmission thresholds, $\Delta_c(\lambda_{ic})$ and $\Delta_i(\lambda_{ic})$, both depend on λ_{ic} , they should be jointly designed to make DICAS increase TC in a more *efficient* way since arbitrarily choosing γ and δ could make A_{ic} and B_{ic} not decrease at the same time. For instance, suppose $\Delta_c(\lambda_{ic}) = \Theta(\lambda_{ic}^\gamma)$ and $\Delta_i(\lambda_{ic}) = \Theta(\lambda_{ic}^\delta)$ where $\gamma > 0$ and $\delta \in \mathbb{R}$. If the network is sparse and $\delta \in (\frac{2}{\alpha}, \infty)$, then $A_{ic} = \Theta\left(\lambda_{ic}^{\frac{\alpha(1+\delta)-2\gamma+4(\gamma/\alpha-1)}{\alpha-2}}\right)$ and $B_{ic} = \Theta\left(\lambda_{ic}^{\frac{\alpha(1+\delta)-4}{\alpha-2}}\right)$. When λ_{ic} decreases, the outage probability can be *efficiently* reduced if $\delta > \frac{2}{\alpha} + (\frac{2\gamma}{\alpha} - 1)(1 - \frac{2}{\alpha})$ (which is equivalent to $\gamma \in (0, \frac{\alpha}{2})$) because A_{ic} and B_{ic} both decrease in this case. So $\Delta_c(\lambda_{ic})$ and $\Delta_i(\lambda_{ic})$ can benefit each other to achieve a much lower outage probability. As a result, TC is increased efficiently under this circumstance. A simulation example of TC for the DICAS scheme is illustrated in Figure 2.5 and we can see that TC achieved by DICAS is much larger than those achieved by DCAS, DIAS and No DICAS⁷. The slope of the DICAS curve does not decrease along with ϵ , which means DCAS and DIAS indeed can benefit each other.

In addition, the following asymptotic tightness of bounds on TC can provide us some insight on how to design $\Delta_c(\lambda_{ic})$ and $\Delta_i(\lambda_{ic})$ for attaining tight bounds.

Lemma 2.7.2. *Assume $\Delta_c(\lambda_{ic}) = \Theta(\lambda_{ic}^\gamma)$ and $\Delta_i(\lambda_{ic}) = \Theta(\lambda_{ic}^\delta)$ where $\gamma > 0, \delta \in \mathbb{R}$. The asymptotic tightness of the bounds on TC in a sparse network is charac-*

⁷No DICAS has the same meaning as No DCAS in Figure 2.3 and No DIAS in Figure 2.4. That is, the transmitting nodes only use slotted Aloha to randomly access the shared channel and thus their intensity is still λ_t .

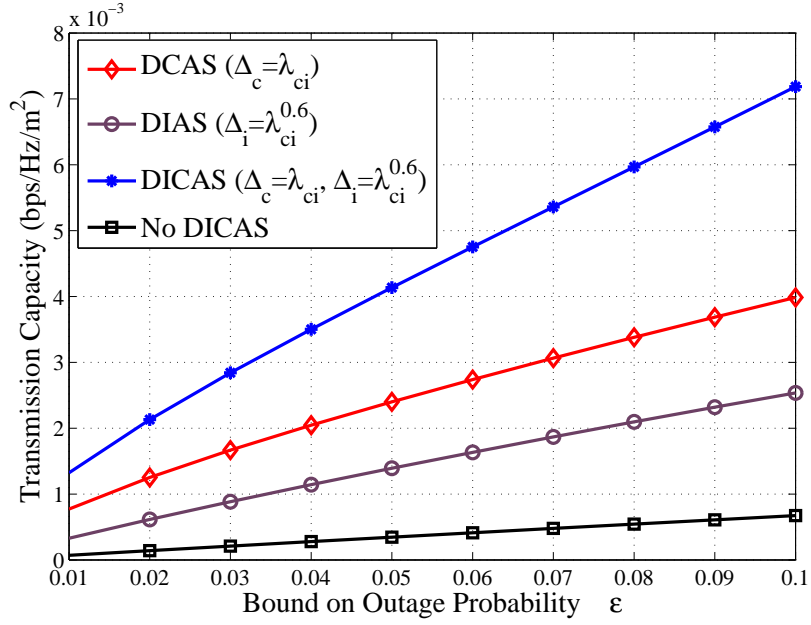


Figure 2.5: The simulation results of TC for the DCAS, DIAS and DICAS schemes. The network parameters for simulation are: $\alpha = 4$, $\beta = 2$, $D_0 = 8m$, $\Delta_c(\lambda_{ic}) = \lambda_{ic}$ and $\Delta_i(\lambda_{ic}) = \lambda_{ic}^{0.6}$.

terized as

$$\lim_{\lambda_{ic} \rightarrow 0} \frac{\bar{\lambda}_{ic}}{\underline{\lambda}_{ic}} = \begin{cases} \left(\frac{\alpha}{\alpha-1} \right)^{\frac{\alpha-2}{2\alpha \left[(\delta - \frac{2}{\alpha}) - (\frac{2}{\alpha}-1)(1-\frac{2}{\alpha}) \right]}}, & \text{for } \delta \in \left(\frac{2}{\alpha}, \infty \right) \text{ and } \gamma \in \left(0, \frac{\alpha}{2} \right) \\ 1, & \text{otherwise} \end{cases}. \quad (2.28)$$

When the network is dense,

$$\lim_{\lambda_{ic} \rightarrow \infty} \frac{\bar{\lambda}_{ic}}{\underline{\lambda}_{ic}} = \begin{cases} \left(\frac{\alpha}{\alpha-1} \right)^{\frac{\alpha-2}{2\alpha \left[(\frac{2}{\alpha} - \delta) - (1-\frac{2}{\alpha})(1-\frac{2}{\alpha}) \right]}}, & \text{for } \delta \in \left(-\infty, \frac{2}{\alpha} \right) \text{ and } \gamma \in \left(\frac{\alpha}{2}, \infty \right) \\ 1, & \text{otherwise} \end{cases}. \quad (2.29)$$

Proof. The proof is omitted since it is similar to the proofs of Lemmas 2.5.4 and

2.7.2 A Geometric Interpretation for the DICAS Scheme

We now provide more insight into the three DOS schemes by considering a geometric interpretation of the lower bounds on the outage probabilities. The Δ -level dominant interferer coverage \mathcal{C}_Δ of a receiver is defined as the region in which any single interferer can cause outage at the receiver with a channel gain bounded below by Δ . More precisely,

$$\mathcal{C}_\Delta \triangleq \left\{ X \in \mathbb{R}^2 : \frac{H_0 D_0^{-\alpha}}{\tilde{H}|X|^{-\alpha}} < \beta \mid H_0 D_0^{-\alpha} \geq \Delta > 0 \right\}. \quad (2.30)$$

If $\Delta = 0$, then \mathcal{C}_Δ reduces to \mathcal{C}_0 which is called dominant interferer coverage and has mean Lebesgue measure $\mu(\mathcal{C}_0) = \beta^{\frac{2}{\alpha}} \psi \mathbb{E}[D_0^2]$ as indicated in Proposition 2.8.2 in Appendix 2.8.2. Without any opportunistic scheme, i.e. when all the nodes transmit,

$$\begin{aligned} q(\lambda_t) &= 1 - \mathbb{E}[\exp(-\lambda_t \beta^{\frac{2}{\alpha}} \psi D_0^2)] \\ &\geq 1 - \exp(-\lambda_t \beta^{\frac{2}{\alpha}} \psi \mathbb{E}[D_0^2]) \\ &= 1 - \exp(-\lambda_t \mu(\mathcal{C}_0)). \end{aligned}$$

Hence, in this simple case, the lower bound on the outage probability is completely characterized by the dominant interferer coverage of a receiver.

Similarly, the low bound on the outage probability of the DICAS scheme can be characterized by $\mu(\mathcal{C}_{\Delta_c})$ as well. By using the Taylor's expansion of an exponential function, the lower bound in (2.26a) can be written as

$$\underline{q}(\lambda_{ic}) = (1 - e^{-A_{ic}}) \lambda_{ic} p_i(\lambda_{ic}) \mu(\mathcal{C}_0) + O(\lambda_{ic}^2 p_i^2). \quad (2.31)$$

According to Proposition 2.8.2 in Appendix 2.8.2, there exists a constant $\tilde{\eta}(\Delta) \in (0, 1)$ such that $\mu(\mathcal{C}_\Delta) = \tilde{\eta}(\Delta)\mu(\mathcal{C}_0)$ so that $\underline{q}(\lambda_{ic})$ can be rewritten as

$$\underline{q}(\lambda_{ic}) = \eta(\lambda_{ic})\lambda_{ic}p_i(\lambda_{ic})\mu(\mathcal{C}_{\Delta_c}) + O(\lambda_{ic}^2p_i^2), \quad \eta(\cdot) \in (0, 1).$$

So in a sparse network, $\underline{q}(\lambda_{ic})$ scales with $\lambda_{ic}p_i(\lambda_{ic})\mu(\mathcal{C}_{\Delta_c})$ which is the average number of interferers in \mathcal{C}_{Δ_c} . By inspecting the above equation, the lower bounds on the outage probabilities in Theorems 2.5.1-2.6.2 also have a smaller dominant interferer coverage compared with \mathcal{C}_0 . For example, the lower bound on the outage probability of the DIAS scheme is

$$\underline{q}(\lambda_i) = 1 - \exp(-\lambda_i p_i(\lambda_i)\mu(\mathcal{C}_0)) = \lambda_i p_i(\lambda_i)\mu(\mathcal{C}_0) + O(\lambda_i^2 p_i^2).$$

Thus we observe that the dominate interferer coverage with DIAS is reduced by $p_i(\lambda_i)$ -fold compared to that without DIAS. In other words, the proposed three DOS schemes are able to *reduce* the dominant interferer coverage of a receiver such that the average number of dominant interferers decreases. An alternative interpretation is that the the dominant interferer coverage remains unchanged but the intensity reduces. According to the conservation property in Proposition 2.8.1, the decrease in the intensity can be alternatively interpreted as interferers moving away from a receiver, thus effectively reducing the number of dominant interferers. We now study interference cancellation in conjunction with the DICAS scheme using the concept of Δ -level dominant interferer coverage.

2.7.3 DICAS with Geometry-based Interference Cancellation

The DICAS scheme can be further improved by interference cancellation at the receiver side. If a receiver is able to first decode its nearby strong interferers,

then interference generated by the interferers can be subtracted out of the received signal and thus a larger SIR can be obtained. From a geometric point of view, the *interference cancellation coverage* of a receiver for DICAS can be defined as follows

$$\mathcal{C}_{ic}^c \triangleq \left\{ X \in \mathbb{R}^2 : \frac{\tilde{H}|X|^{-\alpha}}{I_0 - \tilde{H}|X|^{-\alpha} + H_0 D_0^{-\alpha}} \geq \beta \middle| H_0 D_0^{-\alpha} > \Delta_c(\lambda_{ic}) \right\}. \quad (2.32)$$

Observe that any interferer in the set \mathcal{C}_{ic}^c can be decoded by the typical receiver at the origin and hence any interferer in the coverage \mathcal{C}_{ic}^c can be canceled. Note that I_0 in (2.32) consists of the transmitters whose interference channel gain at their nearest unintended receiver is lower than threshold $\Delta_i(\lambda_{ic})$. Hence, $\Pi_{ic}^c \triangleq \Pi_{ic} \cap \mathcal{C}_{ic}^c$ can be viewed as the (nonhomogeneous) PPP consisting of the transmitters that are *cancelable*, and $\Pi_{ic}^{nc} \triangleq \Pi_{ic} \setminus \Pi_{ic}^c$ is the *noncancelable* part of Π_{ic} and its intensity at location X can be shown to be

$$\lambda_{ic}^{nc}(|X|) = \lambda_{ic} \mathbb{P} \left[\frac{\tilde{H}|X|^{-\alpha}}{I_0 + H_0 D_0^{-\alpha}} < \frac{\beta}{1 + \beta} \middle| H_0 D_0^{-\alpha} \geq \Delta_c(\lambda_{ic}) \right]. \quad (2.33)$$

Hence the residual interference at the receiver Y_0 (after partial interference is canceled) is

$$I_0^{nc} = \sum_{X_j \in \Pi_{ic}^{nc} \setminus X_0} \tilde{H}_j |X_j|^{-\alpha}. \quad (2.34)$$

The outage probability is given by $q(\lambda_{ic}) = \mathbb{P} \left[\frac{H_0 D_0^{-\alpha}}{I_0^{nc}} < \beta \middle| H_0 D_0^{-\alpha} \geq \Delta_c(\lambda_{ic}) \right]$. The following theorem provides bounds on the outage probability for DICAS with interference cancellation.

Theorem 2.7.3. *Consider a network where the transmissions are scheduled using the DICAS scheme. Also, if the receivers are able to completely cancel all*

interferers in their respective interference cancellation coverage C_{ic}^c sets, then the lower and the upper bound on the outage probability are given by

$$\underline{q}(\lambda_{ic}) = \left(1 - e^{-\hat{A}_{ic}}\right) \left(1 - \hat{B}_{ic}\right), \quad (2.35a)$$

$$\bar{q}(\lambda_{ic}) = \left(1 - \frac{(\alpha - 1)\hat{A}_{ic}}{[(\alpha - 1) - \hat{A}_{ic}]^2} e^{-\hat{A}_{ic}}\right)^+ \left(1 - \hat{B}_{ic}\right), \quad (2.35b)$$

where \hat{A}_{ic} and \hat{B}_{ic} equal:

$$\begin{aligned} \hat{A}_{ic} &= \pi\Gamma\left(1 + \frac{2}{\alpha}\right) \beta^{\frac{2}{\alpha}} [\Delta_c(\lambda_{ic})]^{-\frac{2}{\alpha}} p_i(\lambda_{ic}) \left[\lambda_{ic} - \mathcal{G}\left(\lambda_{ic}^c; \frac{2}{\alpha}\right)\right] \\ &= A_{ic} \left[1 - \frac{1}{\lambda_{ic}} \mathcal{G}\left(\lambda_{ic}^c; \frac{2}{\alpha}\right)\right], \\ \hat{B}_{ic} &= \mathbb{E} \left[\exp \left(-p_i(\lambda_{ic}) \beta^{\frac{2}{\alpha}} \psi D_0^2 \left(\lambda_{ic} - \mathcal{B}\left(\lambda_{ic}^c; \frac{\alpha}{2}, 1 - \frac{2}{\alpha}\right) \right) \right) \right]. \end{aligned}$$

$p_i(\cdot)$ is defined in (2.17) and

$$\lambda_{ic}^c(r) = \lambda_{ic} \exp \left(-\pi\psi\tilde{\beta}^{\frac{2}{\alpha}} r^2 \lambda_{ic} p_i(\lambda_{ic}) - \beta\Delta_c(\lambda_{ic})r^\alpha \right) \mathbb{E} \left[\frac{D_0^\alpha}{D_0^\alpha + \tilde{\beta}r^\alpha} \right], \quad (2.36)$$

where $\tilde{\beta} = \frac{\beta}{1+\beta}$. Also, $\mathcal{G}(\lambda_{ic}^c; x)$ and $\mathcal{B}(\lambda_{ic}^c; x, y)$ are called Gamma and Beta mean functional and defined in the following:

$$\mathcal{G}(\lambda_{ic}^c; x) \triangleq \frac{1}{\Gamma(x)} \int_0^\infty \lambda_{ic}^c \left(\sqrt[\alpha]{\beta u / \Delta_c(\lambda_{ic})} \right) u^{x-1} e^{-u} du, \quad (2.37)$$

$$\mathcal{B}(\lambda_{ic}^c; x, y) \triangleq \frac{\Gamma(x+y)}{\Gamma(x)\Gamma(y)} \int_0^\infty \lambda_{ic}^c \left(D_0 \sqrt[\alpha]{\beta t} \right) \frac{t^{x-1}}{(1+t)^{x+y}} dt. \quad (2.38)$$

Obviously, if $\lambda_{ic}^c(\cdot)$ is equal to a constant κ , then we have $\mathcal{G}(\kappa; x) = \mathcal{B}(\kappa; x, y) = \kappa$.

Proof. See Appendix 2.9.6. □

Remark 2.7.4. Observe that $\mathcal{G}(\lambda_{ic}^c; x)$ in (2.37) is deterministic and $\mathcal{B}(\lambda_{ic}^c; x, y)$ in (2.38) is random because it depends on the link distance D_0 which is random.

Moreover,

$$\begin{aligned}\lambda_{ic}^c \left(\sqrt[\alpha]{\beta u / \Delta_c(\lambda_{ic})} \right) &= \lambda_{ic} \exp \left(-\pi \psi(\beta \beta u / \Delta_c(\lambda_{ic}))^{\frac{2}{\alpha}} \lambda_{ic} p_i(\lambda_{ic}) - \beta^2 u \right), \\ \lambda_{ic}^c \left(D_0 \sqrt[\alpha]{\beta t} \right) &= \frac{\lambda_{ic}}{1 + \tilde{\beta} \beta t} \exp \left(-\pi \psi(\tilde{\beta} \beta t)^{\frac{2}{\alpha}} D_0^2 \lambda_{ic} p_i(\lambda_{ic}) - \beta^2 \Delta_c(\lambda_{ic}) D_0^\alpha t \right).\end{aligned}$$

Theorem 2.7.3 indicates that geometry-based interference cancellation can increase TC since bounds on the outage probability are reduced when compared with the results in Theorem 2.7.1. For example, A_{ic} is reduced to \hat{A}_{ic} because we have

$$\hat{A}_{ic} = A_{ic} \left[1 - \frac{\mathcal{G}(\lambda_{ic}^c; \frac{2}{\alpha})}{\lambda_{ic}} \right]$$

and $\mathcal{G}(\lambda_{ic}^c; \frac{2}{\alpha}) / \lambda_{ic} < 1$. Thus $\frac{A_{ic}}{\lambda_{ic}} \mathcal{G}(\lambda_{ic}^c; \frac{2}{\alpha})$ can be interpreted as the average number of the cancellable interferers in coverage \mathcal{C}_{ic}^c that generate interference at the typical receiver which is no less than $\Delta_c(\lambda_{ic}) / \beta$. Similarly, for a given D_0 , $\frac{\mu(\mathcal{C}_{\Delta_c})}{\lambda_{ic}} \mathcal{B}(\lambda_{ic}^c; \frac{2}{\alpha}, 1 - \frac{2}{\alpha})$ can be viewed as the average number of the cancelable interferers in the Δ_c -level dominant interferer coverage \mathcal{C}_{Δ_c} . However, the effect of interference cancellation could become marginal if threshold $\Delta_c(\lambda_{ic})$ is large. Since we know $\lambda_{ic}^c \rightarrow 0$ as $\Delta_c(\lambda_{ic}) \rightarrow \infty$, this leads to $\hat{A}_{ic} \uparrow A_{ic}$ and $\hat{B}_{ic} \uparrow B_{ic}$. This observation indicates that the bounds on the outage probability in Theorem 2.7.3 may just reduce a little if compared to those in Theorem 2.7.1. The intuition behind this phenomenon is that increasing $\Delta_c(\lambda_{ic})$ reduces interference but increases the desired signal power so that decoding strong interference might become difficult while there is not much interference cancellation. Furthermore, we observe that small $p_i(\lambda_{ic})$ and large $\Delta_c(\lambda_{ic})$ weaken the effect of interference cancellation. This is because $p_i(\lambda_{ic})$ is the transmission probability for DIAS and small $p_i(\lambda_{ic})$ can make receivers get rid of strong interferers and large $\Delta_c(\lambda_{ic})$

makes decoding interference difficult. Thus, interference cancellation does not help reduce too much interference in this case. However, interference cancellation can be an auxiliary role for DICAS if two thresholds $\Delta_c(\lambda_{ic})$ and $\Delta_i(\lambda_{ic})$ are not designed properly to optimally benefit each other.

The results in Theorem 2.7.3 can reduce to the cases of the DCAS and DIAS schemes. Note that $\mathcal{G}(\lambda_{ic}^c; x)$ depends on $p_i(\lambda_{ic})$ and $\Delta_c(\lambda_{ic})$, and $\mathcal{B}(\lambda_{ic}^c; x)$ only depends on $p_i(\lambda_{ic})$. Thus, DCAS only affects $\mathcal{G}(\lambda_{ic}^c; x)$, but DIAS affects both $\mathcal{G}(\lambda_{ic}^c; x)$ and $\mathcal{B}(\lambda_{ic}^c; x)$. So if we let $p_i(\lambda_{ic}) = 1$ then the results in Theorem 2.7.3 reduce to the results of DCAS with geometry-based interference cancellation as shown in the following.

Corollary 2.7.5. *In a DCAS network, the interference cancellation coverage \mathcal{C}_c^c can be defined as (2.32) with intensity λ_c . If receivers are able to completely cancel all interferers in their respective coverage \mathcal{C}_c^c sets, then*

$$\bar{q}(\lambda_c) = (1 - e^{-\hat{A}_c}) (1 - \hat{B}_c), \quad (2.39a)$$

$$\underline{q}(\lambda_c) = \left[1 - \left(1 - \frac{(\alpha - 1)\hat{A}_c}{[(\alpha - 1) - \hat{A}_c]^2} \right)^+ e^{-\hat{A}_c} \right] (1 - \hat{B}_c), \quad (2.39b)$$

where $\hat{A}_c = \frac{A_c}{\lambda_c} (\lambda_c - \mathcal{G}(\lambda_c^c; \frac{2}{\alpha}))$ and $\hat{B}_c = \mathbb{E}[\exp(-\beta^{\frac{2}{\alpha}} \psi D_0^2 (\lambda_c - \mathcal{B}(\lambda_c^c; \frac{2}{\alpha}, 1 - \frac{2}{\alpha})))]$.

λ_c^c is the intensity of the cancelable PPP Π_c^c , which is given by

$$\lambda_c^c(r) = \lambda_c \exp\left(-\pi\psi\lambda_c\tilde{\beta}^{\frac{2}{\alpha}}r^2 - \tilde{\beta}r^\alpha\Delta_c(\lambda_c)\right) \mathbb{E}\left[\frac{D_0^\alpha}{D_0^\alpha + \tilde{\beta}r^\alpha}\right], \quad r \in \mathbb{R}_+, \quad (2.40)$$

Proof. The proof is similar to the first part in the proof of Theorem 2.7.3 and thus omitted. \square

It can be easily observed that \hat{A}_c and \hat{B}_c are respectively smaller than A_c and B_c due to interference cancellation. Similarly, if $\Delta_c = 0$ and $p_i \neq 0$, then the results in Theorem 2.7.3 can be shown to transform to the following corollary.

Corollary 2.7.6. *In a DIAS network, the interference cancellation coverage \mathcal{C}_i^c can be defined as (2.32) with intensity λ_i and $\Delta_c = 0$. If receivers are able to completely cancel all interferers in their respective interference cancellation coverage \mathcal{C}_i^c sets, then*

$$\begin{aligned}\underline{q}(\lambda_i) &= 1 - \exp\left(-\lambda_i p_i(\lambda_i) \beta^{\frac{2}{\alpha}} \psi \mathbb{E}\left[D_0^2 \left(1 - \mathcal{B}\left(h(t); \frac{2}{\alpha}, \frac{\alpha-2}{\alpha}\right)\right)\right]\right), \\ \bar{q}(\lambda_i) &= 1 - \exp\left(-2\lambda_i p_i(\lambda_i) \beta^{\frac{2}{\alpha}} \psi \mathbb{E}\left[D_0^2 \left(1 - \mathcal{B}\left(h(t); \frac{2}{\alpha}, \frac{\alpha-2}{\alpha}\right)\right)\right]\right),\end{aligned}$$

where $h(t)$ is given by

$$h(t) = \left(\frac{1}{1 + t\tilde{\beta}\beta}\right) \exp\left(-\pi\psi(\tilde{\beta}\beta t)^{\frac{2}{\alpha}} D_0^2 \lambda_i\right).$$

Proof. The proof is similar to the second part in the proof of Theorem 2.7.1. \square

Corollary 2.7.6 reveals that interference cancellation for DIAS can be viewed as reducing the dominant interferer coverage of a receiver or removing the cancelable part of $\lambda_i p_i(\lambda_i)$. For a given D_0 , $1 - \mathcal{B}(h(t); \frac{2}{\alpha}, 1 - \frac{2}{\alpha})$ can be interpreted as the noncancelable fraction of intensity $\lambda_i p_i(\lambda_i)$ or the area of the dominant interferer coverage (i.e. $\mu(\mathcal{C}_0)$) is reduced by $(1 - \mathcal{B}(h(t); \frac{2}{\alpha}, 1 - \frac{2}{\alpha}))$ -fold. That means, the larger \mathcal{B} , the more interference cancelled. So $h(t)$ should be larger in order to cancel more interference. Reducing the intensity can increase $h(t)$ so that the efficacy of interference cancellation in a sparse network is much better than in a dense network. This makes sense because the mean area

of the interference cancellation coverage is very large due to small I_0 and more (cancelable) interferers are enclosed in the coverage.

2.8 Appendix I : Useful Propositions

2.8.1 The Conservation Property of a Homogeneous PPP

Proposition 2.8.1. *Let $\mathbf{T} : \mathbb{R}^{d_1} \rightarrow \mathbb{R}^{d_2}$ be a linear map from dimension d_1 to dimension d_2 , and it is represented by a non-singular transformation matrix. If Π is a homogeneous PPP of intensity λ , then $\mathbf{T}(\Pi) \triangleq \{\mathbf{T}X_i : X_i \in \Pi\}$ is also a homogeneous PPP and its intensity is $\lambda/\sqrt{\det(\mathbf{T}^\top\mathbf{T})}$. Specifically, if $d_1 = d_2 = 2$ and $\mathbf{T} = \sqrt{\kappa}\mathbf{I}_2$ where \mathbf{I}_2 is a 2×2 identity matrix and $\kappa > 0$, then the intensity of $\mathbf{T}(\Pi)$ changes to λ/κ .*

Proof. The conservation property of a homogeneous PPP for the case of $d_1 = d_2$ can be found in [57]. However, its formal proof is missing. For the convenience of reading this chapter, we here provide a complete proof of a more general case of $d_1 \neq d_2$. The void probability of a point process in a bounded Borel set $\mathcal{A} \subset \mathbb{R}^{d_1}$ is the probability that \mathcal{A} does not contain any points of the process. Since Π is a homogeneous PPP, its void probability is given by

$$\mathbb{P}[\Pi(\mathcal{A}) = 0] = \exp(-\lambda\mu_{d_1}(\mathcal{A})), \quad (2.42)$$

where $\mu_{d_1}(\cdot)$ is a d_1 -dimensional Lebesgue measure. Since the void probability completely characterizes the statistics of a PPP, we only need to show the void probability of $\mathbf{T}[\Pi(\mathcal{A})]$ is given by

$$\mathbb{P}[\mathbf{T}(\Pi(\mathcal{A})) = 0] = \exp\left(-\lambda/\sqrt{\det(\mathbf{T}^\top\mathbf{T})}\mu_{d_2}(\mathbf{T}(\mathcal{A}))\right). \quad (2.43)$$

Recall the result from vector calculus that the absolute value of the determinant of real vectors is equal to the volume of the parallelepiped spanned by those vectors. Therefore, the d_2 -dimensional volume of $\mathbf{T}(\mathcal{A})$, $\mu_{d_2}(\mathbf{T}(\mathcal{A}))$, is given by $\sqrt{\det(\mathbf{T}^\top \mathbf{T})} \mu_{d_1}(\mathcal{A})$. Suppose $\mathbf{T}(\Pi)$ has intensity λ^\dagger and its void probability within the volume of $\mathbf{T}(\mathcal{A})$ is

$$\mathbb{P}[\mathbf{T}(\Pi(\mathcal{A})) = 0] = \mathbb{P}[\Pi(\mathcal{A}) = 0] = \exp\left(-\lambda^\dagger \sqrt{\det(\mathbf{T}^\top \mathbf{T})} \mu_{d_1}(\mathcal{A})\right).$$

Then comparing the above equation with (2.43), it follows that $\lambda^\dagger = \frac{\lambda}{\sqrt{\det(\mathbf{T}^\top \mathbf{T})}}$. \square

2.8.2 The Mean Lebesgue Measure of the Δ -level Dominant Interferer Coverage of a Receiver

Proposition 2.8.2. *Suppose the received signal at the reference receiver is greater than or equal to $\Delta \in \mathbb{R}_+$. The Δ -level interferer coverage of the reference receiver is defined as*

$$\mathcal{C}_\Delta \triangleq \left\{ X \in \mathbb{R}^2 : \frac{H_0 D_0^{-\alpha}}{\tilde{H} |X|^{-\alpha}} < \beta \mid H_0 D_0^{-\alpha} \geq \Delta \right\}, \quad (2.44)$$

where $\{H_0, \tilde{H}\}$ are i.i.d. exponential random variables with unit mean and variance and $D > 1$ is also a random variable independent of $\{H_0, \tilde{H}\}$. For given \tilde{H} , H_0 and D_0 , \mathcal{C}_Δ is the region in which any single interferer is able to cause outage at the reference receiver whose received signal is greater than or equal to Δ . The mean Lebesgue measure of \mathcal{C}_Δ denoted by $\mu(\mathcal{C}_\Delta)$ can be shown as

$$\mu(\mathcal{C}_\Delta) = \beta^{\frac{2}{\alpha}} \psi \mathbb{E} \left[D_0^2 \mathcal{B} \left(e^{-\Delta D_0^{\alpha t}}, \frac{2}{\alpha}, 1 - \frac{2}{\alpha} \right) \right], \quad (2.45)$$

where $\psi = \pi \Gamma\left(1 + \frac{2}{\alpha}\right) \Gamma\left(1 - \frac{2}{\alpha}\right)$ and $\mathcal{B}(\cdot; x, y)$ is the Beta mean functional as defined in (2.38). If $\Delta = 0$, then $\mathcal{B}\left(1; \frac{2}{\alpha}, 1 - \frac{2}{\alpha}\right) = 1$ and $\mu(\mathcal{C}_\Delta) = \mu(\mathcal{C}_0) = \beta^{\frac{2}{\alpha}} \psi \mathbb{E}[D_0^2]$. Also, if $\Delta \neq 0$, there exists a $\eta(\Delta) \in (0, 1)$ which is a monotonically decreasing function of Δ such that

$$\mu(\mathcal{C}_\Delta) = \eta(\Delta) \mu(\mathcal{C}_0). \quad (2.46)$$

Proof. Since \mathcal{C}_Δ is a bounded set for given \tilde{H} , H_0 and D_0 , its mean Lebesgue measure is finite and found as follows:

$$\begin{aligned} \mu(\mathcal{C}_\Delta) &= \mathbb{E} \left[\int_{\mathbb{R}^2} \mathbf{1} \left(\frac{H_0 D_0^{-\alpha}}{\tilde{H} |X|^{-\alpha}} < \beta \mid H_0 D_0^{-\alpha} \geq \Delta \right) \mu(dX) \right] \\ &= \int_{\mathbb{R}^2} \mathbb{P} \left[H_0 D_0^{-\alpha} < \tilde{H} |X|^{-\alpha} \beta \mid H_0 D_0^{-\alpha} \geq \Delta \right] \mu(dX) \\ &= \int_{\mathbb{R}^2} \frac{\mathbb{P}[\tilde{H} |X|^{-\alpha} \beta > \Delta]}{\mathbb{P}[H_0 D_0^{-\alpha} > \Delta]} (\mathbb{P}[H_0 D_0^{-\alpha} \leq \max\{\tilde{H} |X|^{-\alpha} \beta, \Delta\}] \\ &\quad - \mathbb{P}[H_0 D_0^{-\alpha} \leq \Delta]) \mu(dX) \\ &= \int_{\mathbb{R}^2} \mathbb{P}[\tilde{H} |X|^{-\alpha} \beta > \Delta] \mathbb{P}[H_0 D_0^{-\alpha} < \tilde{H} |X|^{-\alpha} \beta] \mu(dX) \\ &= \frac{2\pi}{\alpha} \beta^{\frac{2}{\alpha}} \mathbb{E} \left[D_0^2 \int_0^\infty \frac{t^{\frac{2}{\alpha}-1}}{(1+t)e^{\Delta D_0^\alpha t}} dt \right] \\ &= \beta^{\frac{2}{\alpha}} \psi \mathbb{E} \left[D_0^2 \mathcal{B} \left(e^{-\Delta D_0^\alpha t}; \frac{2}{\alpha}, 1 - \frac{2}{\alpha} \right) \right]. \end{aligned}$$

So if $\Delta = 0$, then it follows that $\mu(\mathcal{C}_\Delta) = \mu(\mathcal{C}_0) = \frac{2\pi}{\alpha} \beta^{\frac{2}{\alpha}} \mathbb{E}[D_0^2] \int_0^\infty \frac{t^{\frac{2}{\alpha}-1}}{1+t} dt$. Since the integral $\int_0^\infty \frac{t^{\frac{2}{\alpha}-1}}{1+t} dt$ is equal to $\Gamma\left(\frac{2}{\alpha}\right) \Gamma\left(1 - \frac{2}{\alpha}\right)$. Thus, $\mu(\mathcal{C}_0) = \beta^{\frac{2}{\alpha}} \psi \mathbb{E}[D_0^2]$.

Using the assumption $D_0 \geq 1$, the upper bound on $\mu(\mathcal{C}_\Delta)$ is given by

$$\mu(\mathcal{C}_\Delta) \leq \beta^{\frac{2}{\alpha}} \psi \mathbb{E}[D_0^2] \mathcal{B} \left(e^{-\Delta t}; \frac{2}{\alpha}, 1 - \frac{2}{\alpha} \right) = \mathcal{B} \left(e^{-\Delta t}; \frac{2}{\alpha}, 1 - \frac{2}{\alpha} \right) \mu(\mathcal{C}_0),$$

and the lower bound on $\mu(\mathcal{C}_\Delta)$ can be shown as follows as

$$\begin{aligned}
\mu(\mathcal{C}_\Delta) &= \frac{2\pi}{\alpha} \beta_{\frac{2}{\alpha}} \mathbb{E} \left[D_0^2 \int_0^\infty \frac{u^{\frac{2}{\alpha}-1}}{(1+u)e^{\Delta D_0^\alpha u}} du \right] \\
&= \frac{2\pi}{\alpha} \beta_{\frac{2}{\alpha}} \mathbb{E} \left[\int_0^\infty \frac{t^{\frac{2}{\alpha}-1} D_0^\alpha}{(D_0^\alpha + t)e^{\Delta t}} dt \right] \\
&\geq \frac{2\pi}{\alpha} \beta_{\frac{2}{\alpha}} \int_0^\infty \frac{t^{\frac{2}{\alpha}-1}}{(1+t)e^{\Delta t}} dt \\
&= \mathcal{B} \left(e^{-\Delta t}; \frac{2}{\alpha}, 1 - \frac{2}{\alpha} \right) \frac{\mu(\mathcal{C}_0)}{\mathbb{E}[D_0^2]}.
\end{aligned}$$

Since $\mathcal{B}(e^{-\Delta t}; x, y) \leq 1$ for all $x, y > 0$ and $\mathbb{E}[D_0^2] \geq 1$, there exists a constant $\eta(\Delta) \in (0, 1)$ depending on $\Delta \neq 0$ such that $\mu(\mathcal{C}_\Delta) = \eta(\Delta)\mu(\mathcal{C}_0)$. \square

2.9 Appendix II : Proofs of Lemmas and Theorems

2.9.1 Proof of Theorem 2.4.1

Let $\hat{\Pi}_n(x) \triangleq \{X_j \in \Pi_n : \tilde{H}_j |X_j|^{-\alpha} \geq x, \forall j \in \mathbb{N}_+\}$. So each point node in $\hat{\Pi}_n$ can generate a shot noise at the origin which is greater than or equal to $x \in \mathbb{R}_+$. Let $\mathcal{C}_{\hat{\Pi}_n}(x) \triangleq \{X \in \mathbb{R}^2 : \tilde{H} |X|^{-\alpha} \geq x\}$ and it is the coverage of $\hat{\Pi}_n(x)$. The probability that there is at least one point node in $\Pi_n(x) \cap \mathcal{C}_{\hat{\Pi}_n}(x)$ is equal to the probability of $\Pi_n(x) \cap \mathcal{C}_{\hat{\Pi}_n}(x) \neq \emptyset$, and thus it is calculated as follows

$$\begin{aligned}
\mathbb{P} [\Pi_n(x) \cap \mathcal{C}_{\hat{\Pi}_n}(x) \neq \emptyset] &= 1 - \exp \left(- \int_{\mathbb{R}^2} \lambda_n(|X|) \mathbb{P}[\tilde{H} |X|^{-\alpha} \geq x] \mu(dX) \right) \\
&= 1 - \exp \left(-2\pi \int_0^\infty \lambda_n(r) r e^{-r^\alpha x} dr \right) \\
&= 1 - \exp \left(-\frac{2\pi}{\alpha x^{\frac{2}{\alpha}}} \int_0^\infty \lambda_n \left(\sqrt[\alpha]{\frac{u}{x}} \right) u^{\frac{2}{\alpha}-1} e^{-u} du \right) \\
&= 1 - \exp(-A(x)).
\end{aligned}$$

Since $F_{\hat{I}_n}^c(x)$ is greater than or equal to the CCDF of the shot-noise \hat{I}_n generated by $\hat{\Pi}_n(x)$, the probability of $(\Pi_n(x) \cap \mathcal{C}_{\hat{\Pi}_n}(x) \neq \emptyset)$ is equal to $\mathbb{P}[\hat{I}_n \geq x]$ and thus it is bounded above by $F_{\hat{I}_n}^c(x)$. Therefore, $\mathbb{P}[\Pi_n(x) \cap \mathcal{C}_{\hat{\Pi}_n}(x) \neq \emptyset]$ is a lower bound of $F_{\hat{I}_n}^c(x)$.

Suppose the complement of $\mathcal{C}_{\hat{\Pi}_n}(x)$ is $\mathcal{C}_{\hat{\Pi}_n}^c(x) = \mathbb{R}^2 \setminus \mathcal{C}_{\hat{\Pi}_n}(x)$ and \tilde{I}_n is the shot-noise process generated by $\Pi_n \cap \mathcal{C}_{\hat{\Pi}_n}^c(x)$. $F_{\hat{I}_n}^c(x)$ is upper bounded by $\mathbb{P}[\hat{I}_n \geq x, \tilde{I}_n \geq x]$ which is found in the following:

$$\begin{aligned} \mathbb{P}[\hat{I}_n \geq x, \tilde{I}_n \geq x] &= \mathbb{P}[\hat{I}_n \geq x] + \mathbb{P}[\tilde{I}_n \geq x] - \mathbb{P}[\hat{I}_n \geq x]\mathbb{P}[\tilde{I}_n \geq x] \\ &= 1 - \left(1 - F_{\hat{I}_n}^c(x)\right) e^{-A(x)}. \end{aligned} \quad (2.47)$$

The variance of \tilde{I}_n can be found and upper bounded as follows

$$\begin{aligned} \text{Var}(\tilde{I}_n) &= 2\pi \int_0^\infty r^{1-2\alpha} \lambda_n(r) \mathbb{P}[\tilde{H} < r^\alpha x] dr \\ &= 2\pi \int_0^\infty r^{1-2\alpha} \lambda_n(r) e^{-xr^\alpha} (e^{xr^\alpha} - 1) dr \\ &\leq \frac{2\pi}{\alpha - 1} x^2 \int_0^\infty r \lambda_n(r) e^{-xr^\alpha} dr \\ &= \frac{x^2}{\alpha - 1} A(x). \end{aligned}$$

Similarly the mean of \tilde{I}_n can be upper bounded as $\mathbb{E}[\tilde{I}_n] \leq x \frac{A(x)}{\alpha - 1}$. Then using Chebyshev's inequality, the upper bound on the CCDF of \tilde{I}_n is found as follows

$$F_{\tilde{I}_n}^c(x) \leq \frac{\text{Var}(\tilde{I}_n)}{\left(x - \mathbb{E}[\tilde{I}_n]\right)^2} \leq \frac{(\alpha - 1)A(x)}{[(\alpha - 1) - A(x)]^2}.$$

Substituting the above result into (2.48), the upper bound in (2.5) can be attained.

2.9.2 Proof of Theorem 2.5.1

The maximum contention intensity for DCAS is given by

$$\bar{\lambda}_\epsilon = \sup\{\lambda_c : q(\lambda_c) \leq \epsilon\},$$

where $q(\lambda_c) = \mathbb{P}[\text{SIR}(\lambda_c) < \beta | H_0 D_0^{-\alpha} \geq \Delta_c(\lambda_c)]$ is the outage probability with DCAS. For Rayleigh fading, the lower bound on $q(\lambda_c)$ can be found as

$$\begin{aligned} q(\lambda_c) &= \mathbb{P}[\Delta_c(\lambda_c) \leq H_0 D_0^{-\alpha} < I_0 \beta] \frac{\mathbb{P}[I_0 \beta > \Delta_c(\lambda_c)]}{\mathbb{P}[H_0 D_0^{-\alpha} > \Delta_c(\lambda_c)]} \\ &= (\mathbb{P}[H_0 D_0^{-\alpha} \leq \max\{I_0 \beta, \Delta_c(\lambda_c)\}] - \mathbb{P}[H_0 D_0^{-\alpha} \leq \Delta_c(\lambda_c)]) \\ &\quad \cdot \frac{\mathbb{P}[I_0 \beta > \Delta_c(\lambda_c)]}{\mathbb{P}[H_0 D_0^{-\alpha} > \Delta_c(\lambda_c)]} \\ &= \mathbb{P}[I_0 \beta > \Delta_c(\lambda_c)] \mathbb{P}[H_0 D_0^{-\alpha} < \beta I_0] \\ &\stackrel{(a)}{=} \mathbb{P}[I_0 > \Delta_c(\lambda_c)/\beta] \left\{ 1 - \mathbb{E} \left[\exp \left(-\beta^{\frac{2}{\alpha}} \psi \lambda_c D_0^2 \right) \right] \right\} \\ &\stackrel{(b)}{\geq} (1 - e^{-A_c}) (1 - B_c) = \underline{q}(\lambda_c), \end{aligned}$$

where (a) follows from the result in [15] and (b) follows from the lower bound in Theorem 2.4.1. Similarly, using the upper bound in Lemma 2.4.1, the upper bound on $q(\lambda_c)$ is given by

$$q(\lambda_c) \leq \left[1 - \left(1 - \frac{(\alpha - 1)A_c}{[(\alpha - 1) - A_c]^2} \right)^+ e^{-A_c} \right] (1 - B_c) = \bar{q}(\lambda_c).$$

2.9.3 Proof of Lemma 2.6.1

The conditional probability in (2.18) can be explicitly written as follows:

$$\mathbb{P}[\tilde{H}_j \tilde{D}_j^{-\alpha} \leq \rho_* | \tilde{H}_* \tilde{D}_*^{-\alpha} \leq \rho_*] = \frac{\mathbb{P}[\max\{\tilde{H}_* \tilde{D}_*^{-\alpha}, \tilde{H}_j \tilde{D}_j^{-\alpha}\} \leq \rho_*]}{\mathbb{P}[\tilde{H}_* \tilde{D}_*^{-\alpha} \leq \rho_*]}.$$

Also, we know

$$\begin{aligned}\mathbb{P}[\max\{\tilde{H}_* \tilde{D}_*^{-\alpha}, \tilde{H}_j \tilde{D}_j^{-\alpha}\} \leq \rho_*] &= \mathbb{P}[\tilde{H}_j \tilde{D}_j^{-\alpha} \leq \rho_*] \mathbb{P}[\tilde{H}_* \tilde{D}_*^{-\alpha} \leq \tilde{H}_j \tilde{D}_j^{-\alpha}] \\ &\quad + \mathbb{P}[\tilde{H}_* \tilde{D}_*^{-\alpha} \leq \rho_*] \mathbb{P}[\tilde{H}_* \tilde{D}_*^{-\alpha} \geq \tilde{H}_j \tilde{D}_j^{-\alpha}],\end{aligned}$$

where

$$\begin{aligned}\mathbb{P}[\tilde{H}_* \tilde{D}_*^{-\alpha} \leq \tilde{H}_j \tilde{D}_j^{-\alpha}] &= 1 - \mathbb{E}[e^{-\tilde{H}_j \tilde{D}_*^\alpha / \tilde{D}_j^\alpha}] = \mathbb{E}\left[\frac{\tilde{D}_*^\alpha}{\tilde{D}_*^\alpha + \tilde{D}_j^\alpha}\right] \\ \mathbb{P}[\tilde{H}_* \tilde{D}_*^{-\alpha} \geq \tilde{H}_j \tilde{D}_j^{-\alpha}] &= \mathbb{E}[e^{-\tilde{H}_j \tilde{D}_*^\alpha / \tilde{D}_j^\alpha}] = \mathbb{E}\left[\frac{\tilde{D}_j^\alpha}{\tilde{D}_*^\alpha + \tilde{D}_j^\alpha}\right].\end{aligned}$$

Therefore, we can have the following result:

$$\begin{aligned}\mathbb{P}[\max\{\tilde{H}_* \tilde{D}_*^{-\alpha}, \tilde{H}_j \tilde{D}_j^{-\alpha}\} \leq \rho_*] &= 1 - \mathbb{E}[e^{-\tilde{D}_*^\alpha \rho_*}] \left(\mathbb{E}\left[\frac{\tilde{D}_j^\alpha}{\tilde{D}_*^\alpha + \tilde{D}_j^\alpha}\right] \right. \\ &\quad \left. + \mathbb{E}\left[\frac{\tilde{D}_*^\alpha}{\tilde{D}_*^\alpha + \tilde{D}_j^\alpha}\right] \frac{\mathbb{E}[e^{-\tilde{D}_j^\alpha \rho_*}]}{\mathbb{E}[e^{-\tilde{D}_*^\alpha \rho_*}]} \right).\end{aligned}$$

It follows that

$$\begin{aligned}\mathbb{P}[\tilde{H}_j |X_0 - Y_j|^{-\alpha} \leq \rho_* | \tilde{H}_* \tilde{D}_*^{-\alpha} \leq \rho_*] &= \\ \frac{1}{1 - \mathbb{E}[e^{-\tilde{D}_*^\alpha \rho_*}]} &\left[1 - \mathbb{E}[e^{-\tilde{D}_*^\alpha \rho_*}] \left(\mathbb{E}\left[\frac{\tilde{D}_j^\alpha}{\tilde{D}_*^\alpha + \tilde{D}_j^\alpha}\right] + \mathbb{E}\left[\frac{\tilde{D}_*^\alpha}{\tilde{D}_*^\alpha + \tilde{D}_j^\alpha}\right] \frac{\mathbb{E}[e^{-\tilde{D}_j^\alpha \rho_*}]}{\mathbb{E}[e^{-\tilde{D}_*^\alpha \rho_*}]} \right) \right].\end{aligned}$$

As $\rho_* \rightarrow 0$, it is easy to observe that $\mathbb{P}[\tilde{H}_j |X_0 - Y_j|^{-\alpha} \leq \rho_* | \tilde{H}_* \tilde{D}_*^{-\alpha} \leq \rho_*]$ approaches to 1, which completes the proof.

2.9.4 Proof of Theorem 2.6.2

For the DIAS scheme, its outage probability can be written as

$$q(\lambda_i) = \mathbb{P}\left[\frac{H_0 D_0^{-\alpha}}{\sum_{X_j \in \Pi_i} \tilde{H}_j |X_j|^{-\alpha}} < \beta \mid \tilde{H}_{j^*} |X_j - X_{j^*}|^{-\alpha} < \Delta_i(\lambda_i)\right].$$

Since the closed-form solution for the above outage probability is unable to be obtained, we resort to finding its upper and lower bounds. Let $\hat{\Pi}_i$ be the following Poisson point process:

$$\hat{\Pi}_i \triangleq \left\{ X_k \in \Pi_i : T_k = \mathbf{1} \left(\frac{H_0 D_0^{-\alpha}}{\tilde{H}_k |X_k|^{-\alpha}} < \beta \right), \forall k \in \mathbb{N}_+ \right\},$$

which means any single transmitter in $\hat{\Pi}_i$ is able to cause outage at the reference receiver. Since the Laplace functional of a PPP completely characterizes the distribution of the PPP, we can find the Laplace functional of $\hat{\Pi}_i$ and it can render us the intensity $\hat{\lambda}_i$ of $\hat{\Pi}_i$. The Laplace functional of $\hat{\Pi}_i$ for a nonnegative function $\phi : \mathbb{R}^2 \rightarrow \mathbb{R}_+$ is defined and shown as follows [17]:

$$\mathcal{L}_{\hat{\Pi}_i}(\phi) \triangleq \mathbb{E} \left[e^{-\int_{\mathbb{R}^2} \phi(X) \hat{\Pi}_i(dX)} \right] = \exp \left(- \int_{\mathbb{R}^2} \hat{\lambda}_i [1 - e^{-\phi(X)}] \mu(dX) \right),$$

where $\mu(\mathcal{A})$ denotes the Lebesgue measure of a bounded set \mathcal{A} . The Laplace functional of $\hat{\Pi}_i$ for $\phi(X) = \hat{\phi}(X) \mathbf{1}(X \in \hat{\Pi}_i)$ is

$$\begin{aligned} \mathcal{L}_{\hat{\Pi}_i}(\phi) &= e^{-\lambda_i \mu(\mathcal{A})} \sum_{k=0}^{\infty} \frac{\lambda_i^k}{k!} \int_{\mathcal{A}} \dots \int_{\mathcal{A}} \prod_{j=1}^k (e^{-\phi(X_j)} \mathbb{P}[X_j \in \hat{\Pi}_i] + \\ &\quad \mathbb{P}[X_j \notin \hat{\Pi}_i]) \mu(dX_1) \dots \mu(dX_k) \\ &= e^{-\lambda_i \mu(\mathcal{A})} \sum_{k=0}^{\infty} \frac{-1}{k!} \left(\int_{\mathcal{A}} \{(1 - e^{-\hat{\phi}(X)}) \mathbb{P}[X \in \hat{\Pi}_i] - 1\} \lambda_i \mu(dX) \right)^k \\ &= \exp \left(- \int_{\mathcal{A}} (1 - e^{-\phi(X)}) \mathbb{P} \left[\frac{H_0 D_0^{-\alpha}}{\tilde{H} |X|^{-\alpha}} < \beta, \tilde{H}_* \tilde{D}_*^{-\alpha} < \Delta_i(\lambda_i) \right] \lambda_i \mu(dX) \right). \end{aligned}$$

Therefore, we have $\hat{\lambda}_i(r) = \lambda_i \mathbb{P}[H_0 D_0^{-\alpha} < \beta \tilde{H} r^{-\alpha}, \tilde{H}_* \tilde{D}_*^{-\alpha} < \Delta_i(\lambda_i)]$. Since $H_0 D_0^{-\alpha}$, $\tilde{H}_* \tilde{D}_*$ and \tilde{H} are independent, it follows that

$$\begin{aligned} \hat{\lambda}_i(r) &= \lambda_i p_i(\lambda_i) \mathbb{P}[H_0 D_0^{-\alpha} < \beta \tilde{H} r^{-\alpha}] \\ &= \lambda_i p_i(\lambda_i) \mathbb{E} \left[\frac{\beta D_0^\alpha}{\beta D_0^\alpha + r^\alpha} \right]. \end{aligned}$$

Let $\mathcal{E}(\hat{\Pi}_i)$ be the outage event caused by $\hat{\Pi}_i$ and its probability is the lower bound on the outage probability because $\mathcal{E}(\hat{\Pi}_i) \subseteq \mathcal{E}(\Pi_i)$. So $\mathbb{P}[\mathcal{E}(\hat{\Pi}_i)]$ can be characterized by the probability that there is at least one transmitter in $\tilde{\Pi}_i$, i.e. $\hat{\Pi}_i(\mathbb{R}^2) \neq \emptyset$. That is,

$$\begin{aligned} \mathbb{P}[\mathcal{E}(\hat{\Pi}_i)] &= 1 - \exp\left(-2\pi \int_0^\infty \hat{\lambda}_i(r) r dr\right) \\ &= 1 - \exp\left(-2\pi \lambda_i p_i(\lambda_i) \int_0^\infty \mathbb{E}\left[\frac{\beta D_0^\alpha}{\beta D_0^\alpha + r^\alpha}\right] r dr\right) \\ &= 1 - \exp\left(-\lambda_i \beta^{\frac{2}{\alpha}} \psi \mathbb{E}[D_0^2] p_i(\lambda_i)\right) = \underline{q}(\lambda_i). \end{aligned}$$

Note that $\beta^{\frac{2}{\alpha}} \psi \mathbb{E}[D_0^2]$ is the mean area of the dominant interferer coverage, as defined in Proposition 2.8.2. Since $\underline{q}(\lambda_i) \leq \epsilon$ and $\bar{\lambda}_i \triangleq \sup\{\lambda_i : \underline{q}(\lambda_i) \leq \epsilon\}$, we have $\bar{\lambda}_i p_i(\bar{\lambda}_i) = \frac{-\ln(1-\epsilon)}{\beta^{\frac{2}{\alpha}} \psi \mathbb{E}[D_0^2]}$.

Suppose the outage event caused by $\Pi_i \setminus \hat{\Pi}_i$ is denoted by $\mathcal{E}^c(\hat{\Pi}_i)$. The upper bound on $q(\lambda_i)$ can be found as follows

$$\begin{aligned} q(\lambda_i) \leq \mathbb{P}[\mathcal{E}(\hat{\Pi}_i) \cup \mathcal{E}^c(\hat{\Pi}_i)] &= \mathbb{P}[\mathcal{E}(\hat{\Pi}_i)] + \mathbb{P}[\mathcal{E}^c(\hat{\Pi}_i)] - \mathbb{P}[\mathcal{E}(\hat{\Pi}_i)]\mathbb{P}[\mathcal{E}^c(\tilde{\Pi}_i)] \\ &= 1 - (1 - \underline{q}(\lambda_i, \Delta_i(\lambda_i)))(1 - \mathbb{P}[\mathcal{E}^c(\hat{\Pi}_i)]), \end{aligned}$$

where $\mathbb{P}[\mathcal{E}^c(\hat{\Pi}_i)] = \mathbb{P}[HD^{-\alpha} < \beta I_0^c]$ and I_0^c is the interference generated by $\Pi_i \setminus \hat{\Pi}_i$. The intensity of $\Pi_i \setminus \hat{\Pi}_i$ is $\lambda_i - \hat{\lambda}_i$, and for $\hat{\lambda}_i > 0$, $\mathbb{P}[\mathcal{E}^c(\hat{\Pi}_i)]$ can be calculated by

$$\begin{aligned} \mathbb{P}[\mathcal{E}^c(\hat{\Pi}_i)] &= 1 - \mathbb{E}\left[e^{-\beta D_0^\alpha I_0^c}\right] \stackrel{(a)}{\leq} 1 - \exp(-\beta \mathbb{E}[D_0^\alpha I_0^c]) \\ &\stackrel{(b)}{=} 1 - \exp\left(-2\pi \lambda_i \beta \mathbb{E}[D_0^\alpha] p_i(\lambda_i) \int_0^\infty \mathbb{P}[H_0 D_0^{-\alpha} \geq \beta \tilde{H} r^{-\alpha}] r^{1-\alpha} dr\right) \\ &= 1 - \exp\left(-2\pi \lambda_i p_i(\lambda_i) \mathbb{E}\left[\int_0^\infty \left(\frac{\beta r}{r^\alpha + \beta D_0^\alpha}\right) dr\right]\right) \\ &= 1 - \exp\left\{-\lambda_i \beta^{\frac{2}{\alpha}} \psi p_i(\lambda_i) \mathbb{E}[D_0^2]\right\}, \end{aligned}$$

where (a) follows from Jensen's inequality because e^{-x} is convex for $x > 0$ and (b) follows from the Campbell theorem [57] by conditioning on D . Thus, it follows that

$$q(\lambda_i) \leq 1 - \exp\left(-2\lambda_i p_i(\lambda_i) \beta^{\frac{2}{\alpha}} \psi \mathbb{E}[D_0^2]\right) = \bar{q}(\lambda_i),$$

which renders us the lower bound on $\bar{\lambda}_\epsilon$. That is, $\underline{\lambda}_i = \sup\{\lambda : \bar{q}(\lambda_i) \leq \epsilon\}$ and thus we have.

$$\underline{\lambda}_i p_i(\lambda_i) = \frac{-\ln(1-\epsilon)}{2\beta^{\frac{2}{\alpha}} \psi \mathbb{E}[D_0^2]}.$$

If $\Delta_i(\lambda_i) = \rho \lambda_i^{\frac{2}{\alpha}}$, then p_i does not depend on λ_i and is a monotonically decreasing function of ρ . Hence, there must exist a sufficiently small ρ such that p_i is less than $\frac{1}{2}$. In this case, $\underline{\lambda}_i > \frac{-\ln(1-\epsilon)}{\beta^{\frac{2}{\alpha}} \psi \mathbb{E}[D_0^2]}$, which indicates the scaling result in (2.22). This completes the proof.

2.9.5 Proof of Theorem 2.7.1

The transmitters using DICAS are a homogeneous PPP which is given by

$$\Pi_{ic} = \{X_j \in \Pi_t : T_j = \mathbf{1}(H_j D_j^{-\alpha} \geq \Delta_c(\lambda_{ic}), \tilde{H}_{j^*} \tilde{D}_{j^*}^{-\alpha} \leq \Delta_i(\lambda_{ic})), \forall j \in \mathbb{N}_+\},$$

where $\tilde{D}_{j^*} \triangleq |X_j - Y_{j^*}|$. Using the result in the proof of Theorem 2.5.1, the outage probability of each pair in Π_{ic} can be written as follows:

$$\begin{aligned} q(\lambda_{ic}) &= \mathbb{P}[\text{SIR}(\lambda_{ic}) < \beta | H_0 D_0^{-\alpha} \geq \Delta_c(\lambda_{ic}), \tilde{H}_{j^*} \tilde{D}_{j^*}^{-\alpha} \leq \Delta_i(\lambda_{ic})] \\ &= \frac{\mathbb{P}[\beta I_0 \geq \Delta_c(\lambda_{ic}) | \tilde{H}_{j^*} \tilde{D}_{j^*}^{-\alpha} \leq \Delta_i(\lambda_{ic})]}{\mathbb{P}[H_0 D_0^{-\alpha} \geq \Delta_c(\lambda_{ic})]} \\ &\quad \cdot \mathbb{P}[\Delta_c(\lambda_{ic}) \leq H_0 D_0^{-\alpha} < \beta I_0 | \tilde{H}_{j^*} \tilde{D}_{j^*}^{-\alpha} \leq \Delta_i(\lambda_{ic})]. \end{aligned}$$

Now, consider the transmitters in Π_{ic} are able to independently generate the interference at the reference receiver that is greater or equal to $\Delta_c(\lambda_{ic})/\beta$, i.e. the point process formed by them can be written as

$$\hat{\Pi}_{ic} = \{X_j \in \Pi_{ic} : \tilde{H}_j |X_j|^{-\alpha} \geq \Delta_c(\lambda_{ic})/\beta\}. \quad (2.48)$$

According to the result in the proof of Theorem 2.6.2, we can infer that $\hat{\Pi}_{ic}$ is a nonhomogeneous PPP with the following intensity:

$$\begin{aligned} \hat{\lambda}_{ic}(r) &= \lambda_{ic} \mathbb{P}[\Delta_c(\lambda_{ic})/\beta \leq \tilde{H}r^{-\alpha}] \mathbb{P}[\tilde{H}_* \tilde{D}_*^{-\alpha} \leq \Delta_i(\lambda_{ic})] \\ &= \lambda_{ic} e^{-r^\alpha \Delta_c(\lambda_{ic})/\beta} \left(1 - \mathbb{E}[e^{-\tilde{D}_*^\alpha \Delta_i(\lambda_{ic})}]\right). \end{aligned} \quad (2.49)$$

Thus, the lower bound on the probability $\mathbb{P}[I_0 \geq \Delta_c(\lambda_{ic})/\beta]$ can be calculated by $1 - \exp(-2\pi \int_0^\infty \hat{\lambda}_{ic}(r) r dr)$, which can be carried out as follows

$$\mathbb{P}[I_0 \geq \Delta_c(\lambda_{ic})/\beta] \geq 1 - \exp\left[-\lambda_{ic} \beta^{\frac{2}{\alpha}} A(\Delta_c(\lambda_{ic})) (1 - \mathbb{E}[e^{-\tilde{D}_*^\alpha \Delta_i(\lambda_{ic})}])\right].$$

Moreover, the probability $\mathbb{P}[\Delta_c(\lambda_{ic}) \leq H_0 D_0^{-\alpha} < \beta I_0 | \tilde{H}_{j*} \tilde{D}_{j*}^{-\alpha} \leq \Delta_i(\lambda_{ic})]$ can be further written as

$$\begin{aligned} &\mathbb{P}[\Delta_c(\lambda_{ic}) \leq H_0 D_0^{-\alpha} < \beta I_0 | \tilde{H}_{j*} \tilde{D}_{j*}^{-\alpha} \leq \Delta_i(\lambda_{ic})] \\ &= \mathbb{E}[e^{-D_0^\alpha \Delta_c(\lambda_{ic})}] - \mathbb{E}\left[e^{-\beta D_0^\alpha \max\{\beta I_0, \Delta_c(\lambda_{ic})\}} | \tilde{H}_{j*} \tilde{D}_{j*}^{-\alpha} \leq \Delta_i(\lambda_{ic})\right] \\ &= \mathbb{E}[e^{-D_0^\alpha \Delta_c(\lambda_{ic})}] - \mathbb{E}\left[e^{-\lambda_{ic} p_{ic}(\lambda_{ic}) \beta^{\frac{2}{\alpha}} \psi D_0^2 - D_0^\alpha \Delta_c(\lambda_{ic})}\right] \\ &= \mathbb{E}[e^{-D_0^\alpha \Delta_c(\lambda_{ic})}] \left(1 - \mathbb{E}\left[e^{-\lambda_{ic} p_{ic}(\lambda_{ic}) \beta^{\frac{2}{\alpha}} \psi D_0^2}\right]\right). \end{aligned}$$

The lower bound on the outage probability is

$$\underline{q}(\lambda_{ic}) = [1 - \exp(-A_{ic})] (1 - B_{ic}).$$

Comparing the above result with the lower bound in (2.9a) in Theorem 2.5.1, we found that they are exactly the same except the intensity term. The intensity term has been changed from λ_c to $\lambda_{ic}p_{ic}$. Hence, the upper bound on the outage probability here can be obtained by following the same steps in the proof of Theorem 2.5.1 and it is exactly the same as the result in (2.9b) by replacing λ_c with $\lambda_{ic}p_{ic}(\lambda_{ic})$. That is,

$$\bar{q}(\lambda_{ic}) = \left[1 - \left(1 - \frac{(\alpha - 1)A_{ic}}{[(\alpha - 1) - A_{ic}]^2} \right)^+ e^{-A_{ic}} \right] (1 - B_{ic}).$$

Bounds on TC can be found by solving $q(\lambda_{ic}) = \epsilon$ and $\bar{q}(\lambda_{ic}) = \epsilon$ for $\bar{\lambda}_{ic}$ and $\underline{\lambda}_{ic}$, respectively.

2.9.6 Proof of Theorem 2.7.3

Here we only prove the lower bound since the proof for the upper bound is similar. The proof consists of three parts. **(i)** First, we only consider the DCAS scheme is adopted (i.e. DICAS with $\Delta_i(\lambda_{ic}) = 0$) and find the lower bound on the outage probability as follows. According to the proof of Theorem 2.5.1, the outage probability for DCAS with interference cancellation has the following identity:

$$q(\lambda_{ic}) = \mathbb{P}[\beta I_0^{\text{nc}} \geq \Delta_c(\lambda_{ic})] (1 - \mathbb{E}[e^{-\beta D_0^\alpha I_0^{\text{nc}}}]).$$

Using the lower bound result in Theorem 2.4.1 and the Laplace transform of a shot-noise process [17, 18], we can obtain

$$q(\lambda_{ic}) \geq \left(1 - \exp \left(-\frac{2\pi}{\alpha} \left(\frac{\beta}{\Delta_c(\lambda_{ic})} \right)^{\frac{2}{\alpha}} \int_0^\infty \lambda_{ic}^{\text{nc}} \left(\sqrt[\alpha]{\frac{\beta u}{\Delta_c(\lambda_{ic})}} \right) u^{\frac{2}{\alpha}-1} e^{-u} du \right) \right) \cdot \left(1 - \mathbb{E} \left[\exp \left(-\frac{2\pi}{\alpha} \beta^{\frac{2}{\alpha}} D_0^2 \int_0^\infty \lambda_{ic}^{\text{nc}} \left(D_0 \sqrt[\alpha]{\beta t} \right) \frac{t^{\frac{2}{\alpha}-1}}{(1+t)} dt \right) \right] \right).$$

Let $\tilde{\beta} = \frac{\beta}{1+\beta}$ and the intensity λ_{ic}^{nc} in (2.33) can be simplified as

$$\begin{aligned} \lambda_{ic}^{\text{nc}}(r) &= \lambda_{ic} \left(1 - \mathbb{E} \left[e^{-\tilde{\beta} r^\alpha I_0} \right] \mathbb{E} \left[e^{-\tilde{\beta} r^\alpha H_0 D_0^{-\alpha}} \mid H_0 D_0^{-\alpha} \geq \Delta_c(\lambda_{ic}) \right] \right) \\ &= \lambda_{ic} \left(1 - \exp \left(-\pi \psi \lambda_{ic} \tilde{\beta}^{\frac{2}{\alpha}} r^2 - \tilde{\beta} r^\alpha \Delta_c(\lambda_{ic}) \right) \mathbb{E} \left[\frac{D_0^\alpha}{D_0^\alpha + \tilde{\beta} r^\alpha} \right] \right) \\ &= \lambda_{ic} - \lambda_{ic}^c(r). \end{aligned}$$

Substituting the above result into the lower bound, it follows that

$$\begin{aligned} q(\lambda_{ic}) &\geq \left(1 - \exp \left(-\frac{A_{ic}}{\lambda_{ic}} \left[\lambda_{ic} - \frac{1}{\Gamma(\frac{2}{\alpha})} \int_0^\infty \lambda_{ic}^c \left(\sqrt[\alpha]{\beta u / \Delta_c(\lambda_{ic})} \right) u^{\frac{2}{\alpha}-1} e^{-u} du \right] \right) \right) \cdot \left(1 - \mathbb{E} \left[\exp \left(-\beta^{\frac{2}{\alpha}} \psi D_0^2 \left[\lambda_{ic} - \int_0^\infty \frac{t^{\frac{2}{\alpha}-1} \lambda_{ic}^c (D_0 \sqrt[\alpha]{\beta t})}{\Gamma(\frac{2}{\alpha}) \Gamma(1 - \frac{2}{\alpha}) (1+t)} dt \right] \right) \right] \right) \\ &= \left\{ 1 - \exp \left(-A_{ic} \left[1 - \frac{1}{\lambda_{ic}} \mathcal{G} \left(\lambda_{ic}^c; \frac{\alpha}{2} \right) \right] \right) \right\} \cdot \left\{ 1 - \mathbb{E} \left[\exp \left(-\beta^{\frac{2}{\alpha}} \lambda_{ic} \psi D_0^2 \left[1 - \frac{1}{\lambda_{ic}} \mathcal{B} \left(\lambda_{ic}^c; \frac{\alpha}{2}, 1 - \frac{\alpha}{2} \right) \right] \right) \right] \right\} \\ &= \left(1 - e^{-\hat{A}_{ic}} \right) \left(1 - \hat{B}_{ic} \right). \end{aligned}$$

(ii) Secondly, we find the lower bound on the outage probability for the DIAS scheme (i.e. DICAS with $\Delta_c(\lambda_{ic}) = 0$). According to the proof of Theorem 2.6.2, we know the PPP $\hat{\Pi}_{ic}$ in which any single transmitter can cause outage at the reference receiver has the intensity $\hat{\lambda}_{ic}(r) = \lambda_{ic} p_i(\lambda_{ic}) \mathbb{E} \left[\frac{\beta D_0^\alpha}{\beta D_0^\alpha + r^\alpha} \right]$. Since the

probability of a transmitter in Π_{ic}^{nc} is $\mathbb{P} \left[\frac{\tilde{H}_k |X_k|^{-\alpha}}{I_0 + H_0 D_0^{-\alpha}} < \tilde{\beta} \right]$, the cancelable part of $\hat{\lambda}_{ic}(r)$ is

$$\begin{aligned} \hat{\lambda}_{ic}^c(r) &= \lambda_{ic} p_i(\lambda_{ic}) \mathbb{E} \left[\frac{\beta D_0^\alpha}{\beta D_0^\alpha + r^\alpha} \right] \mathbb{P} \left[\frac{\tilde{H}_k r^{-\alpha}}{I_0 + H_0 D_0^{-\alpha}} < \tilde{\beta} \right] \\ &= \lambda_{ic} p_i(\lambda_{ic}) \mathbb{E} \left[\frac{\beta D_0^\alpha}{\beta D_0^\alpha + r^\alpha} \right] \mathbb{E} \left[\frac{D_0^\alpha}{D_0^\alpha + \tilde{\beta} r^\alpha} \right] e^{-\pi \psi \tilde{\beta}^{\frac{2}{\alpha}} r^2 \lambda_{ic}}. \end{aligned}$$

Using $\hat{\lambda}_{ic}^{nc}(r) = \hat{\lambda}_{ic}(r) - \hat{\lambda}_{ic}^c(r)$ to find the average number of transmitters which are in the dominant interference coverage and noncancelable, we can obtain the lower bound on $q(\lambda_{ic})$ because $\lambda_{ic}^{nc}(r) > \hat{\lambda}_{ic}^{nc}(r)$. So it follows that

$$\begin{aligned} \underline{q}(\lambda_{ic}) &= 1 - \exp \left(-2\pi \int_0^\infty \hat{\lambda}_{ic}(r) \left[1 - \hat{\lambda}_{ic}^c(r) / \hat{\lambda}_{ic}(r) \right] r dr \right) \\ &= 1 - \exp \left(-2\pi \int_0^\infty \lambda_{ic} p_i(\lambda_{ic}) \mathbb{E} \left[\frac{\beta D_0^\alpha r}{\beta D_0^\alpha + r^\alpha} \right] \right. \\ &\quad \left. \left(1 - \mathbb{E} \left[\frac{D_0^\alpha}{D_0^\alpha + \tilde{\beta} r^\alpha} \right] e^{-\pi \psi \tilde{\beta}^{\frac{2}{\alpha}} r^2 \lambda_{ic}} \right) dr \right) \\ &\stackrel{(\star)}{=} 1 - \exp \left(-\frac{2\pi}{\alpha} \lambda_{ic} p_i(\lambda_{ic}) \beta^{\frac{2}{\alpha}} \mathbb{E} \left[\int_0^\infty D_0^2 [1 - h(t)] \frac{t^{\frac{2}{\alpha}-1}}{1+t} dt \right] \right) \\ &= 1 - \exp \left(-\lambda_{ic} p_i(\lambda_{ic}) \beta^{\frac{2}{\alpha}} \psi \mathbb{E} \left[D_0^2 \left(1 - \mathcal{B} \left(h(t); \frac{\alpha}{2}, 1 - \frac{\alpha}{2} \right) \right) \right] \right), \end{aligned}$$

where (\star) is obtained by doing variable change with $t = \frac{r^\alpha}{\beta D_0^\alpha}$ and $h(t)$ is given by

$$h(t) = \left(\frac{1}{1 + t \tilde{\beta} \beta} \right) \exp(D_0^2 (\tilde{\beta} \beta t)^{\frac{2}{\alpha}} \lambda_{ic}).$$

(iii) Since DIAS only reduces interference, the lower bound found in part **(ii)** indicates that the effect of DIAS is to change the intensity of the interferers by multiplying it with $p_i(\lambda_{ic})$. Therefore, the lower bound for the DICAS scheme can be obtained by replacing λ_{ic} in the lower bound found in part **(i)** with $\lambda_{ic} p_i(\lambda_{ic})$. This completes the proof.

Chapter 3

Multicast Outage and Transmission Capacity

Multicast refers to the scenario whereby a transmitter needs to send a packet to multiple receivers. In a wireless network, this creates a two-edged sword. On one hand, the broadcast nature of wireless transmission assists multicast; but roughly uncorrelated outage probabilities at each receiver (due to spatially distinct fading and interference) require retransmissions that cause interference and waste. Multicast is an important aspect of sensor and tactical networks, and increasingly in commercial networks where streaming is supported. However, the literature on multicast is minuscule compared to unicast – whereby nodes are paired into sources and destinations – and even basic modeling issues such as outage, capacity/throughput definitions, and retransmissions are not widely agreed upon. In this work, we attempt to investigate the fundamental throughput limits of multicast transmission and we develop a metric based on spatial outage capacity which we term *multicast transmission capacity* (MTC).

In order to characterize the MTC in a wireless network we propose a multicast network model in which each transmitter has an intended multicast region (called a cluster) where all the intended receivers are uniformly and independently scattered, and hence a Poisson cluster process can be reasonably used to model

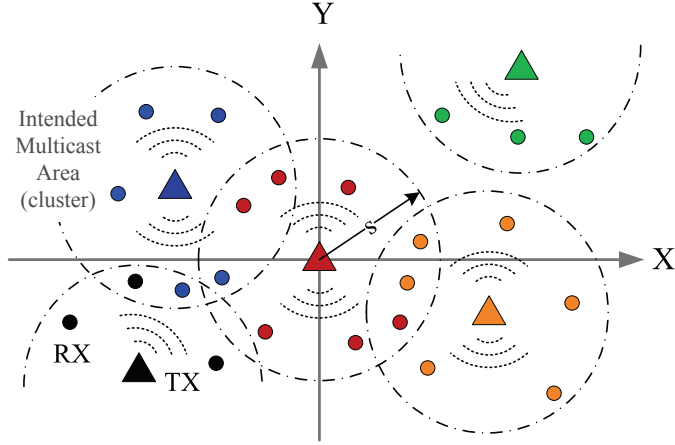


Figure 3.1: Multicast transmission model in a planar wireless ad hoc network: The transmitters in the network form a stationary PPP of intensity λ_t . Each transmitter (triangle) has an intended multicast area of radius s , where all the intended receivers (small circles) also form a stationary PPP of intensity λ_r . A transmitter and its corresponding intended receivers are indicated by the same color in a cluster.

the transmit-receiver location statistics. The active transmitters are modeled as a stationary Poisson point process (PPP) and their associated receiver nodes in the cluster are also a stationary PPP, as shown in Figure 3.1. In other words, each cluster is randomly located in the network and comprises a multicast session. This chapter will develop interference and outage expressions for this model, and analyze some important cases of the network model and design space, including the network intensity, size and the effect of retransmissions.

3.1 Motivation and Related Work

The majority of the existing works on network capacity like Chapter 2 are focused on the *unicast* scenario and built upon the protocol and physical network models proposed in [11]. Generally speaking, the unicast network capacity is the maximum number of point-to-point communication links that can be simultaneously supported in the network under some transmission constraints. For example, transport capacity built upon the protocol model [11] has a geometric constraint on transmitter-receiver pairs. Due to the difficulty in coordinating the transmission constraints between multiple receivers, the unicast capacity, in general, is not readily extended to the multicast capacity. Even the definition of multicast capacity is not widely agreed upon.

Some previous works, such as [30, 58–66], have made significant progress in studying the multicast or broadcast capacity¹. For example, in [58] the protocol model is used where source nodes and their multicast destinations are randomly chosen. The multicast capacity is defined as the sum rate of all multicast flows and it is obtained as a function of the number of multicast sources. In [60], the multicast capacity under the protocol model is defined as the transmission rate summed over all of the multicast traffic flows in the network. Its scaling characterization is obtained by the number of receivers in each multicast session. Reference [64] showed that the broadcast capacity under the protocol model does

¹Broadcast means only one transmitter would like to transmit to all of other nodes in the network, whereas multicast means transmitters transmit to a certain number of nodes in the network. Hence, broadcast capacity can be viewed as a special case of multicast capacity.

not change by more than a constant factor when the number of nodes, the radio range or the area of the network is changed. In [65], the physical model and a stationary PPP of the nodes in the network are considered. It showed that the broadcast capacity is a constant factor of the computed upper bound when the number of nodes goes to infinity under a constant node intensity. The multicast and broadcast capacities in the above works are defined behind the main concept that the transmitted information should be received by all of its intended receivers. However, they are not investigated from the multi-receiver outage point of view and thus their scaling results cannot provide us retransmission guidelines for capacity enhancement.

The multicast capacity problem in this chapter is studied from an outage perspective, which is a departure from previous work. For example, the prior work built on the protocol model in [11] does not consider channel impairments such as fading and path loss, and thus, all transmissions are successful once certain geometric constraints are satisfied. Also, outage and the resulting retransmissions are not considered. This is somewhat unrealistic. The main issues we would like to clarify are (i) how many simultaneous multicast sessions can (and should) coexist when all receivers in a multicast session need to receive the packet from their transmitter, and (ii) when are retransmissions beneficial or detrimental to the multicast capacity? Hence, we introduce the MTC in a planar network, which is defined as the maximum achievable multicast rate per transmission attempt times the maximum number of the coexisting clusters in the network per unit area, subject to decoding delay and multicast outage constraints. This is a logical evolution of the transmission capacity framework originated in [13] to the topic of

multicast. The decoding delay constraint here means a transmitter can multicast a packet to all of its intended receivers up to $\tau \in \mathbb{N}_+$ transmission attempts and multicast outage happens when any of the intended receivers in a cluster does not receive the information multicast by their transmitter during those τ attempts.

Table 3.1: Notation of Main Variables, Processes and Functions in Chapter 3

Symbol	Definition
Φ^t (Φ^r)	Homogeneous PPP of transmitters (receivers)
Φ^c	(Nonhomogeneous) PPP of connected receivers
ϵ	upper bound of multicast outage probability ($\ll 1$)
λ_t (λ_r, λ_c)	intensity of Φ^t (Φ^r, Φ^c)
$\bar{\lambda}_t$	maximum contention intensity of λ_t
$\bar{\lambda}_\epsilon$	first-order Taylor expansion of $\bar{\lambda}_t$ ($\bar{\lambda}_\epsilon \approx \bar{\lambda}_t$)
$\mathcal{E}(\lambda_t)$	multicast outage event depending on λ_t
τ	decoding delay constraint, positive integer
v	number of tessellated regions in a cluster ($v \leq \tau$)
s	radius of a multicast cluster ($s > 1$)
$\mu(\mathcal{A})$	Lebesgue measure of a bounded set \mathcal{A}
β	SIR threshold
α	path loss exponent ($\alpha > 2$)
b	multicast transmission rate (bps/Hz)
C_ϵ	multicast transmission capacity (bps/Hz/m ²)
k ($\pi s^2 \lambda_r$)	average number of intended receivers in a cluster
$f_H(\cdot)$	PDF of channel fading gain H
$F_H(\cdot), F_H^c(\cdot)$	CDF, CCDF of channel fading gain H

3.2 Main Contributions and Chapter Organization

Since unicast outage cannot be directly applied to the outage scenario of multiple receivers, our first contribution is introducing MTC with multicast outage. To the best of our knowledge, this is the first work to study multicast capacity under a multicast outage constraint. According to the proposed Poisson cluster model for multicast, we also propose some new cluster-based definitions for the largeness and denseness of a network in order to characterize the scaling behaviors of the MTC under different conditions. Referring to Table 3.1 for the notation of main variables, we have shown that the scaling of both single-hop and multihop MTC can be expressed in a general form of $\Theta(\rho k^x \log(k)v^y)$ where ρ , x and y are given in Table 3.2 for different network conditions, k is the average number of the intended receivers in a cluster, and v is the number of the tessellated regions of equal area in a cluster². From Table 3.2, we know retransmissions have a significant effect on the MTC and certain number of retransmissions could enhance it. We found that the decoding delay τ can be viewed as a resource which should be allocated properly in every tessellated region to maximize the MTC. In addition, we also show that the MTC scaling holds for the various parameters of Nakagami fading.

We characterize three approaches to improving the MTC – interference-suppression, interference-avoidance and area-shrinking (i.e. reducing the cluster size). The area-shrinking method is able to provide the best capacity gain among

²Throughout this chapter, standard asymptotic notation will be used: $O(\cdot)$, $\Omega(\cdot)$ and $\Theta(\cdot)$ correspond to asymptotic upper, lower, and tight bounds, respectively.

Table 3.2: Summary of Main Results in Chapter 3

Multicast Transmission Capacity C_ϵ	$\Theta(\rho k^x \log(k) v^y)$		
Maximum Contention Intensity $\bar{\lambda}_\epsilon$	$\Theta(\rho k^x v^y)$		
Network Condition	Dense	Large	Large Dense
x	$-\frac{v}{\tau}$	$-(1 + \frac{v}{\tau})$	$-(\frac{\tau+2v}{2\tau})$
ρ	$\frac{1}{\tau^2}(\epsilon(\tau/v + 1))^{\frac{v}{\tau}}$		
y	$\frac{v}{\tau} + 1$		

the three since the multicast outage probability is reduced due to fewer receivers in a cluster. However, shrinking the area of a cluster means some of the intended receivers may have to be excluded, which is not welcome. Thus the multihop multicast method is proposed to improve the MTC without shrinking the cluster. Our main result shows that if the clusters are appropriately tessellated multihop multicast can significantly improve the MTC compared to its single-hop counterpart. This is because an appropriate number of retransmissions largely reduces the multicast outage probability and thus results in the increase of the maximum contention intensity that compensates the loss of spectral efficiency due to retransmissions.

This chapter is organized as follows. In Section 3.3, the network model and its assumptions are described and some preliminaries for the following analysis are provided here. The main results of multicast transmission capacity for the case of single-hop multicast are presented in Section 3.4, whereas Section 3.5 has the main results of multicast transmission capacity with multihop multicast.

3.3 Network Model and Preliminaries

In most of the existing literature, multicast capacity is defined based on the sum of the supportable rates of all multicast sessions. Similarly, the MTC here is characterized by the sum of the multicast rates of the multicast sessions not in (multicast) outage. The multicast rate is affected by the number of the receivers as well as the interference from other multicast sessions. The multicast network model is developed with the principle that it should capture the key traits of a multicast network (for example spatial reuse, retransmissions, broadcast packets, etc.), while being as tractable as possible.

3.3.1 Clustered Network Model for Multicast Transmission

In the network, each transmitter has a multicast cluster of equal area and its receive nodes in the cluster suffer aggregate interference from a Poisson field of transmitters. Specifically, we assume that the network is operating a slotted ALOHA protocol and the distribution of the transmitting nodes in the network is a stationary Poisson point process (PPP) Φ^t of intensity λ_t . As shown in Figure 3.1, any transmitter $X_i \in \Phi^t$ has its own intended multicast cluster \mathcal{R}_i where all of its intended receivers are uniformly and independently distributed and they also form a stationary PPP Φ_i^r of intensity λ_r . *Note that each cluster could contain other transmitters and unintended receivers in addition to its own transmitter and intended receivers.*

Accordingly, the multicast transmission sessions in the network follow a the Poisson cluster process (PCP) $\mathcal{Z}_i \triangleq \Phi_i^r \cup X_i$, *i.e.*, each transmitter is a *parent*

node associated with a cluster of receive *daughter* nodes. The cluster processes $\{\mathcal{Z}_i\}$ corresponding to different transmitters $\{X_i\}$ are assumed to be independent so that the superposition of all clusters yields the resulting cluster process $\Phi = \bigcup_{X_i \in \Phi^t} \mathcal{Z}_i$ of intensity $\lambda = k \lambda_t$ where $k = \pi s^2 \lambda_r$ is the average number of the intended receivers in each cluster assuming all $\{\mathcal{R}_i, \forall i \in \mathbb{N}\}$ have the same radius $s > 1$. The distribution of the intended receiver nodes in each cluster is modeled as a *marked* PPP denoted by $\Phi_i^r \triangleq \{(Y_{ij}, H_{ij}) : Y_{ij} \in \mathcal{R}_i, j \in \mathbb{N}\}$, where H_{ij} is the fading channel gain between transmitter X_i and its intended receiver Y_{ij} . Similarly, the distribution of transmitters in the network is also a marked PPP, *i.e.*, $\Phi^t \triangleq \{(X_i, \{\tilde{H}_{ij}\}), i, j \in \mathbb{N}_+\}$ where \tilde{H}_{ij} denotes the fading channel gain between transmitter X_i and the receiver Y_{0j} located in cluster \mathcal{R}_0 .³ All fading channel gains are i.i.d. with probability density function (PDF) $f_H(\cdot)$.

Without loss of generality, the MTC can be evaluated in the reference cluster \mathcal{R}_0 whose transmitter X_0 is located at the origin. We condition on this typical transmitter X_0 resulting in what is known the Palm distribution for transmitting nodes in the two-dimensional Euclidean space [57]. It follows by Slivnyak's theorem [57] that this conditional distribution also corresponds to a homogenous PPP with the same intensity and an additional point at the origin. The signal propagation in space is assumed to undergo path loss and fading. The path loss

³Since all of the following analysis is based on the nodes in the reference cluster \mathcal{R}_0 , the subscript 0 of some variables will not be explicitly indicated if there is no ambiguity. So Y_j and H_j in \mathcal{R}_0 actually stand for Y_{0j} and H_{0j} , respectively.

model between two nodes X and Y used in this chapter is

$$\ell(|X - Y|) \triangleq \begin{cases} |X - Y|^{-\alpha}, & \text{if } |X - Y| \geq 1 \\ 0, & \text{else,} \end{cases} \quad (3.1)$$

where $|X - Y|$ denotes the Euclidean distance between nodes X and Y , and $\alpha > 2$ is the path loss exponent⁴. The reason of using the model in (3.1) is because the model $|\cdot|^{-\alpha}$ does not behave well in the near field of each transmitter and it thus leads to an unbounded mean of the shot noise process. This model is similar to the idea of the bounded propagation model proposed in [67] [68]. The Nakagami- m fading model is adopted in this chapter because it covers several different fading models, such as Rayleigh (for $m = 1$), Rician fading with parameter K (for $m = (K + 1)^2 / (2K + 1)$) and no fading (for $m \rightarrow \infty$), as well as intermediate fading distributions. It is of unit mean and variance $\frac{1}{m}$ and given by

$$f_H(h) = \frac{m^m}{\Gamma(m)} h^{m-1} \exp(-mh), \quad (3.2)$$

where m is a positive integer and $\Gamma(m) = \int_0^\infty z^{m-1} e^{-z} dz$ is the Gamma function.

Each receiver is able to successfully receive its desired information if its SIR is greater or equal to the target threshold β . That is, receiver node Y_j is “connected” to the typical transmitter if

$$\text{SIR} \triangleq \frac{H_j \ell(|Y_j|)}{I_j} \geq \beta. \quad (3.3)$$

Note that SIR depends on λ_t , i.e. $\text{SIR} = \text{SIR}(\lambda_t)$. All the transmitters are assumed to use the same transmit power, the network is interference-limited, and

⁴Recall that α has to be greater than 2 in order to have bounded interference almost surely, as pointed out in Chapter 2

I_j is the aggregate interference at receive node Y_j and a sum over the marked point processes. Namely,

$$I_j = \sum_{X_i \in \Phi^{\dagger} \setminus \{X_0\}} \tilde{H}_{ij} \ell(|X_i - Y_j|), \quad (3.4)$$

which is a Poisson shot noise process, and \tilde{H}_{ij} is the fading channel gain from transmitter X_i to receiver Y_j in \mathcal{R}_0 . Since Φ^{\dagger} is stationary, according to Slivnyak's theorem the statistics of signal reception seen by receiver Y_j is the same as that seen by any other receivers in the same cluster. Thus I_j can be evaluated at the origin, *i.e.*, (3.4) can be rewritten as $I_0 = \sum_{X_i \in \Phi^{\dagger} \setminus \{X_0\}} \tilde{H}_i \ell(|X_i|)$, where \tilde{H}_i is the fading channel gain between transmitter X_i and the origin.

Suppose the decoding delay is up to the lapse of τ transmission attempts for a transmitter. The connected receiver process for the t -th transmission is denoted by

$$\hat{\Phi}^c(t) = \{(Y_j, H_j(t)) \in \Phi_0^r : H_j(t) \ell(|Y_j|) \geq \beta I_0\}, \quad (3.5)$$

where $\{H_j(t)\}$ are i.i.d. for all $t \in [1, \dots, \tau]$. Also, let $\Phi^c(\tau)$ be the connected receiver process at the τ th attempt, *i.e.*, it is the set of all intended receivers in a cluster connected by their transmitter during the decoding delay, and thus it can be written as $\Phi^c(\tau) = \bigcup_{t=1}^{\tau} \hat{\Phi}^c(t)$. In other words, the connected receiver process can be described by a *filtration* process⁵.

⁵A filtration process means $\Phi^c(1) \subseteq \Phi^c(2) \cdots \subseteq \Phi^c(\tau)$, and for any set $\mathcal{A} \subseteq \mathcal{R}_0$, $\mathcal{A}(\Phi^c(\tau)) \rightarrow \mathcal{A}(\Phi_0^r)$ almost surely as $\tau \rightarrow \infty$ where $\mathcal{A}(\Phi)$ denotes the random number of point process Φ enclosed in set \mathcal{A} .

3.3.2 Multicast Transmission Outage

The transmission capacity of a wireless network introduced in Chapter 1 is defined based on point-to-point transmission with an outage probability constraint $\epsilon \in (0, 1)$. Using the notation of this chapter, its expression can be rewritten as

$$\tilde{c}_\epsilon = \tilde{b} \bar{\lambda}_t (1 - \epsilon), \quad (3.6)$$

where \tilde{b} is the constant transmission rate a communication link can support (for example, about $\log_2(1 + \beta)$), and $\bar{\lambda}_t$ is the maximum contention intensity subject to an outage probability target ϵ . However, (3.6) cannot be directly applied to multicast because the multicast rate would be affected by λ_r and $\bar{\lambda}_t$, and the outage of a multicast transmission is not point-to-point but *point-to-multipoint*. How to declare an outage event for a transmitter multicasting information in the previous multicast transmission model is a key issue.

Since no desired receiver can be assumed to be dispensable, a reasonable way to define multicast outage is when *any of the intended receivers of a transmitter does not receive a multicasted packet* during a period of time up to the decoding delay. That is, after all the allowed retransmissions have been used, if one of the desired receivers in the cluster has not decoded the packet, we declare an outage for this cluster. Thus, a multicast outage event of each multicast cluster can be described as $\mathcal{E}(\lambda_t) = \{\Phi'_0 \setminus \Phi^c(\tau) \neq \emptyset\}$ because \mathcal{E} depends on λ_t . The probability of $\mathcal{E}(\lambda_t)$ can be characterized by the intensity of the connected

receivers during the lapse of τ attempts as follows:

$$\begin{aligned}\mathbb{P}[\mathcal{E}(\lambda_t)] &\triangleq 1 - \mathbb{P}[\{\Phi_0^r \setminus \Phi^c(\tau)\} = \emptyset] \\ &= 1 - \exp \left\{ \int_{\mathcal{R}_0} (\lambda_c(Y, \tau) - \lambda_r) \mu(dY) \right\},\end{aligned}\quad (3.7)$$

where $\mu(\cdot)$ denotes a Lebesgue measure and $\lambda_c(Y, \tau)$ is the intensity of $\Phi^c(\tau)$ at node Y . Using (3.7) to find multicast outage probability can be interpreted as finding the void probability of a “disconnected” PPP in a cluster. Since all of the intended receivers are uniformly distributed in \mathcal{R}_0 , (3.7) can be rewritten as

$$\mathbb{P}[\mathcal{E}(\lambda_t)] = 1 - \exp \left\{ -\pi s^2 (\lambda_r - \mathbb{E}_R[\lambda_c(R, \tau)]) \right\} \leq \epsilon, \quad (3.8)$$

where $R \in [0, s]$ is a random variable whose PDF is $f_R(r) = \frac{2r}{s^2}$. The outage probability in (3.8) cannot exceed its designated upper bound ϵ which is assumed to be a small value throughout this chapter.

Remark 3.3.1. *In Section 3.4.1, we will show that $\Phi^c(\tau)$ is a nonhomogeneous PPP and the average of its intensity $\mathbb{E}_R[\lambda_c(R, \tau)]$ can be found. Thus, the multicast outage probability in (3.8) can be calculated. Also, $\mathbb{E}_R[\lambda_c(R, \tau)]$ is a monotonically decreasing function of λ_t so that the maximum $\bar{\lambda}_t$ is attained when $\mathbb{E}_R[\lambda_c(R, \tau)]$ reduces to its lower bound $\lambda_r + \frac{\ln(1-\epsilon)}{\pi s^2}$ that is obtained by solving (3.8).*

Remark 3.3.2. *The multicast outage probability in (3.8) will accurately approximate the unicast outage probability for a small ϵ if there are no retransmissions ($\tau = 1$) and only one receiver is in a cluster. For a unicast scenario in each cluster, we have $\pi s^2 \lambda_r = 1$ and $\mathbb{E}_R[\lambda_c(R, 1)] = \lambda_r \mathbb{P}[\text{SIR}(\lambda_t) \geq \beta]$. Thus, (3.8)*

becomes

$$\begin{aligned}\mathbb{P}[\mathcal{E}(\lambda_t)] &= 1 - \exp(-\mathbb{P}[\text{SIR}(\lambda_t) < \beta]) \\ &= \mathbb{P}[\text{SIR}(\lambda_t) < \beta] + O(\epsilon^2)\end{aligned}$$

since $\mathbb{P}[\text{SIR}(\lambda_t) < \beta] \leq \epsilon$ and $e^{-\epsilon} = 1 - \epsilon + O(\epsilon^2)$. This shows that the point-to-point outage scenario is covered by our model, i.e. multicast outage is a generalization of point-to-point outage.

3.3.3 Definitions of Multicast Transmission Capacity, Largeness and Denseness of Networks

Since the multicast outage probability is upper bounded by a small ϵ , the maximum contention intensity $\bar{\lambda}_t$ is a function of ϵ and its Taylor expansion for ϵ gives

$$\bar{\lambda}_t(\epsilon) \triangleq \sup\{\lambda_t > 0 : \mathbb{P}[\mathcal{E}(\lambda_t)] \leq \epsilon\} = \bar{\lambda}_\epsilon + O(\epsilon^2), \quad (3.9)$$

where $\bar{\lambda}_\epsilon$ is the Taylor expansion of $\bar{\lambda}_t(\epsilon)$ without the second and higher order terms of ϵ . Since ϵ is small, $\bar{\lambda}_\epsilon \approx \bar{\lambda}_t(\epsilon)$ and thus, for simplicity, we will focus the analysis on $\bar{\lambda}_\epsilon$ in the following.

Definition 3.3.3 (Multicast Transmission Capacity). *The multicast transmission capacity with the multicast outage probability defined in (3.7) for small ϵ is defined as*

$$C_\epsilon \triangleq \frac{1}{\tau} b \bar{\lambda}_\epsilon (1 - \epsilon), \quad (3.10)$$

where $\bar{\lambda}_\epsilon$ is the first order approximation of $\bar{\lambda}_t(\epsilon)$ as indicated in (3.9), b is the maximum achievable multicast rate on average for every cluster and it is not a constant in general.

Multicast transmission capacity C_ϵ gives the number of successful multicast clusters with the maximum achievable multicast rate, that can coexist per unit area subject to decoding delay and multicast outage constraints. In other words, it is the area spectral efficiency of cluster-based multicast transmission. The following definitions of largeness and denseness of a network will be needed to acquire the scaling characterizations of the MTCs in the subsequent analysis. They are defined based on the circumstance that the average number of the intended receivers in a cluster is sufficiently large, *i.e.*, $k = \pi s^2 \lambda_r \gg 1$.

Definition 3.3.4 (Denseness and Largeness of a Network with a PCP).

- (a) We say a network is “large” if the area πs^2 of a cluster in the network is sufficiently large such that for a fixed intended receiver intensity λ_r we have $k \gg 1$.
- (b) If the intended receiver intensity is sufficiently large such that for fixed area πs^2 we have $k \gg 1$, then such a network is called “dense”.
- (c) A “large dense” network, it means that clusters in a network have a sufficiently large size as well as intended receiver intensity; namely, $\lambda_r \propto \pi s^2$ and thus $k \gg 1$.

Here we should point out that Definition 3.3.4 may not be consistent with some popular node-based unicast definitions in prior literature. For example, a dense network usually means it is dense everywhere (*i.e.*, *uniformly* dense); however, our denseness definition could involve the case of *local denseness* if the receiver intensity in a single cluster is sufficiently large whereas the cluster intensity is small.

3.3.4 Multicast Transmission Methods – Single-hop and Multihop

The network model with a PCP for multicast introduced in the previous subsection implicitly assumes that the parent node of each cluster (see Figure 3.1) is the sole transmitter. This is the case of single-hop multicast. Hence, for single-hop multicast, multicast outage probability only depends on the channel conditions between the parent node and its intended receiver nodes. When the size of clusters is large, the path loss of transmitted signals and the average number of the intended receivers for each parent node are both increased significantly. The MTC in this case will correspondingly decrease, so single-hop multicast is not an efficient means of disseminating information for a large and/or dense network.

To alleviate this drawback, we propose a multihop multicast approach. The idea is to allow retransmissions in a cluster by randomly selected receivers that have successfully received the packet already. Each of the selected receivers has its own small local multicast region, and the whole cluster is covered by the combination of small multicast regions. Note that only one selected receiver is allowed to transmit for each time slot in order to make all transmitters in each time slot still form a PPP. The detailed algorithm and modeling assumptions will be presented in Section 3.5.1.

3.4 Multicast Transmission Capacity with Single-Hop Multicast

In this section, we study the MTC when transmitters are multicasting to all of their intended receivers in a single-hop fashion. First we have to find

the multicast outage probability defined in (3.8) and thus we need to study the intensity of the receiver-connected process during the lapse of τ attempts. Then the maximum contention intensity which characterizes the single-hop MTC can be found based on the intensity of the connected receivers in a cluster.

3.4.1 The Receiver-Connected Process

During the allowed transmission τ attempts, the intended receivers in \mathcal{R}_0 connected by the transmitter X_0 form a receiver-connected process whose intensity is the necessary information to estimate the multicast outage probability. Since Φ^c is a filtration process and upper bounded by Φ^r (as explained in Section 3.3.1), the connected receiver intensity in \mathcal{R}_0 is an increasing function of τ as shown in the following lemma.

Lemma 3.4.1. *Consider the stationary PPP Φ_0^r of intensity λ_r in the reference cluster \mathcal{R}_0 . If a transmitter is allowed to transmit a packet up to τ times, then $\Phi^c(\tau)$ is a nonhomogeneous thinning PPP and the intensities of $\Phi^c(\tau)$ for different fading models are shown as follows. For Rayleigh fading, we have*

$$\lambda_c(r, \tau) = \lambda_r (1 - \{1 - \exp[-\pi \Delta_1(\beta r^\alpha, \infty) \lambda_t]\}^\tau), \quad (3.11)$$

and $\Delta_1(\cdot, \cdot)$ is defined in Proposition 3.6.1 in Appendix 3.6.1. For Nakagami- m fading with $m > 1$, we have

$$\lambda_c(r, \tau) = \lambda_r \left\{ 1 - [1 - \Psi^{(m-1)}(m\beta r^\alpha)]^\tau \right\}, \quad r \in [1, s] \quad (3.12)$$

where

$$\Psi^{(m)}(\phi) \triangleq \frac{\phi^{m+1}}{m!} \frac{d^m}{d\phi^m} \left(\frac{(-1)^m}{\phi \exp\{\pi \lambda_t \Delta_1(\phi, \infty)\}} \right). \quad (3.13)$$

Proof. See Appendix 3.7.1. □

The connection intensity λ_c for Rayleigh fading in (3.11) reveals an interesting implication. The term $1 - \exp[-\pi\Delta_1(\beta r^\alpha, \infty)\lambda_t]$ can be interpreted as the probability that there is at least one interferer in the circular area of radius $\sqrt{\Delta_1(\beta r^\alpha, \infty)}$. This circular area can be called the *dominating interferer area* centered at r because any single interferer within this area can cause an outage at the receiver located at r . The effect of retransmission can be said either to make this probability reduce by τ -fold or to enlarge the circular area. In a dense network with $\lambda_t \geq \lambda_r$, for example, the term $(1 - \exp[-\pi\Delta_1(\beta r^\alpha, \infty)\lambda_t])^\tau \approx 1 - \tau \exp[-\pi\Delta_1(\beta r^\alpha, \infty)\lambda_t]$ since $\pi\Delta_1(\beta r^\alpha, \infty)\lambda_t \gg 1$. So the radius of the dominating interferer coverage is approximately increased by $\sqrt{\ln(\tau)}$ -fold if $\tau > 2$ in this case.

In addition, as shown in (3.11)-(3.13), we know that a closed-form expression of the average connection intensity $\mathbb{E}[\lambda_c]$ in terms of λ_t in a general network is difficult to find. However, an upper bound on $\mathbb{E}[\lambda_c]$ can be found in the following lemma, and thus in the special case of clusters with many intended receivers, (3.11) and (3.12) can be simplified to allow a nearly closed-form solution of λ_t (see Section 3.4.2).

Lemma 3.4.2. *The connection intensity λ_c of a non-homogeneous PPP $\Phi^c(\tau)$ in a cluster for Rayleigh fading is shown in (3.11) and its expression for Nakagami- m fading with $m > 1$ is given by (3.12). The upper bound on λ_c for Rayleigh fading is given by*

$$\mathbb{E}_R[\lambda_c(R, \tau)] \leq \lambda_r[1 - (1 - \mathbb{E}_R[\exp(-\pi\lambda_t\Delta_1)])^\tau], \quad (3.14)$$

where $\Delta_1 = \Delta_1(\beta R^\alpha, \infty)$. For Nakagami- m fading with $m > 1$, the upper bound becomes

$$\mathbb{E}_R[\lambda_c(R, \tau)] \leq \lambda_r [1 - (1 - \mathbb{E}_R[\Psi^{(m-1)}(m\beta R^\alpha)])^\tau]. \quad (3.15)$$

Proof. According to the Hölder inequality, for two real-valued random variables D_1 and D_2 , $(\mathbb{E}[D_1 D_2])^p \leq \mathbb{E}[D_1^p] \mathbb{E}[D_2^q]^{p/q}$, where $p, q > 0$ and $1/p + 1/q = 1$. Consider the number of transmission attempts $\tau > 1$ and $D_2 = 1$, and let $p = \tau$ and $q = \frac{\tau}{\tau-1}$. Then it follows that $(\mathbb{E}[D_1])^\tau \leq \mathbb{E}[D_1^\tau]$. For Rayleigh fading, taking average on the both sides of (3.11) and using this property $(\mathbb{E}[D_1])^\tau \leq \mathbb{E}[D_1^\tau]$ by letting $D_1 = 1 - \exp(-\pi \lambda_t \Delta_1(\beta R^\alpha, \infty))$, (3.14) follows. Similarly, (3.15) can be shown in the same way. \square

3.4.2 Single-hop Multicast Transmission Capacity

Now we characterize the MTC in a network when a transmitter directly multicasts its intended receivers in a cluster.

Theorem 3.4.3. *Suppose the multicast outage probability given in (3.8) is upper bounded by small ϵ and the maximum decoding delay is τ transmission attempts. If the average number of the intended receivers in a cluster with radius s is k and $k \geq \frac{1}{\epsilon^{\tau-1}}$, then the maximum contention intensity is*

$$\bar{\lambda}_\epsilon = \frac{\eta \rho \tau^2}{s^2 \beta^\frac{2}{\alpha} \sqrt[\tau]{k}} = \Theta \left(\frac{\rho \tau^2}{s^2 \beta^\frac{2}{\alpha} \sqrt[\tau]{k}} \right), \quad (3.16)$$

where $\rho = \frac{1}{\tau^2} \sqrt[\tau]{\epsilon(\tau+1)}$, β is the SIR threshold for successfully decoding and η is a constant (depending on m , β and α).

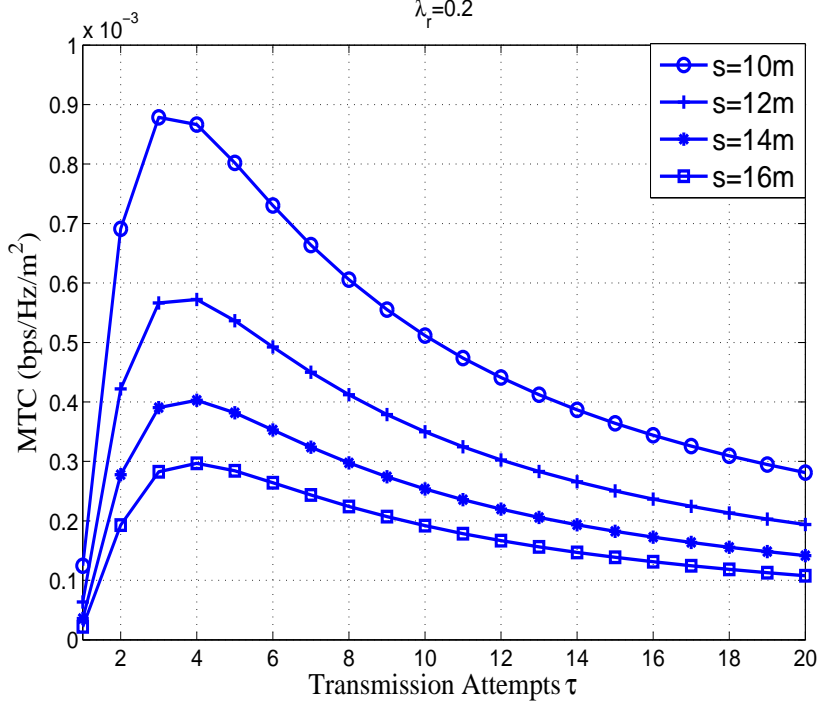


Figure 3.2: The simulated MTC of a large network with Rayleigh fading for $\epsilon = 0.1$, $\beta = 2$, $\alpha = 3$ and $\lambda_r = 0.1$.

Proof. See Appendix 3.7.2. □

Remark 3.4.4. *The scaling function $\Theta(\cdot)$ of $\bar{\lambda}_\epsilon$ in (3.16) only contains the “controllable” network parameters such as s , ϵ , τ and β , which means their values are adjustable if needed. Constant η contains the parameter m of Nakagami fading, which is a channel characteristic and usually uncontrollable and thus η is not left in $\Theta(\cdot)$.*

If a unicast planar network without retransmission is considered (i.e. $k = \tau = 1$), $\bar{\lambda}_\epsilon$ in (3.16) will reduce to the previous results discovered, i.e., $\bar{\lambda}_\epsilon =$

$\Theta\left(\frac{\epsilon}{s^2 \beta^{2/\alpha}}\right)$. In [13], for example, the maximum contention intensities of FH-CDMA and DS-CDMA are $\Theta\left(\frac{\epsilon M}{s^2 \beta^{2/\alpha}}\right)$ and $\Theta\left(\frac{\epsilon M^{2/\alpha}}{s^2 \beta^{2/\alpha}}\right)$ respectively, where M is the channel number of FH-CDMA and the spreading factor of DS-CDMA. It is easy to check that these two results coincide with ours here by considering $\frac{\bar{\lambda}_\epsilon}{M}$ for FH-CDMA and $\frac{\beta}{M}$ for DS-CDMA. In addition, the longest transmission distance in a cluster is s and we know $\bar{\lambda}_\epsilon = \Theta(s^{-2})$ and so is the network capacity, which also coincides with the results in [13] [15].

The result in (3.16) only indicates how much the maximum intensity of transmitters can be supported in a network under the decoding delay and multicast outage constraints. Having the maximum contention intensity only is unable to tell us how much its corresponding MTC should be since the multicast rate b is also affected by the maximum contention intensity. Considering a capacity-approaching code is used, the maximum achievable multicast rate b that is acceptable for all intended receivers is the following ergodic channel capacity evaluated at the boundary of a cluster:

$$b = \mathbb{E} \left[\log \left(1 + \frac{H_{\max} s^{-\alpha}}{I_0} \right) \right]. \quad (3.17)$$

where $H_{\max} = \max_{t \in [1, \dots, \tau]} H(t)$ and $H(t)$ is the fading channel gain for the t -th transmission between typical transmitter X_0 and a receiver located on the cluster boundary. Although there may be no receivers on the boundary of a cluster, multicast rate b should be considered from a worse case point of view because it needs to be acceptable for all intended receivers in any locations within a cluster. The bounds on b are given in the following lemma.

Lemma 3.4.5. *There exists a $\delta \in (0, 1)$ such that the bounds on the multicast rate b in (3.17) can be given by*

$$\delta \log \left(1 + \frac{1}{\pi s^2 \lambda_t} \right) \leq b \leq \log \left(1 + \frac{1}{\pi s^2 \lambda_t} \right) + O(1). \quad (3.18)$$

Proof. See Appendix 3.7.3. □

Remark 3.4.6. *The bounds on the multicast rate in (3.18) are not affected by channel fading because the fading effect has been averaged out. Lemma 3.4.5 suggests that b is significantly reduced by the aggregate interference from the transmitters in the cluster and the transmitters out of the cluster only reduce it by at most a constant.*

Scaling Law of Single-hop MTC. According to Theorem 3.4.3 and Lemma 3.4.5, we found that the multicast rate b is $\Theta(\log(k)/\tau)$ for any network conditions if $\bar{\lambda}_\epsilon$ is achieved and k is sufficiently large. The MTCs in a network without receiver cooperation can be concluded as follows. (i) For a dense network, $\bar{\lambda}_\epsilon = \Theta\left(\frac{\rho\tau^2}{\sqrt[3]{k}}\right)$ since πs^2 is fixed and $k \gg 1$. By the MTC definition, we know $C_\epsilon = \Theta\left(\frac{\rho \log(k)}{\sqrt[3]{k}}\right)$. (ii) If the network is large, then $\bar{\lambda}_\epsilon = \Theta\left(\frac{\rho\tau^2}{k^{1+1/\tau}}\right)$ and thus $C_\epsilon = \Theta\left(\frac{\rho \log(k)}{k^{(1+1/\tau)}}\right)$. (iii) For a large dense network, $\lambda_r = \Theta(s^2)$ and $k \gg 1$. So $\bar{\lambda}_\epsilon$ is $\Theta\left(\rho\tau^2 k^{-\left(\frac{\tau+2}{2\tau}\right)}\right)$ and thus $C_\epsilon = \Theta\left(\rho k^{-\left(\frac{\tau+2}{2\tau}\right)} \log(k)\right)$. In summary, the MTC here can be expressed in a general form as follows:

$$C_\epsilon = \Theta\left(\rho k^x \log(k)\right), \quad (3.19)$$

where x has been given in Table 3.2. Note again that the scaling function $\Theta(\cdot)$ is applied only to the main controllable variables for a specific network. For

example, the main controllable parameters for a dense network are λ_r (or k) and τ whereas πs^2 is a constant.

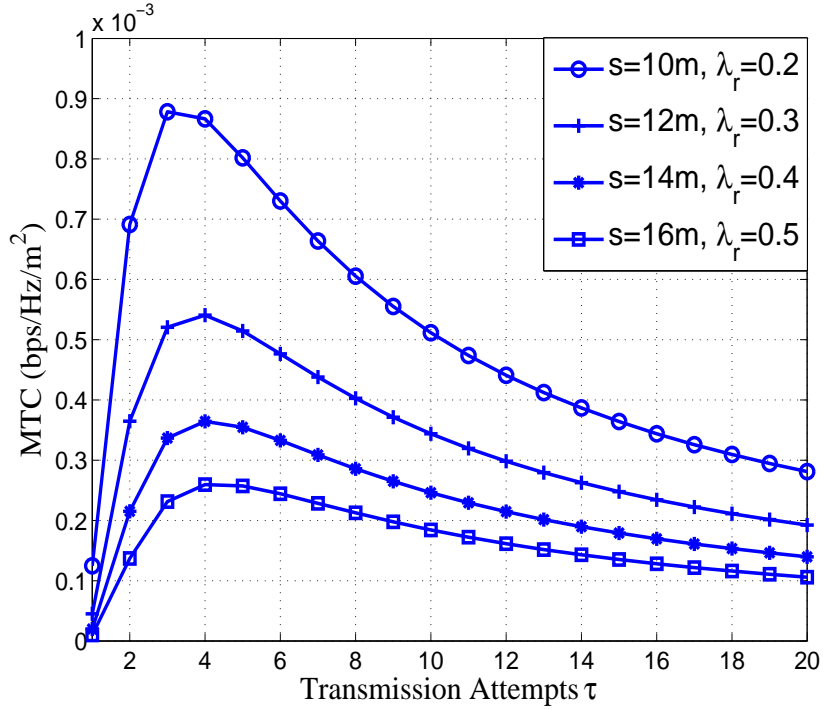


Figure 3.3: The simulated MTC of a large dense network with Rayleigh fading for $\epsilon = 0.1$, $\beta = 2$ and $\alpha = 3$.

A simulation example of the MTCs for a large network with Rayleigh fading is presented in Figure 3.2. One can see that the MTCs decrease when s increases (i.e. k increases), and slightly increasing the radius of a cluster can significantly reduce the MTC. The decoding delay constraint τ has a significant effect on the MTCs as well. Since retransmissions decrease outage probability as well as increase interference, it can be observed from (3.10) that there exists an optimal tradeoff between τ and $\bar{\lambda}_\epsilon$. This can be observed in Figure 3.2, for

example, the MTC of $\tau = 3$ is larger than that of $\tau = 10$, which indicates a few retransmissions indeed increase the MTC and too many retransmissions are, on the contrary, detrimental to it. Figure 3.3 presents the MTC results for a large dense network with Rayleigh fading. If we compare Figure 3.3 with Figure 3.2, we can see that denseness does not have a serious impact on MTC as largeness. This observation coincides with the scaling law stated in above. Thus, path loss is the main key issue of limiting the MTC, which enlightens us the idea of using multihop multicast to deliver packets with a less path loss (see Section 3.5).

3.5 Multicast Transmission Capacity with Multihop Multicast

The MTCs for single-hop multicast investigated in Section 3.4 scale like $\Theta(s^{-2})$ if other network parameters are fixed. Therefore, the single-hop MTC increases when its multicast cluster is shrunk. However, shrinking the cluster is not welcome if the packets must be transmitted over the same coverage. So here we would like to know if there is another method to increase the MTC without shrinking the cluster. From previous results, for sufficiently large k the scaling of the single-hop MTC can be written as

$$C_\epsilon = \Theta\left(\frac{\rho k^x \log(k)}{s^2 \beta_\alpha^{\frac{2}{\alpha}}}\right), \quad (3.20)$$

where $\rho = \frac{1}{\tau^2} \sqrt[\tau]{\epsilon(\tau+1)}$ and $x = -\frac{1}{\tau}$. So (3.20) suggests three approaches to increasing the MTC: interference-avoidance, interference-suppression and area-shrinking methods. The capacity gain due to interference avoidance can be

acquired by removing co-channel interferers such that $\text{SIR}(\lambda_t)$ is improved by reducing λ_t . This is the context when each transmitter independently selects its own transmission channel from several available channels (see the case of FH-CDMA in [13]). Interference avoidance does not affect any network parameters except the multicast rate b . The interference-suppression capacity gain can be obtained by signal processing techniques to increase the SIR so that multicast rate b is increased (see the case of DS-CDMA in [13]). In addition, suppressing interference is equivalent to relaxing the SIR threshold β and thus pre-constant η depending on β is increased. Of course, the area-shrinking capacity gain is attained by multicasting in a smaller region instead of the whole cluster. Shrinking a cluster only leads to a decrease in the cluster radius s and thus the average number of the intended receivers k becomes smaller.

Let $\{g_a, g_s, g_v\} > 1$ be the interference-avoidance, interference-suppression and area-shrinking gain parameters, respectively. Then respectively replacing s^2 , β and $\bar{\lambda}_\epsilon$ by s^2/g_v , β/g_s and $\bar{\lambda}_\epsilon/g_a$ in (3.20), we obtain

$$C_\epsilon = \Theta \left(\frac{\rho g_a g_s^{2/\alpha} g_v^{1-x} k^x \log(k)}{s^2 \beta^\alpha} \right). \quad (3.21)$$

The three gain parameters in (3.21) indicate which method is able to contribute more to the MTC in each context. The interference-avoidance method is superior to interference-suppression when g_a and g_s are equal because $g_a/g_s^{2/\alpha} > 1$ due to $\alpha > 2$. This point has been shown for FH-CDMA and DS-CDMA in [13]. If the cluster is shrunk to a smaller region of area $\pi s^2/g_v$ and all the three gain parameters are equal, then shrinking is the best way to improve the MTC. According to (3.21), we can conjecture that the MTC could be increased if the cluster is

tessellated into several smaller regions and a packet is allowed to be multicasted in each of them up to some times under the condition that the decoding delay and multicast outage constraints both have to be satisfied. This conjecture will be verified later in the following subsection.

3.5.1 Multicast over Multihop

Suppose the cluster \mathcal{R}_0 is tessellated into a certain number of smaller multicast regions of equal area. A packet is multicasted the same number of times (called a multicast time slot) in each tessellated region. So the packet is delivered slot by slot from the central typical transmitter to those regions in a certain order. Note that the number of the tessellated regions cannot exceed the decoding delay constraint τ , *i.e.*, the packet is delivered to all its intended receivers at most $\tau - 1$ hops. As shown in Figure 3.4, for example, each cluster consists of 6 smaller tessellated regions and the decoding delay constraint for each region is 2 if $\tau = 12$.

Delivering a packet by the multihop multicast method proceeds as follows. In the first time slot, the typical transmitter aims at multicasting its own region. In the second time slot, the typical transmitter randomly selects a receiver in the neighboring regions that successfully received the packet in the previous time slot, then the selected receiver becomes the transmitter for the next time slot. The multihop multicast method proceeds slot by slot in this way until all the tessellated regions are visited by the packet. Note that in each time slot the transmitter is asked to ensure all the receivers in its region and at least one

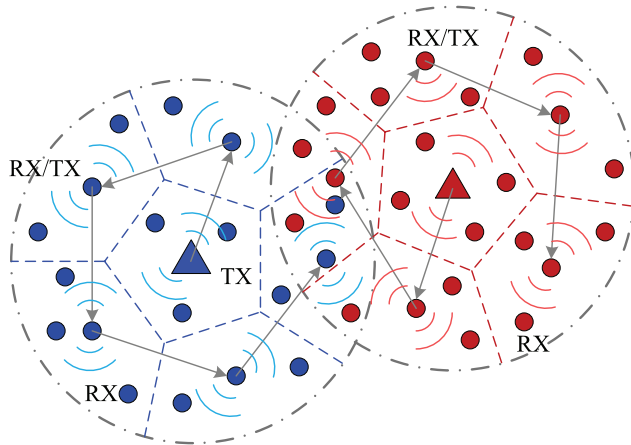


Figure 3.4: Each multicast cluster in a planar network is tessellated into 6 smaller multicast regions of equal area. The arrows in each cluster show an example path of delivering a packet over the tessellated regions by the multihop multicast method.

receiver in the neighboring regions should receive the packet; otherwise, there is an outage. In addition, although there might be more than one receivers in the neighboring regions which successfully receive the packet; however, only one of them is selected to multicast in the next time slot in order to satisfy the assumption of the PPP of the transmitters (see Proposition 3.6.2 in Appendix 3.6.2 for the dual property between PCP and PPP). The scaling realizations of the maximum contention intensity for the above multihop multicast method are shown in the following theorem.

Theorem 3.5.1. *Suppose cluster \mathcal{R}_0 is tessellated into v smaller multicast regions of equal area and each packet is allowed to be multicasted in each region at most τ/v times. If the average number of the intended receivers in a cluster*

$k \geq \frac{v}{\epsilon^{\tau/v-1}}$, then the following scaling characterization of the maximum contention intensity $\bar{\lambda}_\epsilon$ is achieved with high probability:

$$\bar{\lambda}_\epsilon = \frac{\eta k^x v^y \tau^2 \rho}{s^2 \beta^{\frac{2}{\alpha}}} = \Theta \left(\frac{k^x v^y \tau^2 \rho}{s^2 \beta^{\frac{2}{\alpha}}} \right), \quad (3.22)$$

where $x = -\frac{v}{\tau}$, $y = \frac{v}{\tau} + 1$, $\rho = \frac{1}{\tau^2} (\epsilon(\tau/v + 1))^{\frac{v}{\tau}}$ and η is a constant depending on m , β and α .

Proof. See Appendix 3.7.4. □

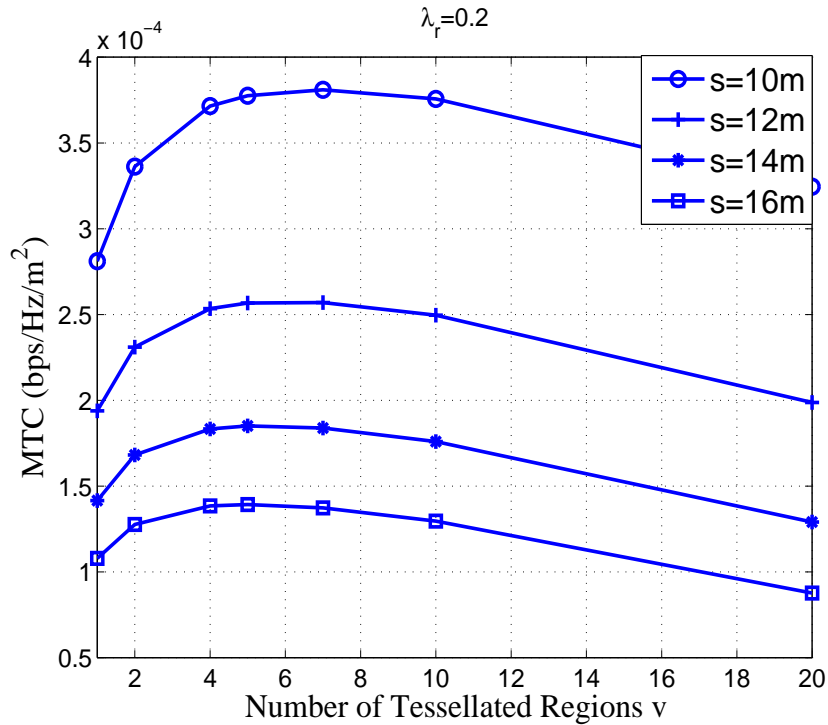


Figure 3.5: The simulated MTC achieved by multihop multicast in a large network with Rayleigh fading for $\epsilon = 0.1$, $\beta = 2$, $\alpha = 3$, $\tau = 20$ and $\lambda_r = 0.2$.

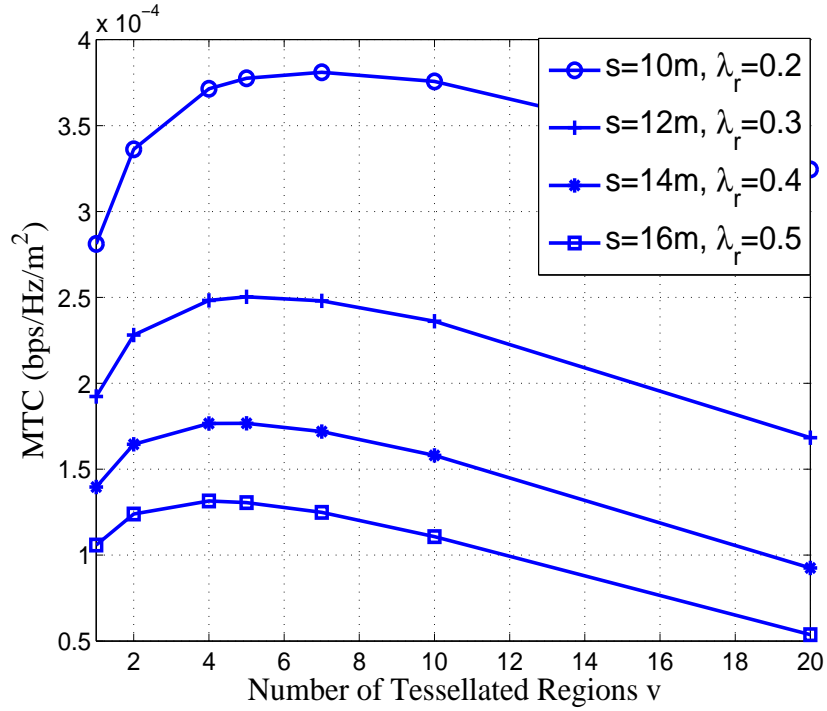


Figure 3.6: The simulated MTC achieved by multihop multicast in a large dense network with Rayleigh fading for $\epsilon = 0.1$, $\beta = 2$, $\alpha = 3$ and $\tau = 20$.

By comparing (3.16) and (3.22), it is hard to see if the multihop multicast method achieves a larger $\bar{\lambda}_\epsilon$. Nevertheless, in the following subsection we will show that $\bar{\lambda}_\epsilon$ and its corresponding MTC indeed achieve a larger value by multihop multicast. The simulation result of the MTC with multihop multicast in a large network with Rayleigh fading and $\lambda_r = 0.2$ is presented in Figure 3.5, and it is easy to observe that tessellating the cluster into a certain number of regions improves the MTC whereas too many tessellations degrades it. Figure 3.6 shows the simulation of the MTC achieved by multihop multicast in a large dense network with Rayleigh fading. If we compare Figure 3.6 with Figure 3.5,

we can find that the curves in these two figures are not very much different. This point is quite different from the case of single-hop multicast (see Figs. 3.2 and 3.3), and therefore, it reveals that multihop multicast is able to efficiently alleviate the impact on MTC due to denseness. How to tessellate the cluster to achieve a larger MTC will be discussed in the following subsection. In addition, there exists another time-division multicast method to multicast in Figure 3.4. Namely, the typical transmitter multicasts a smaller region in each time slot. We can show that this time-division multicast method attains a less $\bar{\lambda}_\epsilon$ than the multihop multicast method. Since it just uses the same transmitter to multicast, the average distance from the transmitter to the intended receivers is longer than that of the multihop multicast method. So time-division multicast has a larger path loss so that the receivers have a lower SIR and thus less cluster transmissions are allowed.

3.5.2 Capacity Gain Achieved by Multihop Multicast

According to Theorem 3.5.1, the MTC with multihop multicast obtained from (3.22) and $b = \Theta(\log(k)/\tau)$ can be concluded as follows

$$C_\epsilon = \Theta \left(\frac{\rho k^x v^y \log(k)}{s^2 \beta_\alpha^{\frac{2}{\alpha}}} \right). \quad (3.23)$$

Since just comparing (3.23) with its single-hop counterpart (3.20) is hard to see if multihop multicast achieves a larger MTC or not, defining a capacity gain g_c as follows can help us understand when multihop multicast is better than single-hop multicast.

$$g_c(v) \triangleq 10 \log_{10} \left[\frac{C_\epsilon \text{ in (3.23)}}{C_\epsilon \text{ in (3.20)}} \right], \text{ (dB)}. \quad (3.24)$$

Since the capacity gain is dependent on v , we can formulate an optimization problem with constraints on v as follows.

$$\begin{aligned} & \min_v -g_c(v), & (3.25) \\ \text{subject to} & \quad 1 - v \leq 0 \text{ and } v - \tau \leq 0. \end{aligned}$$

Hence, if there exists a minimizer v such that the minimum of $-g_c$ is negative, then multihop multicast achieves a higher MTC than single-hop multicast. The problem in (3.25) is a convex optimization problem as shown in the following theorem.

Theorem 3.5.2. *Suppose a packet is delivered by the multihop multicast method and each cluster is tessellated into v smaller multicast regions of equal area. (3.25) is a convex optimization problem and thus there exists a unique feasible solution of v to it.*

Proof. We have to verify that the optimization problem in (3.25) is convex and it has only one optimal solution of v . In other words, we have to show that $-g_c$ is strictly convex. Now considering the noncooperative receiver case, the capacity gain in (3.24) can be explicitly expressed as follows:

$$\begin{aligned} \frac{g_c}{10} &= \left(\frac{1-v}{\tau}\right) \log_{10}\left(\frac{k}{\epsilon}\right) + \frac{v}{\tau} \log_{10}\left(1 + \frac{v}{\tau}\right) + \\ &\quad \left(\frac{v}{\tau} + 2\right) \log_{10}(v) - \frac{\log_{10}(1+\tau)}{\tau} \\ &= z \log_{10}\left(\frac{\tau\epsilon}{k}\right) + z \log_{10}(1+z) + (2+z) \log_{10}(z) \\ &\quad + 2 \log_{10}(\tau) + \frac{1}{\tau} \log_{10}\left(\frac{k}{\epsilon(1+\tau)}\right), \end{aligned}$$

where $z = \frac{v}{\tau}$. Taking the derivative of the above equation with respect to z twice and letting $\frac{d^2 g_c}{dz^2} < 0$, it yields the inequality $(1 + \tau/v)\sqrt{(2\tau - v)/(2\tau + v)} > 1$, which is always true for all $\tau \in \mathbb{N}_+$. Thus, $-g_c$ is strictly convex. \square

Theorem 3.5.2 indicates that the proposed multihop multicast method can achieve a larger MTC than single-hop multicast since g_c is strictly concave. The reason that multicasting in the smaller regions hop by hop can increase the MTC is because the average number of intended receivers in a tessellated region and path loss are largely reduced, and thus merely few retransmissions are able to make the multicast outage probability lower its designated upper bound. So the increase in $\bar{\lambda}_c$ is over the loss in spectral efficiency. For time-division multicast, no capacity gain is achieved by it since its capacity gain function is also negative convex.

3.6 Appendix I : Useful Propositions

3.6.1 Moment Generating Functional of Stationary Independent PPPs

Proposition 3.6.1. *Let $\mathcal{B}(0, r)$ be a circular disc centered at the origin with radius r and $\Phi_i = \{(X_{ij}, H_{ij}) : X_{ij} \in \mathcal{B}(0, r) \cap \mathbb{R}^2, r \geq 1, j \in \mathbb{N}\}$ be a stationary marked PPP of intensity λ_i for all $i \in [1, 2, \dots, L]$ and $\{\sqrt{H_{ij}}\}$ are i.i.d. Nakagami- m random variables with unit mean and variance. Suppose Φ_i has a Poisson shot generating function $I_i : \mathbb{R}_+^2 \times \mathbb{R}_+ \rightarrow \mathbb{R}_+$ which is defined as $I_i \triangleq \sum_{X_i \in \Phi_i} H_{ij} \ell(|X_{ij}|)$ where $\alpha > 2$. If $\{\Phi_i\}$ are independent, then the sum of the Poisson shot generating functions, i.e. $I = \sum_{i=1}^L I_i$, has the following moment*

generating functional:

$$\mathcal{L}_I(\phi_1) = \mathbb{E} [e^{-\phi_1 I}] = \exp \left(-\pi \Delta_1(\phi_1, r) \sum_{i=1}^L \lambda_i \right), (\phi_1 > 0) \quad (3.26)$$

$$\mathcal{M}_I(\phi_2) = \mathbb{E} [e^{\phi_2 I}] = \exp \left(\pi \Delta_2(\phi_2, r) \sum_{i=1}^L \lambda_i \right), (\phi_2 \in (0, m r^\alpha)) \quad (3.27)$$

where

$$\Delta_1(\phi_1, r) \triangleq \frac{2}{\alpha} \left(\frac{\phi_1}{m} \right)^{\frac{2}{\alpha}} \sum_{j=0}^{m-1} \binom{m}{j} \int_{m/\phi_1}^{m r^\alpha / \phi_1} \frac{t^{j-1+\frac{2}{\alpha}}}{(1+t)^m} dt, \quad (3.28)$$

$$\Delta_2(\phi_2, r) \triangleq \frac{2}{\alpha} \left(\frac{\phi_2}{m} \right)^{\frac{2}{\alpha}} \sum_{j=0}^{m-1} (-1)^j \binom{m}{j} \int_{m/\phi_2}^{m r^\alpha / \phi_2} \frac{t^{j+\frac{2}{\alpha}}}{(1-t)^m} dt. \quad (3.29)$$

Proof. Since the marks $\{H_{ij}\}$ for all points $\{X_{ij}\}$ in their corresponding PPP are i.i.d. Nakagami- m random variables with unit mean and variance $\frac{1}{m}$, their probability density function is given in (3.2) and rewritten in below for convenience:

$$f_H(h) = \frac{m^m}{\Gamma(m)} h^{m-1} \exp(-mh).$$

Thus the Laplace transform of $f_H(h)$ is

$$\begin{aligned} \mathcal{L}_H(w) &= \int_0^\infty e^{-wh} f_H(h) dh \\ &= \frac{m^m}{\Gamma(m)} \int_0^\infty e^{-(w+m)h} h^{m-1} dh \\ &= \frac{1}{(1+w/m)^m}. \end{aligned}$$

Moreover, the Laplace transform for a Poisson shot process Φ_i with i.i.d. marks $\{H_{ij}\}$ is given by [69]

$$\mathcal{L}_{I_i}(\phi_1) = \exp \left\{ -\lambda_i \int_{\mathcal{B}(0,r)} (1 - \mathbb{E}_H [e^{-\phi_1 H \ell(|X|)}]) dX \right\}, \quad (3.30)$$

and we also know

$$\begin{aligned}\mathbb{E}_H [e^{-\phi_1 H \ell(|X|)}] &= \int_0^\infty e^{-\phi_1 \ell(|X|)h} f_H(h) dh \\ &= \mathcal{L}_H(\phi_1 \ell(|X|)).\end{aligned}\quad (3.31)$$

Substituting (3.31) into (3.30) and it follows that

$$\begin{aligned}\mathcal{L}_{I_i}(\phi_1) &= \exp\left(-\lambda_i \int_{\mathcal{B}(0,r)} \left[1 - \left(1 + \frac{\phi_1 \ell(|X|)}{m}\right)^{-m}\right] dX\right) \\ &= \exp\left(-2\pi\lambda_i \left\{ \int_1^r \left[1 - \left(\frac{mx^\alpha}{mx^\alpha + \phi_1}\right)^m\right] x dx \right\}\right) \\ &= \exp\left(-\pi\lambda_i \left[\frac{2}{\alpha} \left(\frac{\phi_1}{m}\right)^{\frac{2}{\alpha}} \sum_{j=0}^{m-1} \binom{m}{j} \int_{m/\phi_1}^{mr^\alpha/\phi_1} \frac{t^{j-1+\frac{2}{\alpha}}}{(1+t)^m} dt\right]\right) \\ &= \exp(-\pi\lambda_i \Delta_1(\phi_1, r)).\end{aligned}\quad (3.32)$$

Since all the PPPs are independent, it yields the following desired result:

$$\mathcal{L}_I(\phi_1) = \prod_{i=1}^L \mathbb{E} [e^{-\phi_1 I_i}] = \exp\left(-\pi \Delta_1(\phi_1, r) \sum_{i=1}^L \lambda_i\right).$$

Now consider the case of $\mathcal{M}_I(\phi_2)$. Similar to $\mathcal{L}_{I_i}(\phi_1)$, $\mathcal{M}_{I_i}(\phi_2)$ can be written as

$$\mathcal{M}_{I_i}(\phi_2) = \exp\left\{\lambda_i \int_{\mathcal{B}(0,r)} (1 - \mathbb{E}_H [e^{\phi_2 H \ell(|Y|)}]) dY\right\}.\quad (3.33)$$

We also know $\mathcal{M}_H(w) = \int_0^\infty e^{wh} f_H(h) dh = \frac{1}{(1-w/m)^m}$ if $w \in (0, m)$ and

$\mathbb{E}_H[\exp(\phi_2 H \ell(|Y|))] = \mathcal{M}_H(\phi_2 \ell(|Y|))$ because $\phi_2 \in (0, m r^\alpha)$. Then following the

same steps in (3.32), we can show that

$$\begin{aligned}\mathcal{M}_{I_i}(\phi_2) &= \exp\left(\pi\lambda_i \left[\frac{2}{\alpha} \left(\frac{\phi_2}{m}\right)^{\frac{2}{\alpha}} \sum_{j=0}^m \binom{m}{j} (-1)^j \int_{m/\phi_2}^{mr^\alpha/\phi_2} \frac{t^{j+\frac{2}{\alpha}}}{(1-t)^m} dt\right]\right) \\ &= \exp(\pi\lambda_i \Delta_2(\phi_2, r)).\end{aligned}\quad (3.34)$$

Therefore, $\mathcal{M}_I(\phi_2) = \exp\left(\pi \Delta_2(\phi_2, r) \sum_{i=1}^L \lambda_i\right)$. \square

3.6.2 The Duality between PCP and PPP

Proposition 3.6.2. *A stationary Poisson cluster process (PCP) can be constructed by a given stationary Poisson point process (PPP). Similarly, for a given Poisson cluster process (PCP) a Poisson point process can be constructed from it as well.*

Proof. The first statement is based on the definition of a PCP [57]. Consider a stationary PPP Φ^d of intensity λ_d is given. Then we replace each point $X_j \in \Phi^d$ with a random finite set of points Z_{X_j} which is called the cluster associated with point X_j . Then the superposition of all clusters yields the stationary PCP $\mathcal{Z}^d = \bigcup_{X_j \in \Phi^d} Z_{X_j}$. Suppose now a stationary PCP \mathcal{Z}^d is given. In the following we are going to show that a PPP can be constructed by randomly selecting a point in each cluster. Let \mathcal{A} be a bounded Borel set, Φ^d be the PPP formed by all parent points in \mathcal{Z}^d , and $\tilde{\Phi}^d$ consists of the points randomly selected from all clusters of \mathcal{Z}^d . The capacity functional of $\tilde{\Phi}^d$ is defined as follows [57]:

$$\tilde{T}_d(\mathcal{A}) \triangleq \mathbb{P}[\mathcal{A}(\tilde{\Phi}^d) > 0], \quad (3.35)$$

where $\mathcal{A}(\tilde{\Phi}^d)$ denotes the numbers of points of $\tilde{\Phi}^d$ in a bounded set $\mathcal{A} \subset \mathbb{R}^2$. Since the capacity functional of a point process completely characterizes its distribution, $\tilde{\Phi}^d$ is a stationary PPP if we can show

$$\tilde{T}_d(\mathcal{A}) = \mathbb{P}[\mathcal{A}(\Phi^d) > 0] = 1 - \exp(-\lambda_d \mu(\mathcal{A})),$$

where $\mu(\mathcal{A})$ denotes the Lebesgue measure of set \mathcal{A} .

Consider a large bounded Borel set \mathcal{C} such that $\mathcal{A} \subset \mathcal{C}$ and \mathcal{C} encloses all clusters of \mathcal{Z}^d . So $\mathcal{C}(\Phi^d)$ is a Poisson random variable of parameter $\lambda_d \mu(\mathcal{C})$.

Since $\tilde{\Phi}^d$ is formed by the points that randomly selected by all points in Φ^d , the probability that all points in $\tilde{\Phi}^d$ are not in \mathcal{A} is

$$\begin{aligned} \mathbb{P} \left[\mathcal{A}(\tilde{\Phi}^d) = 0 \right] &= \mathbb{P} \left[\mathcal{A}(\tilde{\Phi}^d) = 0 | \mathcal{C}(\tilde{\Phi}^d) = 0 \right] \mathbb{P} \left[\mathcal{C}(\tilde{\Phi}^d) = 0 \right] \\ &\quad + \mathbb{P} \left[\mathcal{A}(\tilde{\Phi}^d) = 0 | \mathcal{C}(\tilde{\Phi}^d) \neq 0 \right] \mathbb{P} \left[\mathcal{C}(\tilde{\Phi}^d) \neq 0 \right]. \end{aligned}$$

Since $\tilde{\Phi}^d$ is generated from Φ^d and \mathcal{C} covers all clusters of \mathcal{Z}^d , $\mathbb{P} \left[\mathcal{C}(\tilde{\Phi}^d) = 0 \right] = \mathbb{P}[\mathcal{C}(\Phi^d) = 0]$ and thus it follows that

$$\begin{aligned} \mathbb{P} \left[\mathcal{A}(\tilde{\Phi}^d) = 0 \right] &= 1 \cdot \mathbb{P}[\mathcal{C}(\Phi^d) = 0] \\ &\quad + \mathbb{P} \left[\mathcal{A}(\tilde{\Phi}^d) = 0 | \mathcal{C}(\Phi^d) \neq 0 \right] (1 - \mathbb{P}[\mathcal{C}(\Phi^d) = 0]) \\ &= \exp(-\lambda_d \mu(\mathcal{C})) \\ &\quad + \mathbb{P} \left[\mathcal{A}(\tilde{\Phi}^d) = 0 | \mathcal{C}(\Phi^d) \neq 0 \right] (1 - \exp(-\lambda_d \mu(\mathcal{C}))). \end{aligned}$$

Now letting $\mu(\mathcal{C}) \rightarrow \infty$ (i.e. considering an infinitely large network), we can have

$$\mathbb{P} \left[\mathcal{A}(\tilde{\Phi}^d) = 0 | \mathcal{C}(\Phi^d) \neq 0 \right] = \lim_{\mu(\mathcal{C}) \rightarrow \infty} \left(1 - \frac{\lambda_d \mu(\mathcal{A})}{\lambda_d \mu(\mathcal{C})} \right)^{\lambda_d \mu(\mathcal{C})} = \exp(-\lambda_d \mu(\mathcal{A})).$$

Therefore, $\tilde{T}_d(\mathcal{A}) = 1 - \exp(-\lambda_d \mu(\mathcal{A}))$ and $\tilde{\Phi}^d$ is a stationary PPP. \square

3.7 Appendix II : Proofs of Lemmas and Theorems

3.7.1 Proof of Lemma 3.4.1

The Laplace functional of the stationary PPP Φ for a nonnegative function $g : \mathbb{R}^2 \rightarrow \mathbb{R}_+$ is defined and shown as follows [17]:

$$\tilde{\mathcal{L}}_\Phi(g) \triangleq \mathbb{E} \left[e^{-\int_{\mathbb{R}^2} g(X) \Phi(dX)} \right] = \exp \left(- \int_{\mathbb{R}^2} (1 - e^{-g(X)}) \lambda_r \mu(dX) \right).$$

Since the Laplace functional completely characterizes the distribution of the point process, we can find the intensity of Φ^c by looking for $\tilde{\mathcal{L}}_{\Phi^c}(g)$. Recall that $\Phi^c = \{Y_j \in \Phi_0^r : \max_{t \in [1, \dots, \tau]} H_j(t) \ell(|Y_j|) \geq \beta I_0\}$ and $\{H_j(t)\}$ are i.i.d. $\forall t \in [1, 2, \dots, \tau]$. Let $\mathbb{1}_{\mathcal{A}}(x)$ be an indicator function which is equal to 1 if $x \in \mathcal{A}$ and 0, otherwise. The Laplace functional of Φ^c for $g(Y) = \tilde{g}(Y) \mathbb{1}_{\Phi^c}(Y)$ is given by

$$\begin{aligned} \tilde{\mathcal{L}}_{\Phi^c}(g) &= e^{-\pi s^2 \lambda_r} \sum_{i=0}^{\infty} \frac{\lambda_r^i}{i!} \int_{\mathcal{R}_0} \dots \int_{\mathcal{R}_0} \prod_{j=1}^i \left(e^{-g(Y_j)} \mathbb{P}[Y_j \in \Phi^c] + \mathbb{P}[Y_j \notin \Phi^c] \right) \\ &\quad \mu(dY_1) \dots \mu(dY_i) \\ &= e^{-k} \sum_{i=0}^{\infty} \frac{1}{i!} \left(\int_{\mathcal{R}_0} (e^{-g(Y)} \mathbb{P}[Y \in \Phi^c] + 1 - \mathbb{P}[Y \in \Phi^c]) \lambda_r \mu(dY) \right)^i \\ &= \exp \left(- \int_{\mathcal{R}_0} (1 - e^{-g(Y)}) \mathbb{P}[Y \in \Phi^c] \lambda_r \mu(dY) \right). \end{aligned}$$

Also, for all $r \in [1, s]$ and considering $\lambda_t = \Theta(\epsilon)$, we have

$$\begin{aligned} \mathbb{P}[Y \in \Phi^c] &= \mathbb{P}[H_j(t) \ell(|Y|) \geq \beta I_0(t), t = 1, \dots, \tau] \\ &\stackrel{(a)}{=} 1 - (\mathbb{P}[H \ell(|Y|) < \beta I_0])^\tau \\ &= 1 - (\mathbb{E}_I[F_H(\beta r^\alpha I_0 | I_0)])^\tau. \end{aligned} \tag{3.36}$$

where (a) follows from the fact that the temporal correlation of interference can be neglected for small λ_t [70]. Thus, we have

$$\tilde{\mathcal{L}}_{\Phi^c}(g) = \exp \left(- \int_1^s (1 - e^{-g(r)}) \lambda_c(r, \tau) \mu(dr) \right),$$

where $\lambda_c(r, \tau) = \lambda_r (1 - (\mathbb{E}_I[F_H(\beta r^\alpha I_0 | I_0)])^\tau)$. From the above result we know that $\Phi^c \subseteq \Phi_0^r$ is a nonhomogeneous PPP because its intensity $\lambda_c(r, \tau)$ is the intensity λ_r of Φ_0^r scaled by (3.36).

First consider \sqrt{H} is Rayleigh fading. We can have the following:

$$\begin{aligned}\mathbb{E}_I [F_H(\beta r^\alpha I_0)|I_0] &= \int_{\mathbb{R}_+} F_H(\beta r^\alpha \omega) f_{I_0}(\omega) d\omega \\ &= 1 - \int_0^\infty e^{-\beta r^\alpha w} f_{I_0}(w) dw \\ &\stackrel{(b)}{=} 1 - \mathcal{L}_{I_0}(\beta r^\alpha),\end{aligned}$$

where (b) follows from the result of Proposition 3.6.1 in Appendix 3.6.1. So using (3.26) and (3.28), it follows that

$$\lambda_c(r, \tau) = \lambda_r \{1 - [1 - \exp(-\pi \Delta_1(\beta r^\alpha, \infty) \lambda_t)]^\tau\}.$$

Now if \sqrt{H} is a Nakagami- m random variable, then we can have the following:

$$\begin{aligned}\mathbb{E}_I [F_H(\beta r^\alpha I_0)|I_0] &= \int_{\mathbb{R}_+} F_H(\beta r^\alpha \omega) f_{I_0}(\omega) d\omega \\ &= 1 - \int_0^\infty \frac{\Gamma(m, m\beta r^\alpha \omega)}{\Gamma(m)} f_{I_0}(\omega) d\omega,\end{aligned}$$

where $\Gamma(y, x) = \int_x^\infty t^{y-1} e^{-t} dt$ is the incomplete Gamma function and $\Gamma(m, 0) = \Gamma(m) = (m-1)!$. Also, if $f_W(w)$ is a probability density function of random variable W then we can have the following result for $m > 1$:

$$\begin{aligned}\int_0^\infty \Gamma(m, aw) f_W(w) dw &= \int_0^\infty \int_{aw}^\infty t^{m-1} e^{-t} f_W(w) dt dw \\ &= (-1)^{m-1} a^m \frac{d^{m-1}}{da^{m-1}} \left(\frac{\mathcal{L}_W(a)}{a} \right).\end{aligned}\quad (3.37)$$

According to Proposition 3.6.1 in Appendix 3.6.1, we can have $\mathcal{L}_{I_0}(\phi)$ with $\Delta_1(\phi, \infty)$. Thus,

$$\begin{aligned}\mathbb{E}_I [F_H(\beta r^\alpha I_0|I_0)] &= 1 + \frac{(-\phi)^m}{\Gamma(m)} \frac{d^{m-1}}{d\phi^{m-1}} \left(\frac{\mathcal{L}_{I_0}(\phi)}{\phi} \right) \Big|_{\phi=m\beta r^\alpha} \\ &= 1 - \Psi^{(m-1)}(m\beta r^\alpha).\end{aligned}\quad (3.38)$$

Substituting (3.38) into (3.36), then the result in (3.12) can be arrived.

3.7.2 Proof of Theorem 3.4.3

Here we only provide the proof for Nakagami- m fading with $m > 1$ since the proof for Rayleigh fading is similar. According to the outage probability (3.8) upper bounded by ϵ , we know

$$\mathbb{E}_R[\lambda_c(R, \tau)] \geq \lambda_r + \frac{\log(1 - \epsilon)}{\pi s^2} = \lambda_r \left(1 - \frac{\epsilon}{k}\right) + \Theta(\epsilon^2),$$

for sufficiently small ϵ . Using the upper bound in (3.15) and the lower bound on $\mathbb{E}_R[\lambda_c(R, \tau)]$ obtained in above, it follows that

$$\mathbb{E}_R \left[(1 - \Psi^{(m-1)}(m\beta R^\alpha))^\tau \right] \leq \frac{\epsilon}{k}. \quad (3.39)$$

Therefore, we further have

$$\mathbb{E}_R[\Psi^{(m-1)}(m\beta R^\alpha)] \geq 1 - \sqrt[\tau]{\frac{\epsilon}{k}}. \quad (3.40)$$

Note that $\mathbb{E}_R[\Psi^{(m-1)}(m\beta R^\alpha)]$ is upper bounded by one and thus it approaches to unity when ϵ/k is sufficiently small such that $\sqrt[\tau]{\epsilon/k} \leq \epsilon$. That means $\Psi^{(m-1)}(m\beta R^\alpha)$ is very close to 1 almost surely and thus $\lambda_t = \Theta(\epsilon)$. If k is sufficiently large, then we have $\exp(-\pi \lambda_t \Delta_1) = 1 - \pi \lambda_t \Delta_1 + \Theta(\epsilon^2)$. Substituting this expression into (3.13), $\Psi^{(m-1)}(m\beta R^\alpha)$ can be reduced to $1 - \pi \lambda_t \Delta_1 \prod_{j=1}^{m-1} (1 - 2/j\alpha) + \Theta(\epsilon^2)$. Define $\hat{\Delta}_1(\phi) \triangleq [\Delta_1(\phi, \infty) - \Delta_1(\phi, \hat{a})] \prod_{j=1}^{m-1} (1 - 2/j\alpha)$. Choosing $0 \leq \hat{a} \leq 1$, we have

$$\begin{aligned} \mathbb{E}_R \left[(1 - \Psi^{(m-1)}(m\beta R^\alpha))^\tau \right] &\leq \left[\hat{\Delta}_1(\beta) \pi \lambda_t \right]^\tau \mathbb{E}[R^{2\tau}] + \Theta(\epsilon^2) \\ &= \frac{\left[\pi s^2 \hat{\Delta}_1(\beta) \lambda_t \right]^\tau}{(\tau + 1)} + \Theta(\epsilon^2). \end{aligned}$$

According to (3.39) and the above result, these two upper bounds should coincide when the maximum contention intensity $\bar{\lambda}_t$ is reached. Namely, (3.16) is obtained from the following:

$$\bar{\lambda}_t = \frac{\sqrt[\tau]{\epsilon(\tau+1)}}{\pi s^2 \beta_\alpha^{\frac{2}{\alpha}} \sqrt[\tau]{k} \hat{\Delta}_1(\beta)} + \Theta(\epsilon^2),$$

which gives

$$\bar{\lambda}_\epsilon = \eta \cdot \frac{\sqrt[\tau]{\epsilon(\tau+1)}}{\pi s^2 \beta_\alpha^{\frac{2}{\alpha}} \sqrt[\tau]{k}}, \quad (3.41)$$

where $\eta \triangleq 1/\hat{\Delta}_1(\beta)$. This completes the proof.

3.7.3 Proof of Lemma 3.4.5

According to Campbell's theorem, we know $\mathbb{E}[I_0] = \frac{2\pi\lambda_t}{\alpha-2}$ and then the lower bound on b can be reduced as follows.

$$\begin{aligned} b &\stackrel{(a)}{\geq} \mathbb{E} \left[\log \left(1 + \frac{H_{\max}}{s^\alpha \mathbb{E}[I_0]} \right) \right] \stackrel{(b)}{\geq} \mathbb{E} \left[\log \left(1 + \frac{H_{\max}(\alpha-2)}{2\pi s^2 \lambda_t} \right) \right] \\ &\geq \log \left(1 + \frac{1}{\pi s^2 \lambda_t} \right) F_{H_{\max}}^c \left(\frac{2}{\alpha-2} \right), \end{aligned}$$

where (a) follows from Jensen's inequality since $\log(1+a/x)$ is convex for $x > 0$ and constant $a > 0$, (b) is due to $s^{\alpha-2} \geq 1$, and $F_{H_{\max}}^c$ is the CCDF of random variable H_{\max} . In addition, we also know b in (3.17) is upper bounded as follows.

$$b \leq \log(\mathbb{E}[I_0] + \mathbb{E}[H_{\max}]s^{-\alpha}) + \mathbb{E}[\log(1/I_0)].$$

The upper bound is obtained by first conditioning on I_0 and then using Jensen's inequality. We know the term $\log(1/I_0)$ in the upper bound is convex and thus $\mathbb{E}[\log(1/I_0)] \geq \log(1/\mathbb{E}[I_0])$. Since the network is interference-limited, $\mathbb{E}[I_0]$ must be bounded above zero. Thus there exists a $\gamma_1 > 0$ such that $\log(\gamma_1) \leq$

$\mathbb{E}[\log(I_0)] \leq \log(\mathbb{E}[I_0])$, which means $\mathbb{E}[\log(I_0)] \geq \log(\gamma_2 \mathbb{E}[I_0])$ for any $\gamma_2 \in (0, \gamma_1/\mathbb{E}[I_0])$. So the upper bound can be simplified as follows:

$$\begin{aligned} & \log(\mathbb{E}[I_0] + \mathbb{E}[H_{\max}]s^{-\alpha}) + \mathbb{E}\left[\log\left(\frac{1}{I_0}\right)\right] \\ & \leq \log\left(\frac{\mathbb{E}[I_0]}{\mathbb{E}[H_{\max}]} + \mathbb{E}[R^{-\alpha}]\right) + \log\left(\frac{\mathbb{E}[H_{\max}]}{\gamma_2 \mathbb{E}[I_0]}\right) \\ & \leq \log\left(1 + \frac{1}{\pi s^2 \lambda_t}\right) + \log\left(\frac{\mathbb{E}[H_{\max}]}{\gamma_2}\right) \end{aligned}$$

because $s^{-\alpha} \leq \mathbb{E}[R^{-\alpha}] \leq \frac{2}{s^{2(\alpha-2)}}$ and $\mathbb{E}[H_{\max}] \geq 1$. Note that the CDF of H_{\max} , $F_{H_{\max}}$, is equal to $(F_H)^\tau$ since $\{H_j(t), t = 1, \dots, \tau\}$ are i.i.d. random variables. The proof is complete.

3.7.4 Proof of Theorem 3.5.1

We start with the derivation of the upper bound on $\mathbb{E}[\lambda_c]$ as follows. **(i) The upper bound on $\mathbb{E}[\lambda_c]$:** Suppose the multicast cluster \mathcal{R}_0 is tessellated into v smaller multicast regions of equal area $\pi s^2/v$. Let \mathcal{T} denote the set of all the pathes from the source multicast region (*i.e.*, the tessellated region in which the central transmitter is located) to the last multicast region. Let $T_* \in \mathcal{T}$ be the chosen path for multicasting a packet and \mathcal{S}_i denote the i th tessellated region on T_* . Since there are v multicast regions on T_* , the duration of a time slot for multicasting a packet in each region is at most τ/v transmission attempts. In order to implement multihop multicast, the multicast outage event should be redefined here as follows. We say there exists a multihop multicast outage in a multicast time slot if any of the receivers in the current multicast region does not receive the packet or no receivers in the next multicast region receive the

packet after τ/v transmission attempts. In addition, T_* is chosen according to the following criteria:

$$T_* = \arg \min_{T \in \mathcal{T}} \left[1 - \prod_{i=1}^v (1 - \mathbb{P}[\mathcal{E}_i|T]) \right], \quad (3.42)$$

where \mathcal{E}_i is the multicast outage event happening in \mathcal{S}_i . So T_* is the path with the minimum probability of end-to-end multicast outage.

If Φ_{s_i} is the receiver-connected process in \mathcal{S}_i after τ attempts, then \mathcal{E}_i can be expressed as $\{\Phi_{s_i} \subset (\Phi_r \cap \mathcal{S}_i) \cup (\tilde{Y}_{i+1} \in \mathcal{S}_{i+1})\}$ where \tilde{Y}_{i+1} is any intended receiver in \mathcal{S}_{i+1} and it could be the transmitter in the $(i+1)$ th time slot. Due to the broadcast nature of wireless communication, the intended receivers in the regions other than \mathcal{S}_i could also receive the packet which is merely multicasted to \mathcal{S}_i in the i th time slot. Thus, if the average intensity of Φ_{s_i} at the end of the t th time slot is $\mathbb{E}_X[\lambda_{s_i}(X, t\tau/v)]$ where $X \in \mathcal{R}_0$, then we know $\mathbb{E}_X[\lambda_{s_1}(X, t\tau/v)] \leq \mathbb{E}_X[\lambda_{s_2}(X, t\tau/v)] \leq \dots \leq \mathbb{E}_X[\lambda_{s_v}(X, t\tau/v)]$ since Φ_{s_i} is a filtration process.

Since the Lebesgue measure of \mathcal{S}_i is $\frac{\pi s^2}{v}$, the probability of E_i on T_* is given by

$$\begin{aligned} \mathbb{P}[\mathcal{E}_i|T_*] &= 1 - \exp\left(-\int_{\mathcal{S}_i} (\lambda_r - \lambda_{s_i}(X, i\tau/v)) \mu(dX)\right) \\ &\quad \cdot \left[1 - \exp\left(-\frac{\pi s^2 \mathbb{E}_X[\lambda_{s_{i+1}}(X, i\tau/v)]}{v}\right)\right] \\ &\leq \epsilon_v, \end{aligned}$$

where $\epsilon_v = 1 - (1 - \epsilon)^{1/v}$ is the upper bound constraint on the multicast outage probability in each tessellated region. Considering sufficiently large k , the above equation can be simplified as

$$\mathbb{P}[\mathcal{E}_i|T_*] = 1 - \exp\left(-\int_{\mathcal{S}_i} (\lambda_r - \lambda_{s_i}(X, i\tau/v)) \mu(dX)\right) + \Theta(\epsilon^2).$$

The multicast outage event in \mathcal{R}_0 is the union of all the multihop multicast outage events, *i.e.*, $\mathcal{E} = \bigcup_{i=1}^v \mathcal{E}_i = (\bigcap_{i=1}^v \mathcal{E}_i^c)^c$. Since all multihop multicast outage events are independent, the probability of \mathcal{E} can be explicitly expressed as

$$\begin{aligned} \mathbb{P}[\mathcal{E}|T_*] &= 1 - \prod_{i=1}^v \mathbb{P}[\mathcal{E}_i^c|T_*] \\ &= 1 - \exp \left\{ -\pi s^2 \lambda_r + \sum_{i=1}^v \int_{\mathcal{S}_i} \lambda_{s_i}(X, i\tau/v) \mu(dX) \right\} + \Theta(\epsilon^2) \leq \epsilon. \end{aligned}$$

According to (3.8) and the above equation, it follows that

$$\begin{aligned} \mathbb{E}_X[\lambda_c(X, \tau)] &= \frac{1}{v} \sum_{i=1}^v \int_{\mathcal{S}_i} \lambda_{s_i}(X, i\tau/v) \frac{\mu(dX)}{\pi s^2/v} \\ &= \frac{1}{v} \sum_{i=1}^v \mathbb{E}_X[\lambda_{s_i}(X, i\tau/v)]. \end{aligned}$$

From the results in Lemma 3.4.2, we can know $\mathbb{E}_X[\lambda_{s_i}(X, i\tau/v)]$ with Rayleigh and Nakagami- m fading at the i th time slot. Let $A(r) = 1 - \exp(-\pi \Delta_1(\beta r^\alpha, \infty) \lambda_t)$ for Rayleigh fading or $A(r) = 1 - \Psi^{(m-1)}(m\beta r^\alpha)$ for Nakagami- m fading with $m > 1$, and thus the upper bound on $\mathbb{E}_R[\lambda_c(R, \tau)]$ can be shown as

$$\mathbb{E}_R[\lambda_c(R, \tau)] \leq \lambda_r \left(1 - \frac{1}{v} \sum_{i=1}^v \mathbb{E}_R[A(R)]^{\frac{i\tau}{v}} \right).$$

(ii) The scaling law of $\bar{\lambda}_\epsilon$: Using the upper bound on $\mathbb{E}_R[\lambda_c(R, \tau)]$ obtained from (3.8) and the above result, it yields the following inequality:

$$\frac{\epsilon v}{k} \geq \sum_{i=1}^v \mathbb{E}_R[A(R)]^{\frac{i\tau}{v}} = \frac{\mathbb{E}_R[A]^{\frac{\tau}{v}} (1 - \mathbb{E}_R[A]^\tau)}{1 - \mathbb{E}_R[A]^{\frac{\tau}{v}}}.$$

Also, we know $\epsilon_v = 1 - \sqrt[v]{1 - \epsilon} = \frac{\epsilon}{v} + \Theta(\epsilon^2)$ and $\mathbb{E}_R[A]^{\frac{\tau}{v}} \leq \frac{\epsilon_v v}{k} = \frac{\epsilon}{k} + \Theta(\epsilon^2)$. Thus, we know

$$1 - \left(\frac{\epsilon v}{k} \right)^{\frac{v}{\tau}} \leq \mathbb{E}_R[\Psi^{(m-1)}(m\beta R^\alpha)].$$

$\mathbb{E}_R[\Psi^{(m-1)}(m\beta R^\alpha)] \approx 1$ since $\mathbb{E}_R[\Psi^{(m-1)}(m\beta R^\alpha)] \leq 1$ and $k \geq \frac{v}{\epsilon^{\tau/v-1}}$. So the random variable $\Psi^{(m-1)}(m\beta R^\alpha)$ is very close to one almost surely and thus λ_t is $\Theta(\epsilon)$. Then following the same steps in the proof of Theorem 3.4.3, we can show that

$$\bar{\lambda}_\epsilon = \eta \cdot \frac{v^{\frac{v}{\tau}+1} \tau^2 \rho}{\pi s^2 \beta_\alpha^{\frac{2}{\tau}} k^{\frac{v}{\tau}}} = \Theta\left(\frac{v^{\frac{v}{\tau}+1} \tau^2 \rho}{\pi s^2 \beta_\alpha^{\frac{2}{\tau}} k^{\frac{v}{\tau}}}\right). \quad (3.43)$$

Thus, (3.22) is arrived, which completes the proof.

Chapter 4

Ergodic Transmission Capacity

In the past decade, our understanding of large wireless network capacity has increased considerably, but perhaps still comprises more questions than answers, especially for realistic models. Gupta and Kumar's landmark work [11], for example, introduced the transport capacity metric and derived scaling laws on it in a size-limited network. Another more recent example is transmission capacity proposed in [13] which is a spatial throughput metric for Poisson-distributed transmitters in an infinite network with outage constraints. Almost all of the studies following the aforementioned approaches did not consider temporal affections. For a wireless network with long-term time-varying channels, its *snapshot* throughput may not provide a full picture of how the throughput evolves over time.

In this chapter, we introduce a metric capable of characterizing the network throughput induced by channels with temporal and spatial ergodicity¹. This metric is called the *ergodic transmission capacity* (ETC), and it measures the maximum long-term average rate (in bps/Hz) that can be sent per unit area in

¹Spatial ergodicity means that the mean of a random variable can be characterized by averaging the random variable over an infinitely large space.

the network with an outage constraint. We evaluate the ETC under assuming all transmitters form a homogeneous Poisson point process (PPP) with a unique receiver. The channel models span many blocks of time, and so the throughput variations over time can be characterized with our framework but not with prior frameworks. Thus, ETC may be better able to accurately suggest how to effectively use transmissions over time and space, such as multi-antenna transmission and opportunistic scheduling, and how much such techniques will improve area spectral efficiency in a long-term sense.

4.1 Motivation and Related Work

In the literature on wireless network throughput (see [11–13, 22, 51, 71, 72] and the references therein), a unified and time-invariant channel model is typically adopted over the entire network, but channels in a large-scale wireless network usually are diverse across time and/or space. Using a channel model without temporal correlation does not capture how channel states evolve over time and thus the impact on network throughput from the temporal (and spatial) variations of channels is ignored, and techniques which exploit the variations and correlations cannot be properly quantified. For example, we observe that transmission techniques that increase the snapshot network throughput may not increase ETC or may even degrade it. In particular, we will show that threshold scheduling proposed in [51], i.e. the DCAS scheme with a constant threshold introduced in Chapter 1, does not always improve ETC, which is perhaps surprising.

ETC requires the use of different channel models that include temporal

discrepancies. We propose a finite-state Markov chain (FSMC) to model the fading channels, in particular a m -state Markov chain that is irreducible and positive recurrent. Each channel undergoes path loss and fading and has an ergodic property in that its fading state has an invariant (steady-state) probability [73]. This idea can be traced back to the early work of Gilbert and Elliott [74] [75] that used a two-state Markov chain to represent *good* and *bad* channel conditions which was extended to a finite state case in [76].

4.2 Contributions

The first contribution in this work is the model for ETC itself. We then calculate the ETC, which requires the outage probability for each fading channel state to be found, for which we find tight closed-form bounds based on a proposed δ -level interfering coverage area around a receiver. Any single transmitter in the δ -level region of its unintended receiver will cause an outage if its interference power is enlarged by a factor δ . We show that appropriately choosing δ admits bounds on outage probability that are much tighter than those found in previous work.

Bounds on ETC and their corresponding scaling laws for some special cases are then found. They reveal several interesting implications, e.g. the scaling of ETC for a *sparse* or *dense* network is

$$C_E = \Theta(\Phi^T \mathbf{s}_\epsilon), \quad (4.1)$$

where C_E denotes ETC, $\mathbf{s}_\epsilon = \left[\tilde{s}_1^{\frac{2}{\alpha}}, \tilde{s}_2^{\frac{2}{\alpha}}, \dots, \tilde{s}_m^{\frac{2}{\alpha}} \right]^T$ in which \tilde{s}_k is the function of the k th state s_k of a Markov fading channel with m states, $\Phi = [\phi_1 \ \phi_2 \ \dots \ \phi_m]^T \in$

$[0, 1]^m$ is the invariant probability vector² of the Markov fading channel model and $\alpha > 2$ is the path loss exponent. From (4.1), we notice that a single deep fading state is not necessary to have a significant negative effect on ETC if its invariant probability is very small. This point is not revealed in prior work that neglects temporal variations. Also, we observe that ETC has a geometric interpretation because it can be viewed as an inner product of two vectors. Thus, ETC is maximized when the directions of Φ_k and \mathbf{s}_ϵ coincide. In addition, we show that the DCAS scheme with a constant threshold³, which is a scheme to allow transmitters to transmit only when their channels are in good states, does not necessarily provide an ETC gain. Although DCAS is able to increase the transmission capacity contributed by good channel states, it loses the transmission capacity contributed by bad channel states. So DCAS cannot benefit ETC if the improvement is no larger than the loss from bad channel states.

Three interference management methods – avoidance, suppression and cancellation – are applied to the network to reduce outage probability. Bounds on the outage probability and ETC with interference management are found which provide geometric insight into the efficiency of each technique in different scenarios. For example, we show that interference cancellation is not effective for significantly increasing ETC in a sparse or dense network. Also, we show interference management can control the direction and magnitude of vector \mathbf{s}_ϵ . Finally, we show that DCAS should not be used if interference management can

²The physical meaning of ϕ_k is the fraction of time that channel state s_k sojourns as time goes to infinity.

³Throughout this chapter, the DCAS scheme always uses a constant threshold.

significantly lower interference.

4.3 Network Model and Definitions

4.3.1 The Network Model

The wireless network considered in this chapter is similar to the model in Chapter 2 where all nodes in the network are independently and randomly scattered. Thus, we employ a marked homogeneous Poisson point process (PPP) Π on the plane \mathbb{R}^2 to represent the locations of all transmitting nodes in the network, which can be written at time τ as⁴

$$\Pi \triangleq \{(X_i \in \mathbb{R}^2, H_i(\tau) \in \mathbb{R}_+, e_i(\tau)) : e_i(\tau) = 1\}, \quad (4.2)$$

where X_i denotes node X_i as well as its location, $H_i(\tau)$ is the fading channel gain between node X_i and its receiver Y_i , and $e_i(\tau) \in \{0, 1\}$ represents the transmitting index of node X_i : $e_i(\tau) = 1$ means node X_i is transmitting; otherwise, it is idle. The intensity (density) of Π is λ for all $\tau \in \mathbb{N}$.

Each transmitter has a unique receiver and the distance between a TX-RX pair is a constant $d > 1$. All of the transmitters use the same transmit power and the channel model between each TX-RX pair is subject to path loss and fading. So the channel gain for TX-RX pair i can be written as

$$H_i(\tau)\ell(|X_i - Y_i|) = H_i(\tau)\ell(d),$$

⁴Here it is better to use $\Pi(\tau)$ instead of Π . However, to simplify notation, we will use Π to stand for $\Pi(\tau)$ throughout this chapter if ignoring time indices does not induce any ambiguity. This custom is applied to other set and variable notations.

where $H_i(\tau)$ is the fading channel gain, $|X_i - Y_i|$ denotes the Euclidean distance between nodes X_i and Y_i and $\ell(|\cdot|)$ is the path loss function. In order to avoid the singularity where $|X| \rightarrow 0$, we will use

$$\ell(|X|) = |X|^{-\alpha} \mathbf{1}(|X| \in [1, \infty)), \quad X \in \mathbb{R}^2, \quad (4.3)$$

where $\alpha > 2$ is the path loss exponent⁵ and $\mathbf{1}(x \in \mathcal{X})$ denotes the *indicator* function: $\mathbf{1}(x \in \mathcal{X}) = 1$ if $x \in \mathcal{X}$ and 0, otherwise.

Specifically, we use an m -state FSMC model to characterize the fading effect of all channels in the network. The FSMC is irreducible and positive recurrent, and its m states are ordered. The FSMC model with transition matrix \mathbf{P} is denoted by $\mathcal{S}(\mathbf{P}) \in \mathbb{R}_+^m$ and \mathcal{S} is an order set of the m states, i.e. for any two states $s_i, s_j \in \mathcal{S}$ we have $s_i < s_j$ where $i < j$ and $i, j \in \mathcal{M} \triangleq \{1, 2, \dots, m\}$. Since \mathcal{S} is irreducible and positive recurrent, the fading channel gain $H(\tau)$ for all TX-RX pairs must satisfy the following conditions [73]:

$$\phi_k \triangleq \lim_{L \rightarrow \infty} \frac{1}{L} \sum_{\tau=0}^{L-1} \mathbf{1}(H(\tau) \in s_k) \quad \text{and} \quad \mathbf{u}^\top \Phi = \sum_{k=1}^m \phi_k = 1, \quad (4.4)$$

where $\Phi \triangleq [\phi_1, \phi_2, \dots, \phi_m]^\top$ is the invariant probability vector of \mathbf{P} and $\mathbf{u} \triangleq [1 \ 1 \ \dots \ 1]^\top$ is an m -tuple vector. Namely, at any time τ , $H(\tau)$ must belong to one of the states in \mathcal{S} and ϕ_k represents the probability that $H(\tau)$ visits state s_k in a long-term sense. Since this m -state Markov channel model is irreducible and positive recurrent, it has a temporal ergodic property and we can have the

⁵In a planar network, we require $\alpha > 2$ to have bounded interference, i.e. $I_t < \infty$ almost surely if $\alpha > 2$ [15, 18].

following result:

$$\mathbb{P} \left[\lim_{L \rightarrow \infty} \frac{1}{L} \sum_{\tau=0}^{L-1} \mathbb{1}(Z(\tau) \in \mathcal{S}) = \sum_{i=1}^m \phi_k \mathbb{1}(s_k) \right] = 1, \quad (4.5)$$

where $\mathbb{1} : \mathcal{S} \rightarrow [0, 1]$ is a state measurable function of \mathcal{S} , $\{\phi_k, k = 1, \dots, m\}$ are the invariant (steady state) distribution of \mathbf{P} , and s_k is the k th state of \mathcal{S} .

The definition of ergodic transmission capacity in the following subsection is built based on the result in (4.5). In addition, the following lemma shows that the fading channel model of a FSMC also has a spatial ergodic property.

Lemma 4.3.1 (Spatial Ergodicity). *Consider a marked homogeneous PPP Π with an independent mark $H(\tau) \in \mathcal{S}$, and let $g : \Pi \rightarrow \mathbb{R}_+$ be a measurable function on Π . For any bounded subset $\mathcal{A}_n \subset \mathbb{R}^2$ and $\mu(\mathcal{A}_n) \rightarrow \infty$ as $n \rightarrow \infty$, we have*

$$\mathbb{E}[g(\Pi_k)] \triangleq \lim_{n, \tau \rightarrow \infty} \frac{1}{\mu(\mathcal{A}_n)} \int_{\mathcal{A}_n} g((X, H \in s_k)) \mu(dX) = \phi_k \mathbb{E}[g(\Pi)], \quad a.s., \quad (4.6)$$

where $\Pi_k \triangleq \{(X_i, H_i) \in \Pi : H_i \in s_k\}$ is the PPP with channel state s_k .

Proof. Since Π is homogeneous, we know

$$\mathbb{E}[g(\Pi)] = \lim_{n, \tau \rightarrow \infty} \frac{1}{\mu(\mathcal{A}_n)} \int_{\mathcal{A}_n} \mathbb{E}_H[g((X, H))] \mu(dX).$$

Since $\{H_i\}$ are independent, Π_k is just the thinning homogeneous PPP of Π and thus we have

$$\begin{aligned} \mathbb{E}[g(\Pi_k)] &= \lim_{n, \tau \rightarrow \infty} \frac{1}{\mu(\mathcal{A}_n)} \int_{\mathcal{A}_n} g((X, H \in s_k)) \mu(dX) \\ &= \lim_{n, \tau \rightarrow \infty} \frac{1}{\mu(\mathcal{A}_n)} \int_{\mathcal{A}_n} \mathbb{E}[g((X, H))] \mathbb{E}[\mathbb{1}(H \in s_k)] \mu(dX) \\ &\stackrel{(*)}{=} \phi_k \mathbb{E}[g(\Pi)], \end{aligned}$$

where (\star) follows from the temporal ergodicity result in (4.5). \square

Lemma 4.3.1 indicates that the spatial average of $g(\Pi_k)$ is equal to $\phi_k \mathbb{E}[g(\Pi)]$. So we know the intensity of Π_k is $\lambda_k = \phi_k \lambda$ provided that $g(\cdot)$ is an intensity measure.

The interference channel gain from transmitter X_j to its non-intended receiver Y_i is denoted by $\tilde{H}_{ji}(\tau) \ell(|X_j - Y_i|)$ where $\tilde{H}_{ji}(\tau) \in \mathcal{S}$. The aggregate interference normalized by the transmit power at receiver Y_i can thus be expressed as

$$I_i(\tau) = \sum_{X_j \in \Pi \setminus X_i} \tilde{H}_{ji}(\tau) \ell(|X_j - Y_i|), \quad (4.7)$$

where I_i is also called a spatial shot noise process [15, 53, 54, 56] since it captures the cumulative effect at location Y_i of a set of random shocks appearing at random locations X_j , and $\tilde{H}_{ji} \ell(|X_j - Y_i|)$ can be viewed as the impulse function that gives the attenuation of the transmit power in space. In order to have a successful transmission for TX-RX pair i , the following signal-to-interference ratio (SIR) condition at receiver node Y_i must hold at time τ :

$$\text{SIR}_i(\tau, \lambda) \triangleq \frac{H_i(\tau)}{d^\alpha I_i(\tau)} \geq \beta, \quad (4.8)$$

where β is the SIR threshold for TX-RX pair i to successfully decode the received data. The network is assumed to be interference-limited.

Note that according to Slivnyak's theorem [57] the statistics of I_i seen by any node in the network is the same if the nodes form a homogeneous PPP. That means the average outage probability of each receiver node may be found by evaluating the SIR seen by a receiver located at the origin. Intuitively, the

distribution of the point process is unaffected by the addition of a receiver at the origin, and this receiver is called a *typical* receiver. The performance measured at the origin is often referred to the Palm measure, and in keeping with simplified notation we will denote the probability and expectation of functionals of evaluated at the origin \mathbf{o} by \mathbb{P} and \mathbb{E} , respectively. Also, Table 4.1 summaries the main mathematical notation used in this chapter.

4.3.2 Definitions

Consider the typical TX-RX pair and its steady state outage probability is

$$\lim_{\tau \rightarrow \infty} \mathbb{P}[\text{SIR}(\tau, \lambda) < \beta] \in \{q_k(\lambda), k \in \mathcal{M}\}, \quad (4.9)$$

where $q_k(\lambda) \triangleq \lim_{\tau \rightarrow \infty} \mathbb{P}[\text{SIR}(\tau, \lambda) < \beta | H(\tau) = s_k]$ is the outage probability for channel state s_k as time τ goes to infinity. Now we are ready to use (4.9) to define ergodic transmission capacity in this chapter.

Definition 4.3.2 (Ergodic Transmission Capacity). *Suppose transmitting nodes in a wireless ad hoc network form a homogeneous PPP of intensity λ . For a given $\epsilon \in (0, 1)$, the ergodic transmission capacity (ETC) of a wireless ad hoc network is defined by*

$$C_E \triangleq b \bar{\lambda}_\epsilon (1 - \epsilon), \quad (4.10)$$

where b is the supportable transmission rate, ϵ is the upper bound on the outage probability of each channel state, and $\bar{\lambda}_\epsilon = \sup\{\lambda > 0 : \sum_{k=1}^m \phi_k q_k(\lambda) \leq \epsilon\}$ is called maximum contention intensity achieved under the outage probability constraint ϵ .

Table 4.1: Summary of Main Mathematical Notation in Chapter 4

Symbol	Definition
Π	Homogeneous PPP of transmitters
λ	Intensity (density) of Π
C_E	Ergodic transmission capacity
$\bar{\lambda}_E$	Maximum Contention Intensity
ϵ	Upper bound of outage probability
d	Transmission distance of a TX-RX pair
$\mathcal{S} \in \mathbb{R}_+^m$	m -state Markov chain for modeling fading
s_k	k th state of Markov chain \mathcal{S}
ϕ_k	Invariant (steady state) probability of channel state s_k
$H(\tau)$	Fading channel gain at time τ , $H(\tau) \in \mathcal{S}$
$\alpha > 2$	Path loss exponent
β	SIR threshold for successful decoding
\mathcal{I}_k^δ	δ -level interfering coverage for channel state s_k
$\delta \geq 1$	Parameter of defining \mathcal{I}_k^δ
ν	Mean area of \mathcal{I}_k^δ for $s_k = 1$
\mathcal{C}_k^ξ	Interference cancellation coverage for channel state s_k
$\gamma_k \in (0, 1)$	Interference reduction factor for channel state s_k
$\ell(\cdot)$	Path loss function
$q_k(\cdot)$	Outage probability for channel state s_k
$\mu(\mathcal{A})$	Lebesgue measure of set \mathcal{A}

The definition of C_E in (4.10) originates from the following definition:

$$C_E \triangleq \frac{b \bar{\lambda}_E}{L} \sum_{\tau=0}^{L-1} \mathbb{P}[\text{SIR}(\tau, \bar{\lambda}_\epsilon) \geq \beta]. \quad (4.11)$$

Since all channels are an irreducible and positive current Markov chain, according to (4.5) they all have temporal ergodicity. Thus, the definition in (4.11) is equivalent to $C_{\mathbf{E}} = b \bar{\lambda}_{\mathbf{E}} \sum_{k=1}^m \phi_k [1 - q_k(\bar{\lambda}_{\mathbf{E}})]$. This is the reason why we directly use the invariant probability of a Markov chain to define ETC instead of using (4.11). For ease of analysis, we need to quantitatively define the sparseness and denseness of a network with Poisson-distributed nodes.

Definition 4.3.3 (Spatial Sparseness and Denseness of a Poisson-Distributed Network). *Suppose the transmission coverage of a transmitter is the circular area of radius d . A network whose transmitting nodes form a homogeneous PPP of intensity λ is called “dense” (“sparse”) if the average number of transmitting nodes in the coverage is sufficiently large (small), i.e. $\pi d^2 \lambda \gg 1$ ($\pi d^2 \ll 1$).*

4.4 General Results on Ergodic Transmission Capacity

In this section, we study the general results of ETC. First, we have to calculate the outage probability for each channel state; however, only the bounds on the outage probability and ETC can be characterized due to the complicated distribution of the interference. According to the found bounds, the scaling behaviors of ETC are characterized and they reveal several observations.

4.4.1 Bounds on the Outage Probability

Since a closed-form expression of the outage probability defined in (4.9) is difficult to find⁶, we resort to bounds. The idea of approaching the lower bound for a receiver with channel state s_k is to use a δ -level *interfering coverage* \mathcal{I}_k^δ for the typical receiver Y_0 with fading state s_k , and it is defined as follows⁷:

$$\mathcal{I}_k^\delta \triangleq \left\{ X \in \mathbb{R}^2 : \frac{s_k d^{-\alpha}}{\delta \ell(|X|) \tilde{H}} < \beta \right\}, \quad \delta \in [1, \infty), \quad (4.12)$$

which means any single interferer within it can cause outage at receiver Y_0 with a SIR threshold $\delta\beta$. If \mathcal{I}_k^δ is not empty, it could contain dominant interferers and non-dominant interferers. In addition, $\Pi_k^\delta \triangleq (\Pi \cap \mathcal{I}_k^\delta) \setminus X_0$ is called δ -level interfering point process.

The lower bound on the outage probability $q_k(\lambda)$ can be acquired by considering the outage events caused by Π_k^δ . The upper bound can be approached by finding the probability of the union outage events separately caused by the interferers in Π_k^δ and $\Pi \setminus \Pi_k^\delta$. These two bounds found are tighter than those in the previous works [13] [77], as the following theorem shows.

Theorem 4.4.1. *The outage probability $q_k(\lambda)$ in (4.9) can be bounded as*

$$1 - e^{-\lambda(\nu s_k^{-\frac{2}{\alpha}} - \pi)} \leq q_k(\lambda) \leq 1 - (1 - \Lambda_k(\lambda))^+ e^{-\lambda(\nu s_k^{-\frac{2}{\alpha}} - \pi)}, \quad (4.13)$$

⁶If all channels are instead Rayleigh fading, the closed-form of the outage probability can be found by the Laplace transform of the aggregate interference contributed by Poisson-distributed transmitters [15] [69]. However, such closed-form outage probability cannot be obtained for the case of channels without fading [13] [77] or with a single state at any time.

⁷If $\delta = 1$, then \mathcal{I}_k^δ is called the dominant interferer coverage in which a single interferer causes outage at receiver Y_0 .

where $(x)^+ \triangleq \max\{x, 0\}$ and $\Lambda_k(\cdot)$ is defined as

$$\Lambda_k(\lambda) = \frac{s_k^{\frac{3}{\alpha}-1} \lambda \sigma^2}{(s_k^{\frac{2}{\alpha}-1} / d^\alpha \delta \beta - \lambda \eta)^2}, \quad (4.14)$$

and ν , η , σ^2 are respectively given by

$$\nu = \pi d^2 \sum_{k=1}^m \phi_k (\delta \beta s_k)^{\frac{2}{\alpha}}, \quad \eta = \frac{2\nu}{(\alpha - 2)d^\alpha \delta \beta}, \quad \sigma^2 = \frac{\pi d^{2-2\alpha}}{\alpha - 1} (\delta \beta)^{\frac{1}{\alpha}-1} \sum_{k=1}^m \phi_k s_k^{\frac{1}{\alpha}+1}.$$

Proof. See Appendix 4.6.1. □

The physical meanings of ν , η and σ^2 are the mean area of \mathcal{I}_k^δ with $s_k = 1$, the mean, and the variance of the interference contributed by the interferers of $\Pi \setminus \Pi_k^\delta$ for $\lambda = s_k = 1$. When the channel state s_k is high, the outage probability is reduced because SIR is large or equivalently the target SIR β is reduced. Nevertheless, it also can be explained from a geometric point of view. In (4.8), we can let fading gain s_k be incorporated into the path loss model of all interference channels, and according to the conservation property of a homogeneous PPP [57], the intensity of the original PPP is changed from λ to $\lambda/s_k^{\frac{2}{\alpha}}$. This is why λ in the bounds is scaled by $s_k^{-\frac{2}{\alpha}}$ and thus interference generated by the PPP with intensity $\lambda/s_k^{\frac{2}{\alpha}}$ is small when s_k is large. So tightness of the bounds in (4.13) can also be observed.

If $(\cdot)^+$ in (4.13) is non-zero, the gap between the upper and lower bounds is $\Lambda_k(\lambda)e^{-\lambda(\nu s_k^{-\frac{2}{\alpha}} - \pi)}$ which is a function of δ , λ and s_k . Since $e^{-\nu \lambda s_k^{-2/\alpha}}$, σ^2 and η are all monotonically decreasing functions of δ , and the denominator of $\Lambda_k(\lambda)e^{-\lambda(\nu s_k^{-\frac{2}{\alpha}} - \pi)}$ is convex for δ , it is easy to realize that $\Lambda_k(\lambda)e^{-\lambda(\nu s_k^{-\frac{2}{\alpha}} - \pi)}$ is smaller than that without δ if δ is chosen appropriately. Figure 4.1 shows the

simulation results for channel fading modeled by a 2-state Markov chain. As expected, the two gaps decrease along with δ so that using $\delta > 1$ can make the bounds (much) tighter. In addition, the gap for a good channel state is much larger than that for a bad channel state. Hence, we should choose a sufficiently large δ in order to have tight bounds when the Markov chain has very good channel states.

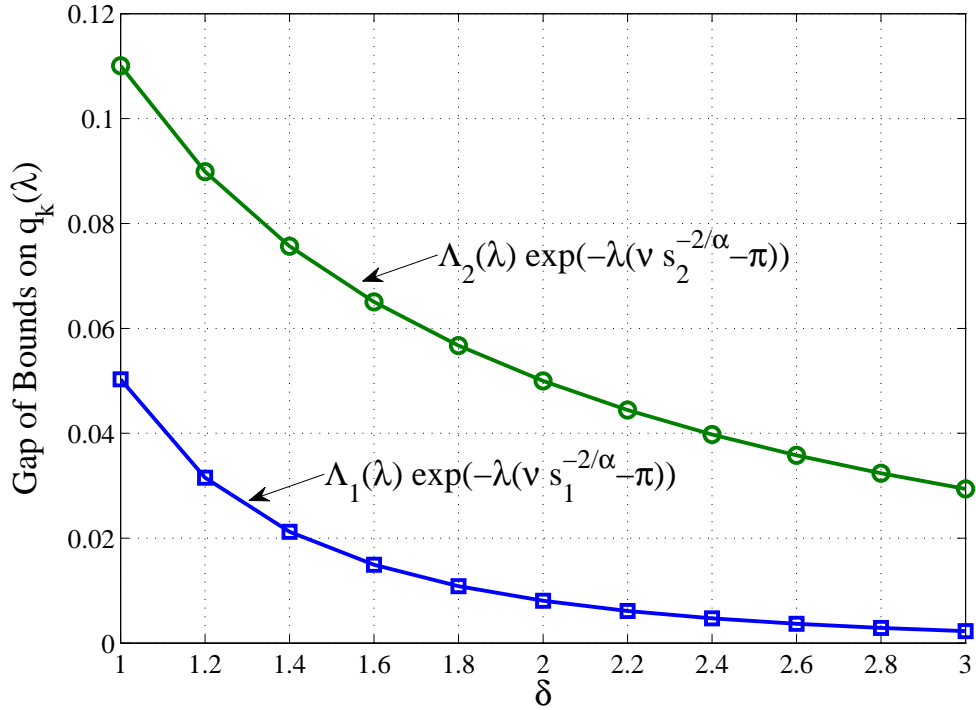


Figure 4.1: The gap between the upper and lower bounds on $q_k(\lambda)$. Channel fading is modeled by a Markov chain with 2 states. The network parameters for simulation are: $d = 5m$, $\lambda = 0.01$, $\alpha = 3$, $\beta = 2$, $s_1 = 0.5$, $s_2 = 2$ and $\phi_1 = \phi_2 = 0.5$.

The result in (4.13) will become slightly different if a transmitter uses a

channel-aware opportunistic transmission (DCAS) policy. Recall that the states of a Markov fading channel are ordered so that a better state has a higher subscript index. Suppose we call a channel state “good” in each FSMC if its subscript index is greater than or equal to g and $s_g > 1$, which means channel gain H is good if $H \in \mathcal{S}_g \triangleq \{s_g, \dots, s_m\}$. Therefore, the PPP with good channel states can be expressed as

$$\Pi_g = \{(X_i, H_i(\tau)) \in \Pi : H_i(\tau) \in \mathcal{S}_g\}. \quad (4.15)$$

According to (4.5) and Lemma 4.3.1, its intensity is $\lambda_g = \lambda \mathbb{P}[H \in \mathcal{S}_g] = \lambda \sum_{k=g}^m \phi_k$ as time goes to infinity. Therefore, the bounds on the outage probability with DCAS can be obtained from (4.13) by replacing λ with λ_g , which yields

$$1 - e^{-\lambda_g(\nu s_k^{-\frac{2}{\alpha}} - \pi)} \leq q_k(\lambda_g) \leq 1 - (1 - \Lambda_k(\lambda_g))^+ e^{-\lambda_g(\nu s_k^{-\frac{2}{\alpha}} - \pi)}. \quad (4.16)$$

Note that the bounds decrease in (4.13) when λ decreases. Thus, the bounds in (4.16) decrease compared with (4.13). So DCAS improves the bounds on the outage probability of each channel state because nodes with bad channel states refrain from transmitting. In Section 4.4.3, however, we will point out that it may not always improve ETC.

4.4.2 Ergodic Transmission Capacity

By using the bounds on the outage probability of each channel state in Theorem 4.4.1, the ETC in (4.10) has bounds as shown in the following theorem.

Theorem 4.4.2. *Suppose the outage probability $q_k(\lambda)$ in (4.9) is upper bounded by $\epsilon \in (0, 1)$. Using the inequality in (4.13), bounds on the maximum contention intensity $\bar{\lambda}_E$ which maximize $\sum_{k=1}^m \phi_k q_k(\bar{\lambda}_E)$ under the constraint of ϵ can be given by*

$$\sum_{k=1}^m s_k^{\frac{2}{\alpha}} \phi_k \bar{\lambda}_k^\epsilon \leq \bar{\lambda}_E \leq -\ln(1 - \epsilon) \sum_{k=1}^m \frac{s_k^{\frac{2}{\alpha}} \phi_k}{\nu - s_k^{\frac{2}{\alpha}} \pi}, \quad (4.17)$$

where $\bar{\lambda}_k^\epsilon$ is given by in the following.

$$\bar{\lambda}_k^\epsilon = \inf \left\{ \lambda > 0 : \frac{1}{\lambda} \ln \left[\frac{(1 - \Lambda_k(\lambda))^+}{1 - \epsilon} \right] \leq \left(\nu s_k^{-\frac{2}{\alpha}} - \pi \right) \right\}, \quad (4.18)$$

where $\Lambda_k(\lambda)$ is defined in (4.14).

Proof. See Appendix 4.6.2. □

Scaling Laws of Ergodic Transmission Capacity. If we consider $\epsilon \rightarrow 0$, the upper bound in (4.17) will reduce to $\epsilon \sum_{k=1}^m s_k^{\frac{2}{\alpha}} \phi_k / (\nu - s_k^{\frac{2}{\alpha}} \pi) + \Theta(\epsilon^2)$ since $-\ln(1 - \epsilon) \rightarrow \epsilon$. So we know $\bar{\lambda}_k^\epsilon \ll 1$ and thus the solution in (4.18) is $\bar{\lambda}_k^\epsilon = s_k^{\frac{2}{\alpha}} \epsilon / [(\sigma^2 d^{2\alpha} \beta^2 \delta^2 s_k^{1+\frac{1}{\alpha}} + \nu) - s_k^{\frac{2}{\alpha}} \pi] + \Theta(\epsilon^2)$. We can conclude that the lower bounds in (4.17) is $\epsilon \sum_{k=1}^m \phi_k s_k^{\frac{2}{\alpha}} / [(\sigma^2 d^{2\alpha} \beta^2 \delta^2 s_k^{1+\frac{1}{\alpha}} + \nu) - s_k^{\frac{2}{\alpha}} \pi] + \Theta(\epsilon^2)$ as $\epsilon \rightarrow 0$. So the bounds in (4.17) are asymptotically tight when the network is sparse because $\lambda = \Theta(\epsilon)$ as $\epsilon \rightarrow 0$. The scaling behavior of $\bar{\lambda}_E$ in this case turns out to be

$$\bar{\lambda}_E = \Theta \left(\frac{\epsilon}{\nu} \sum_{k=1}^m \frac{\phi_k s_k^{\frac{2}{\alpha}}}{1 - \pi s_k^{\frac{2}{\alpha}} / \nu} \right), \quad (4.19)$$

where the argument in $\Theta(\cdot)$ only keeps the *key* parameters of interest. The above result is also the scaling law for a dense network because $\nu \lambda \gtrsim -\ln(1 - \epsilon)$ as $\pi d^2 \lambda$ is sufficiently large. Note that (4.19) is only valid for small λ but large $\pi d^2 \lambda$

since for small λ we have to keep ϵ small and πd^2 sufficiently large in order to make $\pi d^2 \lambda$ large and the outage probability lower than ϵ . In addition, if $\nu \rightarrow \infty$ (i.e. d and/or $\delta \rightarrow \infty$), then (4.19) further reduces to

$$\bar{\lambda}_E = \Theta \left(\frac{\epsilon}{\pi d^2 (\delta \beta)^{\frac{2}{\alpha}}} \right), \quad (4.20)$$

which means ETC is not affected by the fading channel states if the received signal is very weak. This makes sense in that channels can be equivalently viewed in a bad state all the time when the received signal is very weak due to long transmission distance.

ETC with Distributed Channel-Aware Scheduling (DCAS). The result in Theorem 4.4.2 is obtained without any transmission scheduling. Suppose now the channel state information (CSI) is available at each transmitter. Then transmitters can use their CSI to do DCAS and thus we have the following corollary.

Corollary 4.4.3. *If all transmitters transmit only when their channel fading gains are in \mathcal{S}_g , the bounds on the ergodic transmission capacity are*

$$\frac{1}{\varphi_g} \sum_{k=g}^m s_k^{\frac{2}{\alpha}} \phi_k \bar{\lambda}_k^\epsilon \leq \bar{\lambda}_E \leq \frac{-\ln(1-\epsilon)}{\varphi_g} \sum_{k=g}^m \frac{s_k^{\frac{2}{\alpha}} \phi_k}{\nu - s_k^{\frac{2}{\alpha}} \pi}, \quad (4.21)$$

where $\varphi_g = \sum_{k=g}^m \phi_k$.

Proof. For DCAS, the bounds on the outage probability for channel state s_k is shown in (4.16). Hence, the bounds in (4.21) can be acquired by first taking off the terms with an index i lower than g in (4.17) and replacing $\bar{\lambda}_E$ in the bounds with $\varphi_g \bar{\lambda}_E$. Since ν , η and σ^2 do not depend on λ_g , we can replace λ_g in (4.16) by

$\bar{\lambda}$. Then following the same steps in the proof of Theorem 4.4.2 to derive (4.18), the lower bound in (4.21) is completely achieved. \square

4.4.3 Observations and Discussion

In the previous subsection, we have obtained bounds on ETC and discussed the scaling laws of ETC for a sparse and dense network. From the bounds and scaling laws, we have made three interesting observations.

ETC implicitly possesses a geometric interpretation. The scaling law of ETC in (4.19) can be expressed in a general form by vectors Φ and \mathbf{s}_ϵ as

$$C_E = \Theta(\Phi^T \mathbf{s}_\epsilon), \quad (4.22)$$

where $\Phi = [\phi_1, \phi_2, \dots, \phi_m]^T$ and \mathbf{s}_ϵ is defined as

$$\mathbf{s}_\epsilon \triangleq \epsilon \left[\frac{s_1^{\frac{2}{\alpha}}}{\nu - \pi s_1^{\frac{2}{\alpha}}}, \frac{s_2^{\frac{2}{\alpha}}}{\nu - \pi s_2^{\frac{2}{\alpha}}}, \dots, \frac{s_m^{\frac{2}{\alpha}}}{\nu - \pi s_m^{\frac{2}{\alpha}}} \right]^T = \left[\tilde{s}_1^{\frac{2}{\alpha}}, \tilde{s}_2^{\frac{2}{\alpha}}, \dots, \tilde{s}_m^{\frac{2}{\alpha}} \right]^T. \quad (4.23)$$

In other words, C_E is scaled by the inner product of vectors Φ and \mathbf{s}_ϵ . So the result in (4.22) can be interpreted from a geometric point of view. Suppose the Markov channel model has two fading states (i.e. $m = 2$, this is so called Gilbert-Elliott channel model [74] [75]). Then C_E in (4.22) can be schematically presented in Figure 4.2. Note that \mathbf{s}_ϵ must be above on the 45° line because s_2 is larger than s_1 . The inner product of \mathbf{s}_ϵ and Φ can be written as $\Phi^T \mathbf{s}_\epsilon = |\Phi| |\mathbf{s}_\epsilon| \cos \theta$ and θ is the angle between vectors \mathbf{s}_ϵ and Φ . So we will have a larger ETC if Φ has the same direction as \mathbf{s}_ϵ . The optimal Φ_* that maximizes ETC can be given by $\Phi_* = \frac{\mathbf{s}_\epsilon}{\mathbf{u}^T \mathbf{s}_\epsilon}$. Therefore, if all Markov fading channels have the optimal distribution

Φ_* , then C_E in (4.22) becomes

$$C_E = \Theta \left(\frac{\mathbf{s}_\epsilon^\top \mathbf{s}_\epsilon}{\mathbf{u}^\top \mathbf{s}_\epsilon} \right), \quad (4.24)$$

and thus it is completely characterized by all channel fading states.

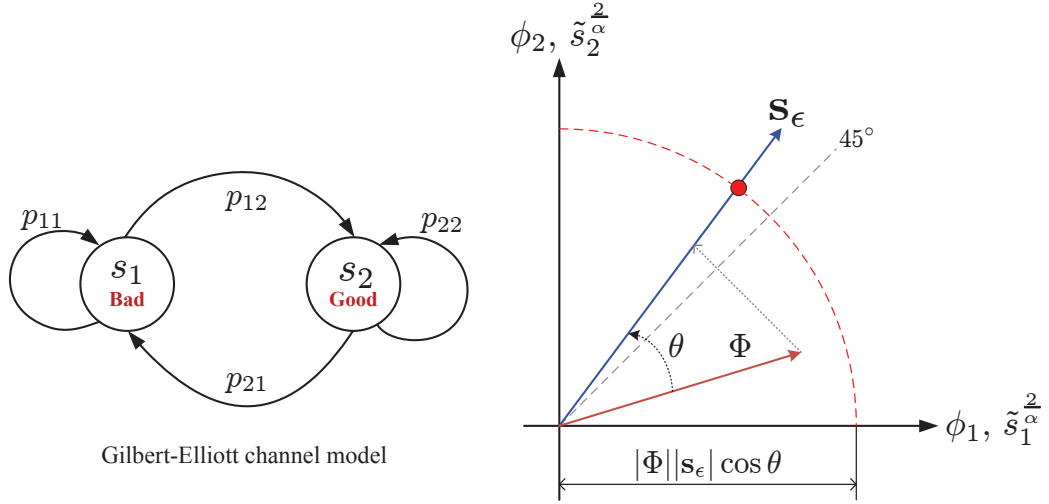


Figure 4.2: The Gilbert-Elliott channel model and its corresponding geometric presentation of C_E , where $\{p_{ij}\}$ are the state transition probabilities for the FSMC model

and $\tilde{s}_k = \frac{\epsilon^{\frac{\alpha}{2}} s_k}{\left(\nu - \pi s_k^{\frac{\alpha}{2}}\right)^{\frac{\alpha}{2}}}$.

Dominant channel states may not dominate ETC. Dominant states in a Markov chain means that their invariant probabilities are much larger than other states' invariant probabilities. In other words, if a channel has dominant states then it is in these states most of the time. Dominant channel states may not contribute too much ETC since their state magnitudes could be very small (very bad states). Thus, dominant channel states which really *dominates* ETC only when they have a large magnitude. This point can also be visually explained

by Figure 4.2. Suppose s_2 dominates and it is much larger than s_1 . In this case, Φ and \mathbf{s}_ϵ will move up and be close to the vertical axis. The projection of Φ on \mathbf{s}_ϵ will largely increase and it is mostly contributed by the vertical component. Thus, whether a channel state dominates ETC or not depends on the product of its magnitude and invariant probability.

DCAS may not benefit ETC. If we compare the results in Theorem 4.4.2 and Corollary 4.4.3, we can find DCAS indeed increases the bounds with good channel states. Nevertheless, *it may not always improve ETC since it loses the throughput contributed by bad channel states.* To show this, let the upper bound in (4.17) be greater than the upper bound in (4.21). This leads to the following inequality:

$$\left(\frac{1}{\varphi_g} - 1\right) \sum_{k=g}^m \frac{s_k^{\frac{2}{\alpha}} \phi_k}{\nu - \pi s_k^{\frac{2}{\alpha}}} < \sum_{k=1}^{g-1} \frac{s_k^{\frac{2}{\alpha}} \phi_k}{\nu - \pi s_k^{\frac{2}{\alpha}}}. \quad (4.25)$$

The LHS in the above expression is the ETC improved by DCAS and the RHS is the ETC loss because of bad channel states. If this inequality is valid, apparently DCAS may not improve ETC because the ETC increase in the good states could not compensate the ETC loss in the bad states. A schematic example of ETC with two-state Markov fading channels is shown in Figure 4.3 to geometrically explain why DCAS may not benefit ETC. If DCAS is not used to schedule transmissions, the ETC is the scaled length of segment $\overline{\mathbf{od}}$, i.e. for a positive constant ρ , $C_E = \rho \Phi^T \mathbf{s}_\epsilon$. Suppose now DCAS is used and the ETC can be shown as $\rho \tilde{s}_2^{\frac{2}{\alpha}}$ which is the scaled length of segment $\overline{\mathbf{ao}}$ (i.e. it is the vertical component of \mathbf{s}_ϵ scaled by ρ). Obviously, we can observe that segment $\overline{\mathbf{od}}$ is longer than segment $\overline{\mathbf{oa}}$ so that DCAS does not benefit ETC in this case.

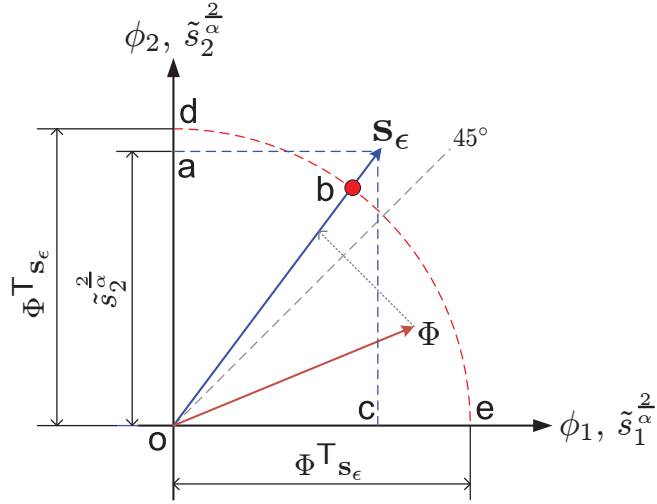


Figure 4.3: A geometric example of illustrating why DCAS does not always benefit ETC.

Following from (4.25), the better policy of using DCAS for a transmitter is when the following condition holds

$$\varphi_g \leq \frac{\epsilon \sum_{k=g}^m s_k^{\frac{2}{\alpha}} \phi_k / (\nu - \pi s_k^{\frac{2}{\alpha}})}{\Phi^T \mathbf{s}_\epsilon}. \quad (4.26)$$

However, the above condition is not implementable by transmitters in a wireless ad hoc network without knowing Φ in advance. So DCAS is not always an effective means to enhance ETC in a real-time situation. A simulation example for ETC with and without DCAS is shown in Figure 4.4. Channel fading is modeled by a 2-state Markov chain and the simulation condition is set to let the bad channel state be dominant. Obviously, we can see that ETC with DCAS is worse than ETC without DCAS.

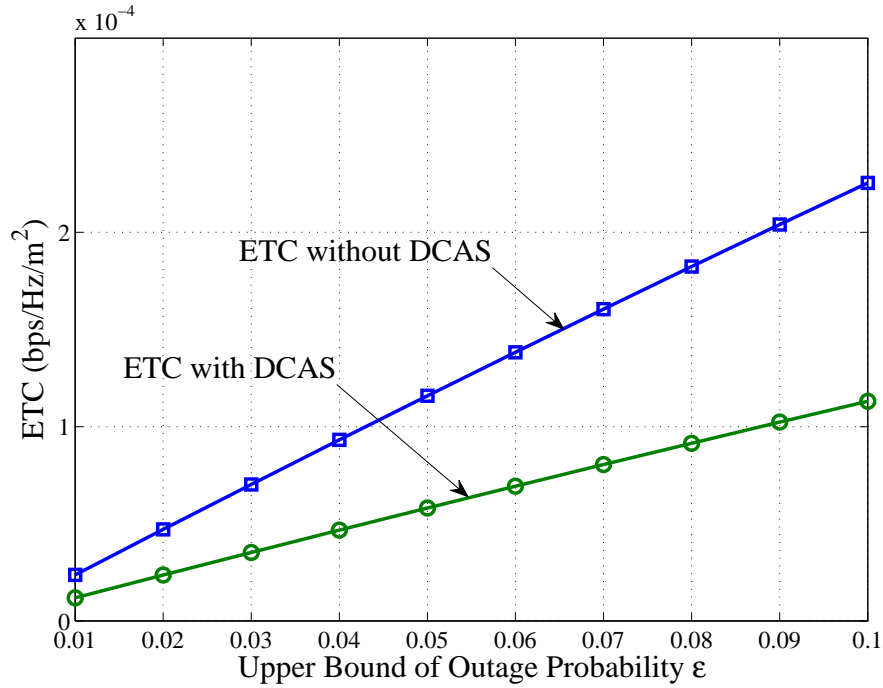


Figure 4.4: Numerical results for ETC with and without DCAS. The network parameters for simulation are : $d = 10m$, $\beta = 2$, $\alpha = 3$, $\delta = 1.5$, $s_1 = 0.5$, $s_2 = 2$, $\phi_1 = 0.8$, $\phi_2 = 0.2$ and $\lambda = 0.01$.

4.5 Ergodic Transmission Capacity with Interference Management

In Section 4.4.3, we observed that refraining from transmitting when channels are in bad states does not necessarily increase ETC. This is because the DCAS scheme increases the transmission capacity for good channel states but further lowers the transmission capacity for users in bad channel states. That is, the throughput increase does not in general compensate for the throughput loss, particularly when bad channel states are dominant (i.e. channels are bad

most of the time). Thus, the key to increasing ETC is to boost every entry of vector \mathbf{s}_ϵ and not to sacrifice transmission opportunities of users with bad channel states. Two possible approaches to attaining this goal are through power control and interference management. In general, power control makes the analysis of the outage probability more intractable due to the complex structure of the interference. In addition, it is not a very effective means to increase SIR in a interference-limited ad hoc work [77] [78].

4.5.1 Interference Management – A Stochastic Geometry Perspective

Interference management can be classified into three categories: *interference avoidance, suppression and cancellation*. Avoiding interference in a wireless ad hoc network is typically accomplished by using space, time or frequency orthogonality to eliminate the co-reception of strong interferers. Frequency-hopping and CSMA are prominent examples of avoiding interference in an ad hoc network. Interference suppression deploys signal processing at the transmitter and/or receiver to (linearly) suppress interference without actually cancelling it. Direct-Sequence CDMA (DS-CDMA) is a typical example of this category. In addition, receivers can try to cancel strong interference from their nearby unintended transmitters (e.g. successive interference cancellation (SIC) [79–81]). Although avoiding interference and suppressing interference are two different methods of reducing interference, we know there exists a duality property between them in a wireless network with Poisson-distributed nodes. According to the conserva-

tion property of a homogeneous PPP [57]⁸, these two methods both reduce the original intensity of transmitters so that their effect can be demonstrated via another homogeneous PPP with a new intensity. However, interference avoidance has a better efficiency in reducing the intensity of interferers than interference suppression [13] [78].

The effect of interference cancellation can also be grasped from a geometric perspective. To explain this, suppose now any receiver Y_i in the network is able to cancel some interference from its nearby interferers after the interference is avoided and/or suppressed. As time goes to infinity, the *interference cancellation coverage* of receiver Y_0 with channel state s_k is defined in the following.

$$\mathcal{C}_k^c = \left\{ X \in \mathbb{R}^2 : \frac{\tilde{H}|X|^{-\alpha}}{s_k d^{-\alpha} + \gamma_k I_0} \geq \frac{\beta}{\beta + 1} \right\}, \quad (4.27)$$

where I_0 is the interference of receiver Y_0 and $\gamma_k \in (0, 1)$ is called interference reduction factor for channel state s_k ⁹. Coverage \mathcal{C}_k^c means that any received interference within this region can be decoded by receiver Y_0 with channel state s_k , and all transmitters in \mathcal{C}_k^c have a larger received power than transmitter X_0 if $\mathcal{C}_k^c \cap (\Pi \setminus X_0)$ is not empty and $\beta > 1$. Also, \mathcal{C}_k^c is a random compact set so that its mean Lebesgue measure $\mu(\mathcal{C}_k^c)$ is finite. If each receiver can perfectly cancel all interferers in its cancellation coverage after suppressing and/or avoiding some

⁸The conservation property of a homogeneous PPP with intensity λ is that the intensity will change to λ/a if all locations of the nodes in the PPP are scaled by a constant \sqrt{a} .

⁹Reduction factor γ_k can account for the joint effect of interference avoidance and suppression. For example, if there are $M > 1$ available channels for DS-CDMA with spreading gain $G > 1$, then $\gamma_k = 1/GM^{\frac{\alpha}{2}}$.

interference, then its SIR for channel state s_k is

$$\text{SIR}_k = \frac{s_k d^{-\alpha}}{\sum_{X_j \in \Pi_k^{\text{nc}}} \tilde{H}_j(\tau) |X_j|^{-\alpha}}, \quad (4.28)$$

where $\Pi_k^{\text{nc}} \triangleq \Pi \setminus (\mathcal{C}_k^c \cap \Pi \cup X_0)$ is the noncancelable part of Π with intensity $\lambda \gamma_k^{\frac{2}{\alpha}}$. So equation (4.28) essentially suggests that interference management can be equivalently reflected by constructing a new PPP with a reduced intensity. The above SIR_k expression will be used in the following subsection to find the bounds on the outage probability. Those bounds are used to characterize the bounds on ETC with interference management.

4.5.2 Bounds on Outage Probability with Interference Management

Bounds on the outage probability with interference management are shown in the following theorem.

Theorem 4.5.1. *If each receiver is able to avoid and/or suppress interference, and cancel interferers in its cancellation coverage, then bounds on the outage probability for channel state s_k are given by*

$$1 - e^{-\lambda_k^m (\nu s_k^{-\frac{2}{\alpha}} - \pi)} \leq q_k(\lambda) \leq 1 - \left(1 - \Lambda_k \left(\gamma_k^{\frac{2}{\alpha}} \lambda\right)\right)^+ e^{-\lambda_k^m (\nu s_k^{-\frac{2}{\alpha}} - \pi)}, \quad (4.29)$$

where $\lambda_k^m \triangleq \gamma_k^{\frac{2}{\alpha}} \lambda \left(1 - \frac{\nu_k^c}{\nu}\right)^+$ is the average intensity of the transmitters in \mathcal{I}_k^δ with interference management and ν_k^c is the mean Lebesgue measure of \mathcal{C}_k^c .

Proof. See Appendix 4.6.3. □

There are a couple of observations that can be drawn from Theorem 4.5.1. First, the upper and lower bounds in (4.29) are smaller than those in (4.13).

Canceling interference can be viewed as constructing a new PPP with reduced intensity $\gamma_k^{\frac{2}{\alpha}} \lambda (1 - \nu_k^c / \nu)^+$ in \mathcal{I}_k^δ , and it is more efficient to reduce interference than suppressing interference since it completely eliminates transmitters with strong interference power and thus the $1 - \nu_k^c / \nu$ term does not have an exponent of $\frac{2}{\alpha}$. Thus, we can infer that imperfect interference cancellation (i.e. interference suppression) is not as efficient as perfect interference cancellation (i.e. intensity reduction) and interference avoidance since it merely decreases transmitters' interference and does not directly reduce transmitter intensity.

Second, interference cancellation is not equally useful for all networks. For example, in a dense network, canceling the strong interferences from the nearby transmitters can significantly reduce outage probability such that network throughput is substantially increased. This point can be easily verified by letting $\lambda \nu$ be sufficiently large. In this case, $q_k(\lambda)$ is close to unity if no interference is canceled. On the other hand, for sparse networks, interference cancellation may merely have a marginal reduction in outage probability. For sufficiently small $\lambda \nu$ and $\nu > \nu_k^c$, (4.29) can be simplified as $q_k(\lambda) = \left(\frac{\gamma_k}{s_k}\right)^{\frac{2}{\alpha}} \lambda (\nu - \nu_k^c) + O((\lambda \nu)^2)$. So when receivers cancel more interferers, its outage probability is reduced by amount of $O(\lambda \nu_k^c)$ which is really a small and trivial improvement. From this observation, we see that canceling strong interferers for each channel state may not be an effective means to increase transmission capacity for small ϵ since the maximum contention intensity of transmission capacity for each channel state is already a small value in this case.

4.5.3 ETC with Interference Management

According to the bounds on the outage probability in Theorem 4.5.1, ETC with interference management is bounded as shown in the following theorem.

Corollary 4.5.2. *Suppose interference management is used in the network and each receiver is able to perfectly cancel all interferers in the interference cancellation coverage of each channel state. Let the outage probability be upper bounded by $\epsilon \in (0, 1)$. If $\mathcal{C}_k^c \subset \mathcal{I}_k^\delta$, the maximum contention intensity for channel state s_k has the bounds given by*

$$\sum_{k=1}^m \left(\frac{s_k}{\gamma_k} \right)^{\frac{2}{\alpha}} \phi_k \bar{\lambda}_k^\epsilon \leq \bar{\lambda}_E \leq -\ln(1 - \epsilon) \sum_{k=1}^m \left(\frac{s_k}{\gamma_k} \right)^{\frac{2}{\alpha}} \frac{\phi_k}{(\nu - s_k^\alpha \pi)(1 - \nu_k^c/\nu)}, \quad (4.30)$$

where $\nu > \nu_k^c$ and $\bar{\lambda}_k^\epsilon$ is given by

$$\bar{\lambda}_k^\epsilon = \inf \left\{ \lambda > 0 : \frac{1}{\lambda} \ln \left[\frac{(1 - \Lambda_k(\lambda))^+}{1 - \epsilon} \right] \leq \left(1 - \frac{\nu_k^c}{\nu} \right) \left(\nu - s_k^\alpha \pi \right) \right\}. \quad (4.31)$$

However, if $\mathcal{I}_k^\delta \subseteq \mathcal{C}_k^c$, then (4.30) becomes

$$\lambda_E \geq \sum_{k=1}^m \left(\frac{s_k}{\gamma_k} \right)^{\frac{2}{\alpha}} \phi_k \bar{\lambda}_k^\epsilon, \quad (4.32)$$

where $\bar{\lambda}_k^\epsilon = \inf \left\{ \lambda > 0 : \left(1/d^\alpha \delta \beta - \lambda \eta s_k^{1-\frac{2}{\alpha}} \gamma_k^{-\frac{2}{\alpha}} \right)^2 \leq s_k^{1-\frac{1}{\alpha}} \gamma_k^{\frac{2}{\alpha}} \frac{\sigma^2}{\epsilon} \lambda \right\}$.

Proof. See Appendix 4.6.4. □

By comparing (4.30) with (4.17), we can perceive that the effect of interference cancellation on ergodic transmission capacity can be interpreted to shrink ν by $(1 - \nu_k^c/\nu)$ -fold. This is equivalent to saying channel gain s_k increases $(1 - \nu_k^c/\nu)^{-\frac{\alpha}{2}}$ -fold. Suppose ϵ is small and thus from (4.30) and (4.31) we know

$\bar{\lambda}_{\mathbf{E}} \approx \epsilon \sum_{k=1}^m \left(\frac{s_k}{\gamma_k}\right)^{\frac{2}{\alpha}} \frac{\phi_k}{(\nu - \pi s_k^{\frac{2}{\alpha}})(1 - \nu_k^c/\nu)}$. So interference cancellation in a sparse network can make the transmission capacity for channel state s_k increase $(1 - \nu_k^c/\nu)^{-1}$ -fold. Although avoiding and suppressing interference can linearly augment ETC in a sparse network, interference cancellation could contribute much more ETC than them if ν_k^c is very close to ν . Figure 4.5 presents a simulation example showing how interference management improves ETC. We first notice that interference management does not provide too much ETC gain when ϵ is extremely small. On the other hand, if the network is very dense, the efficacy of interference cancellation is seriously weakened because interference is large. So the solid-circle curve of ETC looks like a concave function of ϵ . Therefore, interference management in an extremely sparse or dense network can merely have marginal improvement on outage probability.

How should interference management be used for each channel state to maximize ETC? In Section 4.4.3, we have pointed out that ETC has a geometric interpretation since its bounds can be viewed as the inner product of two vectors: vectors Φ and \mathbf{s}_ϵ should roughly align. Since vector Φ is a channel characteristic, it cannot be manipulated to the desired direction. Therefore, the only option is to design vector \mathbf{s}_ϵ such that it is enlarged and rotated to the direction of Φ as closely as possible. This can be attained by interference management. To illustrate the idea of how to change \mathbf{s}_ϵ , the right part of Figure 4.2 is redrawn in Figure 4.6. Let $\mathbf{s}_\epsilon = \left[\tilde{s}_1^{\frac{2}{\alpha}} \tilde{s}_2^{\frac{2}{\alpha}}\right]^T$ where $\tilde{s}_k = s_k \epsilon^{\frac{\alpha}{2}} \left(\nu - \pi s_k^{\frac{2}{\alpha}}\right)^{-\frac{\alpha}{2}}$ and $\mathbf{s}_\epsilon^* = \left[(\tilde{s}_1^*)^{\frac{2}{\alpha}} (\tilde{s}_2^*)^{\frac{2}{\alpha}}\right]^T$ represent the optimal vector that \mathbf{s}_ϵ can achieve by interference management. Note that $\tilde{s}_k^* = \frac{\tilde{s}_k}{\gamma_k} (1 - \nu_k^c/\nu)^{-\frac{\alpha}{2}}$, $k = 1, 2$. Therefore, after interference is reduced, vertices $\mathbf{c} \left(\tilde{s}_1^{\frac{2}{\alpha}}, 0\right)$ and $\mathbf{a} \left(0, \tilde{s}_2^{\frac{2}{\alpha}}\right)$ can be maximally pushed out to vertices $\mathbf{h} \left((\tilde{s}_1^*)^{\frac{2}{\alpha}}, 0\right)$ and

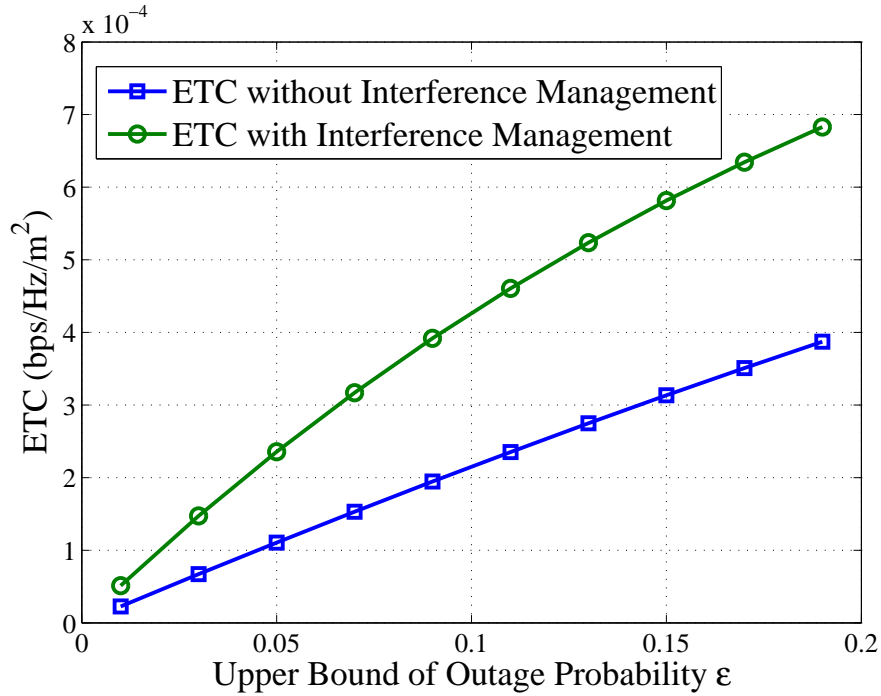


Figure 4.5: Numerical results for ETC with and without interference management. The network parameters for simulation are : $d = 10m$, $\beta = 2$, $\alpha = 3$, $\delta = 2$, $s_1 = 0.5$, $s_2 = 2$, $\phi_1 = \phi_2 = 0.5$, $\gamma_1 = \gamma_2 = 0.6$ and $\lambda = 0.02$.

$\mathbf{f} (0, (\tilde{s}_2^*)^{\frac{2}{\alpha}})$. Vertex \mathbf{i} is the point where \mathbf{s}_ϵ^* is projected on Φ and Vertex \mathbf{d} is the point where \mathbf{s}_ϵ is projected on Φ . The distance from \mathbf{m} to \mathbf{e} represents the increase of ETC due to interference management.

Since \mathbf{s}_ϵ^* is the best vector \mathbf{s}_ϵ can achieve, how can we make vector \mathbf{s}_ϵ move to vector \mathbf{s}_ϵ^* ? Namely, how should we choose γ_k and ν_k^c for each channel state s_k such that \mathbf{s}_ϵ can approach \mathbf{s}_ϵ^* ? The policy is to reduce interference for each channel state as much as possible because we can formulate the following

nonlinear programming problem to optimize all γ_k :

$$\max_{\gamma_k} \sum_{k=1}^m \left(\frac{\phi_k s_k^{\frac{2}{\alpha}}}{\nu - \pi s_k^{\frac{2}{\alpha}}} \right)^{\frac{\alpha}{2}} \frac{1}{\gamma_k [(1 - \nu_k^c/\nu)]^{\frac{\alpha}{2}}} \quad (4.33)$$

$$\text{subject to } \gamma_k \geq \gamma_{\min_k}, \quad \text{for all } k \in \mathcal{M}, \quad (4.34)$$

where γ_{\min_k} is the lower bound of γ_k and it can be determined by the system resources or limitations such as number of available channels and the maximum spreading gain, etc. Note that ν_k^c is a monotonically decreasing and nonlinear function of γ_k so that $1/\gamma_k [(1 - \nu_k^c/\nu)]^{\frac{\alpha}{2}}$ is also a monotonically decreasing function of γ_k . Therefore, the optimal solution of γ_k must happen at $\gamma_k = \gamma_{\min_k}$, which means interference should be avoided, suppressed and cancelled as much as possible in order to achieve \mathbf{s}_ϵ^* . In addition, using interference management could make DCAS perform poorly because it may make most of channel states become “good” so that $\varphi_g \approx 1$.

4.6 Appendix : Proofs of Lemmas and Theorems

4.6.1 Proof of Theorem 4.4.1

First of all, we have to find the intensity λ_δ of Π_k^δ . According to [17], the Laplace functional of a stationary PPP Π for a nonnegative function $w : \mathbb{R}^2 \rightarrow \mathbb{R}_+$ is given by

$$\begin{aligned} \mathcal{L}_\Pi(w) &\triangleq \mathbb{E} \left[e^{-\int_{\mathbb{R}^2} w(X) \Pi(dX)} \right] \\ &= \exp \left(- \int_{\mathbb{R}^2} \lambda (1 - e^{-w(X)}) \mu(dX) \right). \end{aligned} \quad (4.35)$$

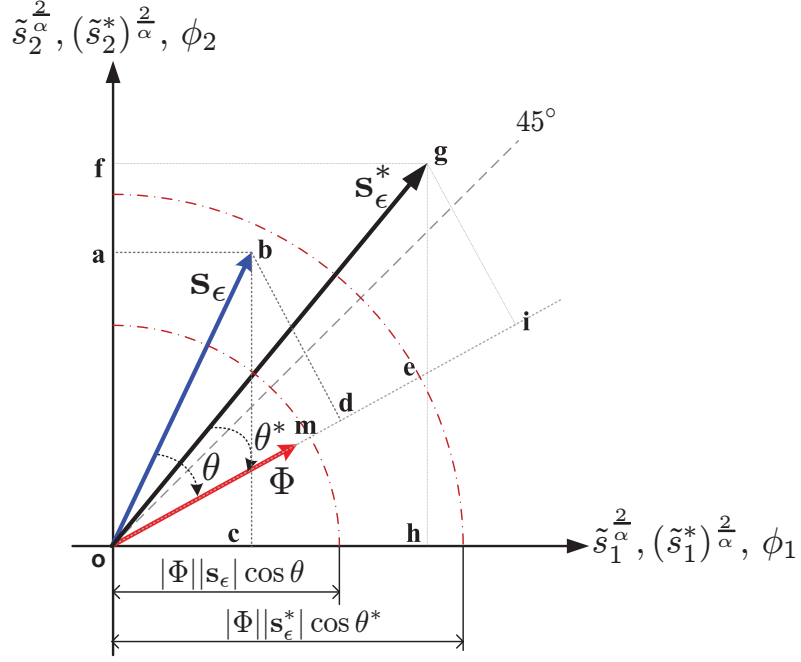


Figure 4.6: The geometric representation of the ETC for an FSMC with 2 states. \mathbf{s}_ϵ^* is the optimal vector that \mathbf{s}_ϵ can achieve by interference management. By using interference management, vertices \mathbf{a} and \mathbf{c} can be optimally moved to \mathbf{f} and \mathbf{h} , respectively. The projection points of vertices \mathbf{b} and \mathbf{g} on Φ are \mathbf{d} and \mathbf{i} , respectively.

Since the Laplace functional completely characterizes the distribution of a point process, we can find the intensity of Π_k^δ by calculating $\mathcal{L}_{\Pi_k^\delta}(w)$. For a bounded Borel set $\mathcal{A} \subset \mathbb{R}^2$, The Laplace functional of Π_k^δ with $w(X) = \tilde{w}(X)\mathbb{1}_{\Pi_k^\delta}(X)$ can

be written as follows:

$$\begin{aligned}
\mathcal{L}_{\Pi_k^\delta}(w) &= e^{-\lambda\mu(\mathcal{A})} \sum_{i=0}^{\infty} \frac{\lambda^i}{i!} \int_{\mathcal{A}} \cdots \int_{\mathcal{A}} \prod_{j=1}^i (e^{-w(X_j)} \mathbb{P}[X_j \in \Pi_k^\delta] + \mathbb{P}[X_j \notin \Pi_k^\delta]) \\
&\quad \mu(dX_1) \cdots \mu(dX_i) \\
&= e^{-\lambda\mu(\mathcal{A})} \sum_{i=0}^{\infty} \frac{1}{i!} \left\{ \int_{\mathcal{A}} (e^{-g(Y)} \mathbb{P}[Y \in \Pi_k^\delta] + 1 - \mathbb{P}[Y \in \Pi_k^\delta]) \lambda \mu(dY) \right\}^i \\
&\stackrel{(a)}{=} \exp \left(-\lambda \int_{\mathcal{A}} (1 - e^{-g(Y)}) \left[\sum_{i=1}^m \mathbb{1} \left(s_i \in \left[\frac{s_k d^{-\alpha}}{\ell(|Y|) \delta \beta}, \infty \right) \right) \phi_i \right] \mu(dY) \right),
\end{aligned}$$

where (a) follows from the property of spatial ergodicity. Letting $\mathcal{A} \rightarrow \mathbb{R}^2$ and according to (4.35), we know the intensity of Π_k^δ is

$$\lambda_k^\delta(x) = \lambda \sum_{i=1}^m \phi_i \mathbb{1} \left(s_i \in \left[\frac{s_k d^{-\alpha}}{\ell(x) \delta \beta}, \infty \right) \right), \quad x \in \mathbb{R}_+. \quad (4.36)$$

So Π_k^δ is a non-homogeneous PPP since λ_k^δ depends on x .

Since $\Pi_k^\delta(\mathcal{I}_k^\delta)$ is a Poisson random variable, its mean can be found as follows:

$$\begin{aligned}
\mathbb{E}[\Pi_k^\delta(\mathcal{I}_k^\delta)] &= \mathbb{E} \left[\sum_{X_j \in \Pi \setminus X_0} \mathbb{1}_{\Pi_k^\delta}(X_j) \right] \\
&\stackrel{(b)}{=} \int_{\mathbb{R}^2} \mathbb{E}[\mathbb{1}_{\Pi_k^\delta}(X)] \mu(dX) = \int_{\mathbb{R}^2} \lambda_\delta(|X|) \mu(dX) \\
&= 2\pi \lambda \int_0^\infty \left[\sum_{i=1}^m \mathbb{1} \left(s_i \in \left[\frac{s_k d^{-\alpha}}{\ell(x) \delta \beta}, \infty \right) \right) \phi_i \right] x dx \\
&= 2\pi \lambda \sum_{i=1}^m \phi_i \int_1^{d \sqrt{\frac{\delta \beta s_i}{s_k}}} x dx = \pi \lambda s_k^{-\frac{2}{\alpha}} \left(d^2 (\delta \beta)^{\frac{2}{\alpha}} \sum_{i=1}^m \phi_i s_i^{\frac{2}{\alpha}} - s_k^{\frac{2}{\alpha}} \right) \\
&= \lambda (s_k^{-\frac{2}{\alpha}} \nu - \pi).
\end{aligned}$$

where (b) follows from the Campbell theorem [57]. Let $\mathcal{E}(\Pi_k^\delta)$ denote the outage

event caused by any transmitters in Π_k^δ and its probability is

$$\mathbb{P}[\mathcal{E}(\Pi_k^\delta)] = 1 - \exp\left(-\lambda\left(\nu s_k^{-\frac{2}{\alpha}} - \pi\right)\right) \leq q_k(\lambda),$$

which is a lower bound of $q_k(\lambda)$ because it ignores the interference contributed by the transmitters that are not in Π_k^δ .

Let $\mathcal{E}^c(\Pi_k^\delta)$ be the complement event of $\mathcal{E}(\Pi_k^\delta)$ and $\mathcal{E}^c(\Pi_k^\delta)$ means the outage event caused by the transmitters of $\Pi \setminus \Pi_k^\delta$. So the upper bound of $q_k(\lambda)$ is given by

$$\begin{aligned} q_k(\lambda) &\leq \mathbb{P}[\mathcal{E}(\Pi_k^\delta) \cup \mathcal{E}^c(\Pi_k^\delta)] \\ &= 1 - e^{-\lambda(\nu s_k^{-\frac{2}{\alpha}} - \pi)} + \mathbb{P}[\mathcal{E}^c(\Pi_k^\delta)] e^{-\lambda(\nu s_k^{-\frac{2}{\alpha}} - \pi)}, \end{aligned} \quad (4.37)$$

where $\mathbb{P}[\mathcal{E}^c(\Pi_k^\delta)] = \mathbb{P}[s_k d^{-\alpha} < \beta I_k^c]$ and I_k^c is the interference contributed by the transmitters of $\Pi \setminus \Pi_k^\delta$. Unfortunately, it is impossible to explicitly calculate $\mathbb{P}[\mathcal{E}(\mathcal{I}_k^c)]$ and thus we resort to find its upper bound by Chebyshev's inequality. Using Campbell's theorem, the mean and variance of interference I_k^c can be calculated as follows:

$$\begin{aligned} \mathbb{E}[I_k^c] &= \mathbb{E}\left[\sum_{X_l \in \Pi} \tilde{H}_l \ell(|X_l|) \mathbf{1}_{\Pi \setminus \Pi_k^\delta}(X_l)\right] \\ &= \mathbb{E}[\tilde{H}] \int_{\mathbb{R}^2} \ell(|X|) [\lambda - \lambda_\delta(|X|)] \mu(dX) = \lambda s_k^{1-\frac{2}{\alpha}} \eta, \end{aligned}$$

$$\begin{aligned} \text{Var}[I_k^c] &= \mathbb{E}[(I_k^c)^2] - \mathbb{E}[I_k^c]^2 \\ &= \mathbb{E}[\tilde{H}^2] \int_{\mathbb{R}^2} [\ell(|X|)]^2 [\lambda - \lambda_\delta(|X|)] \mu(dX) = \lambda s_k^{1-\frac{1}{\alpha}} \sigma^2, \end{aligned}$$

where σ^2 is bounded is due to bounded η since $[\ell(x)]^2 \leq \ell(x)$. The upper bound of $\mathbb{P}[\mathcal{E}^c(\Pi_k^\delta)]$ can be obtained by

$$\begin{aligned} \mathbb{P}[\mathcal{E}^c(\Pi_k^\delta)] &= \mathbb{P}[d^{-\alpha} < \delta\beta I_k^c] \\ &\leq \mathbb{P}\left[\frac{d^{-\alpha} - s_k^{1-\frac{2}{\alpha}}\delta\beta\lambda\eta}{|d^{-\alpha} - s_k^{1-\frac{2}{\alpha}}\delta\beta\lambda\eta|} \leq \frac{\delta\beta|I_k^c - s_k^{1-\frac{2}{\alpha}}\lambda\eta|}{|d^{-\alpha} - s_k^{1-\frac{2}{\alpha}}\delta\beta\lambda\eta|}\right] \\ &\stackrel{(c)}{\leq} \frac{s_k^{\frac{3}{\alpha}-1}\lambda\sigma^2}{(s_k^{\frac{2}{\alpha}-1}/d^\alpha\delta\beta - \lambda\eta)^2}, \end{aligned}$$

where (c) follows from Chebyshev's inequality. Substituting the above result into (4.37), the proof is complete.

4.6.2 Proof of Theorem 4.4.2

Since $\sum_{k=1}^m \phi_k q_k(\lambda) \leq \epsilon$, the lower bound in (4.13) with $\bar{\lambda}_E$ can be rewritten as

$$\sum_{k=1}^m \phi_k \exp\left(-\bar{\lambda}_E(\nu s_k^{-\frac{2}{\alpha}} - \pi)\right) \geq 1 - \sum_{k=1}^m \phi_k q_k(\bar{\lambda}_E) \geq 1 - \epsilon,$$

which gives us

$$\bar{\lambda}_E \sum_{k=1}^m \phi_k e^{-\bar{\lambda}_E(\nu s_k^{-\frac{2}{\alpha}} - \pi)} \geq \bar{\lambda}_E \Rightarrow \sum_{k=1}^m \bar{\lambda}_k^\epsilon \phi_k e^{-\bar{\lambda}_k^\epsilon(\nu s_k^{-\frac{2}{\alpha}} - \pi)} \geq \sum_{k=1}^m \phi_k \bar{\lambda}_k^\epsilon (1 - \epsilon),$$

where $\bar{\lambda}_k^\epsilon = \arg \max_\lambda \lambda e^{-\lambda(\nu s_k^{-\frac{2}{\alpha}} - \pi)}$. Hence, $e^{-\bar{\lambda}_k^\epsilon(\nu s_k^{-\frac{2}{\alpha}} - \pi)} \geq 1 - \epsilon$ so that we have

$$\bar{\lambda}_k^\epsilon \leq \frac{-\ln(1 - \epsilon)}{s_k^{-\frac{2}{\alpha}}\nu - \pi} \Rightarrow \bar{\lambda}_E \leq \frac{-\ln(1 - \epsilon)}{s_k^{-\frac{2}{\alpha}}\nu - \pi} \sum_{k=1}^m \phi_k s_k^{\frac{2}{\alpha}}. \quad (4.38)$$

So the upper bound on $\bar{\lambda}_E$ is acquired.

Similarly, we know $1 - \sum_{k=1}^m \phi_k q_k(\bar{\lambda}_E) \geq 1 - \epsilon$ and (4.13) with $\bar{\lambda}_E$ can give us another lower bound on $1 - \sum_{k=1}^m \phi_k q_k(\bar{\lambda}_E)$. Combining these two lower

bounds, it yields the following result:

$$1 - \sum_{k=1}^m \phi_i q_i(\bar{\lambda}_{\mathbf{E}}) \geq \max \left\{ 1 - \epsilon, \sum_{k=1}^m \phi_k (1 - \Lambda_k(\bar{\lambda}_{\mathbf{E}}))^+ e^{-\bar{\lambda}_{\mathbf{E}}(\nu s_k^{-\frac{2}{\alpha}} - \pi)} \right\}. \quad (4.39)$$

Since $(1 - \Lambda_k(\bar{\lambda}_{\mathbf{E}}))^+ e^{-\bar{\lambda}_{\mathbf{E}}(\nu s_k^{-\frac{2}{\alpha}} - \pi)}$ is a monotonically decreasing function of $\bar{\lambda}_{\mathbf{E}}$, the lower bound on $\bar{\lambda}_{\mathbf{E}}$ must happen when $(1 - \Lambda_k(\bar{\lambda}_{\mathbf{E}}))^+ e^{-\bar{\lambda}_{\mathbf{E}}(\nu s_k^{-\frac{2}{\alpha}} - \pi)}$ is equal to $1 - \epsilon$, which means $\bar{\lambda}_k^\epsilon = \inf\{\lambda : (1 - \Lambda_k(\lambda))^+ e^{-\lambda(\nu s_k^{-\frac{2}{\alpha}} - \pi)} \leq 1 - \epsilon\}$. We can explicitly write the relationship $(1 - \Lambda_k(\lambda))^+ e^{-\lambda(\nu s_k^{-\frac{2}{\alpha}} - \pi)} \leq 1 - \epsilon$ in the following.

$$\ln \left[\frac{(1 - \Lambda_k(\lambda))^+}{1 - \epsilon} \right] \leq \lambda(\nu s_k^{-\frac{2}{\alpha}} - \pi),$$

which implies

$$\bar{\lambda}_k^\epsilon = \inf \left\{ \lambda > 0 : \frac{1}{\lambda} \ln \left[\frac{(1 - \Lambda_k(\lambda))^+}{1 - \epsilon} \right] \leq \left(\nu s_k^{-\frac{2}{\alpha}} - \pi \right) \right\}.$$

Thus, the lower bound on $\bar{\lambda}_{\mathbf{E}}$ can be written as $\sum_{k=1}^m \phi_k s_k^{\frac{2}{\alpha}} \bar{\lambda}_k^\epsilon$. The proof is complete.

4.6.3 Proof of Theorem 4.5.1

Since the interference generated by Π is scaled by γ_k , it is equivalent to the interference generated by a stationary PPP with intensity $\gamma_k^{\frac{2}{\alpha}} \lambda$. The intensity of Π_k^{nc} at location X can be shown to be

$$\lambda_k^{\text{nc}}(|X|) = \gamma_k^{\frac{2}{\alpha}} \lambda \mathbb{P} \left[\frac{\tilde{H}|X|^{-\alpha}}{s_k d^{-\alpha} + I_0} < \frac{\beta}{1 + \beta} \right].$$

The average number of nodes in \mathcal{C}_k^c is $\int_0^\infty [\gamma_k^{\frac{2}{\alpha}} \lambda - \lambda_k^{\text{nc}}(|X|)] \mu(dX) = \gamma_k^{\frac{2}{\alpha}} \lambda \nu_k^c$. The lower bound on the outage probability can be characterized by the average number of noncancelable nodes within \mathcal{I}_k^δ , that means we have to find $\gamma_k^{\frac{2}{\alpha}} \lambda \mu(\mathcal{C}_k^c \cap \mathcal{I}_k^\delta)$ which is the average number of nodes in $\Pi_k^{\text{nc}} \cap \mathcal{I}_k^\delta$.

Transmitters in \mathcal{I}_k^δ and \mathcal{C}_k^c must satisfy the following in two equalities, respectively:

$$|X_j| \leq \left(\frac{\delta\beta\tilde{H}_j}{s_k} \right)^{1/\alpha} d \quad (\text{for } X_j \in \mathcal{I}_k^\delta),$$

$$|X_j| \leq \left[\frac{\tilde{H}_j(\beta+1)}{\beta(d^\alpha\gamma_k I_0 + s_k)} \right]^{1/\alpha} d \quad (\text{for } X_j \in \mathcal{C}_k^c).$$

So for any $X_j \in \mathcal{I}_k^\delta \cap \mathcal{C}_k^c$, we must have

$$|X_j| \leq d \left(\frac{\delta\beta\tilde{H}_j}{s_k} \min \left\{ 1, \frac{1+\beta}{\delta\beta^2(1+d^\alpha\gamma_k I_0/s_k)} \right\} \right)^{1/\alpha}. \quad (4.40)$$

If $\mathcal{C}_k^c \subseteq \mathcal{I}_k^\delta$ a.s., then we must have

$$\delta \geq \frac{1+\beta}{\beta^2(1+d^\alpha\gamma_k I_0/s_k)}, \quad a.s. \Rightarrow \delta \geq \frac{1+\beta}{\beta^2}.$$

In this case, the average number of noncancelable δ -level interferers is $\lambda\gamma_k^{\frac{2}{\alpha}}(\mu(\mathcal{I}_k^\delta) - \mu(\mathcal{C}_k^c))$ which is equal to $\lambda\gamma_k^{\frac{2}{\alpha}}\nu(1 - \nu_k^c/\nu)$. On the other hand, if $\mathcal{I}_k^\delta \subset \mathcal{C}_k^c$ a.s., $\delta < \frac{1+\beta}{\beta^2}$ and thus $\nu_k^c > \nu$ in this case and thus all interferers in \mathcal{I}_k^δ are cancelable. Combining these two cases, the average number of noncancelable δ -level interferers should be written as $\nu\lambda_k^m$. Using λ_k^m to replace λ of the lower bound in (4.13), we can have the lower bound on the outage probability.

The $(\cdot)^+$ term of the upper bound is due to the outage caused by the transmitters out of \mathcal{I}_k^δ so that the intensity of $\Pi \setminus \Pi_k^\delta$ is $\gamma_k^{2/\alpha}\lambda$ because no interferers are canceled in $\Pi \setminus \Pi_k^\delta$. So we can just replace λ in the $(\cdot)^+$ term of (4.13) by $\gamma_k^{2/\alpha}\lambda$ and also replace λ in the exponential term with λ_k^m . Then the upper bound is obtained.

4.6.4 Proof of Corollary 4.5.2

By considering the given condition $\sum_{k=1}^m \phi_k q_k(\bar{\lambda}_{\mathbf{E}}) \leq \epsilon$, the success probability for channel state s_k obtained from (4.29) is bounded as follows.

$$1 - \sum_{k=1}^m \phi_k \epsilon \leq 1 - \sum_{k=1}^m \phi_k q_k(\bar{\lambda}_{\mathbf{E}}) \leq \sum_{k=1}^m \phi_k e^{-\nu \delta s_k^{-2/\alpha} \lambda_k^m}.$$

If $\mathcal{C}_k^c \subset \mathcal{I}_k^\delta$, then using the above inequality and following the same steps of finding the upper and lower bounds in the proof of Theorem 4.4.2, we can show the results in (4.30) and (4.31). If $\mathcal{I}_k^\delta \subseteq \mathcal{C}_k^c$, then the upper bound on success probability is no longer available since all δ -level interferers are canceled and thus $(\nu - \nu_k^c)^+ = 0$. As shown in the proof of Theorem 4.4.2, there are two lower bounds on the success probability: one is $1 - \epsilon$, the other is $\sum_{k=1}^m \phi_k \left(1 - \Lambda_k \left(\bar{\lambda}_k \gamma_k^{\frac{2}{\alpha}}\right)\right)^+$. Considering $\Lambda_k(\cdot) < 1$, the lower bound on the success probability can be expressed as

$$1 - \sum_{k=1}^m \phi_k q_k(\bar{\lambda}_{\mathbf{E}}) \geq 1 - \min \left\{ \epsilon, \sum_{k=1}^m \phi_k \Lambda_k \left(\bar{\lambda}_k \gamma_k^{\frac{2}{\alpha}}\right) \right\},$$

which yields the following inequality

$$\frac{s_k^{\frac{3}{\alpha}-1} \lambda \sigma^2 / \gamma_k^{\frac{2}{\alpha}}}{\left[s_k^{\frac{2}{\alpha}-1} / \gamma_k^{\frac{2}{\alpha}} d^\alpha \delta \beta - \lambda \eta \right]^2} \geq \epsilon.$$

This leads to the following condition:

$$\bar{\lambda}_k^\epsilon = \inf \left\{ \lambda > 0 : s_k^{\frac{1}{\alpha}-1} \gamma_k^{-\frac{2}{\alpha}} \left(1/d^\alpha \delta \beta - \lambda \eta s_k^{1-\frac{2}{\alpha}} \gamma_k^{-\frac{2}{\alpha}} \right)^2 \leq \lambda \frac{\sigma^2}{\epsilon} \right\},$$

which renders us the lower bound $\sum_{k=1}^m (s_k / \gamma_k)^{\frac{2}{\alpha}} \phi_k \bar{\lambda}_k^\epsilon$. This completes the proof.

Chapter 5

Conclusions

In this dissertation, we have investigated the fundamental issues of distributed transmission in a wireless network from three directions. In this chapter, we summarize the main results of each direction and point out a couple of possible directions for future research.

5.1 Summary of Main Results

5.1.1 Distributed Opportunistic Scheduling

In Chapter 2, the problem of how to do distributed opportunistic scheduling (DOT) for a potential transmitter in a large-scale wireless random network is studied from a transmission-capacity point of view. We proposed three DOS schemes which are distributed channel-aware scheduling (DCAS), distributed interferer-aware scheduling (DIAS), and distributed interferer-channel-aware scheduling (DICAS). These three schemes are inspired by the physical meaning of transmission capacity (TC). They are essentially a threshold-based distributed scheduling scheme which aims at increasing signal-to-interference ratio (SIR) as much as possible. DCAS can avoid transmitting in deep fading, DIAS can make receivers

get rid of strong interferers, whereas DICAS is the scheme that integrates the two ideas of DCAS and DIAS.

To capture the transmitting activities (i.e. interference level) in the network, the transmission thresholds of the three schemes are designed as a function of transmitter intensity. As a result, very tight bounds on TC can be obtained and they provide some insight on how to design the thresholds. We have theoretically showed that TC is significantly increased by the three schemes and DICAS is the most efficient scheme to increase TC among the three. In addition, we showed that the outage probability performance of three schemes can be further improved by geometry-based interference cancellation and the corresponding results provide a fundamental tradeoff between interference cancellation and interference avoidance.

5.1.2 Multicast Outage Probability and Transmission Capacity

In Chapter 3, multicast transmission in a wireless ad hoc network is modeled by a Poisson cluster process, where transmitters in the network follow a stationary Poisson point process (PPP) and each of them is associated with an area-fixed cluster in which the intended receivers are an another stationary PPP. The MTC is defined under the constraints on the multicast outage probability and the decoding delay. Three network conditions, dense, large, and large dense, are specified in order to attain scaling characterizations on multicast transmission capacity (MTC). The scaling behaviors of the single-hop and multihop MTCs under the three network conditions are presented by a general expression. They are

affected significantly by the decoding delay but not by the fading channel models. In addition, for multihop multicast our main result shows that the MTC is superior to its single-hop counterpart if all clusters are tessellated appropriately.

5.1.3 Ergodic Transmission Capacity

We presented a long-term look at the transmission capacity problem in Chapter 4, which is completely different from the previous works on investigating network throughput at a particular time point. The motivation of this work is to understand how the temporal characteristic of a channel influences the network throughput with an outage probability constraint. Therefore, channel fading is modeled by an m -state Markov chain that has temporal and spatial ergodic properties. Bounds the on outage probability of each channel state and ergodic transmission capacity (ETC) for the case with and without interference management are all found and they show that ETC can be characterized by the inner product of vectors Φ and \mathbf{s}_ϵ . For a sparse or dense network, the scaling law of ETC that is derived from those bounds provides some guidelines on when to use distributed channel-aware scheduling and how to do interference management.

5.2 Future Work

The ideas proposed in the previous chapters can be utilized to many other transmission scenarios wherein distributed transmission has to be implemented with some specific constraints or requirements. The following subsections are some exemplary research directions where those ideas could be successfully ap-

plied.

5.2.1 Distributed Physical Layer Security

Recall that the transmission protocol used is slotted ALOHA with certain transmitting constraint, and thus the receivers of idle transmitters would cause a security issue – they could successfully *eavesdrop* on their unintended transmitters. Maintaining secure transmission in a wireless environment is challenging because information could be grasped illegally due to the broadcast nature of wireless communication. Physical layer security can also be achieved by using the concept of the proposed DOS schemes in Chapter 2 and it is completely different from the most existing approaches of achieving security [82–88].

The idea of achieving the distributed physical layer security is roughly stated as follows. Suppose the eavesdroppers (i.e. the idle receivers) are a homogeneous PPP and each eavesdropper intends to seize the information from its nearest active transmitter. When the channel from a transmitter to its nearest eavesdropper is in deep fading and the channel from the transmitter to its intended receiver is good, it is a good transmitting opportunity because the transmitter can transmit as fast as its communication link can reliably support whereas its eavesdropper is unable to decode reliably because of the low capacity of the eavesdropped channel. So transmitters with a strong eavesdropped channel should not transmit. This is the essential idea of achieving distributed secure transmission. This eavesdropper-aware scheme can be combined with the three proposed DOS schemes in Chapter 2 to achieve a better TC performance.

Note that the eavesdropper-aware scheme induces a fundamental tradeoff between transmission capacity and physical layer security, i.e. *increasing transmission capacity reduces security*, because increasing TC means the intensity of the eavesdroppers is also increased. In addition, how to achieve distributed physical layer security in a *multicast* scenario is also an interesting research direction.

5.2.2 Distributed Opportunistic Relaying

How to route or relay packets is an important problem in a network since it is involved in many network issues such as resource allocation, flow control, queueing stability, etc. Relaying in a wireless network should follow a basic rule, that is, it should be used when it is very helpful for the desired receiver and be less/no detrimental to the undesired receivers. So it is important to understand how to select a relay and/or which method to relay can lead to a better network throughput. Relaying should be in a (distributed) opportunistic sense, which means it should be used only when it provides significant benefits in terms of diversity, reliability and rate, etc. Previous works on relay selection in a random wireless network, such as [89] [90], used a static and independent point process for relay deployment, and did not develop the relay selection algorithms from a throughput point of view. For opportunistic relaying in a random wireless network, our focus is on in how to select an optimal relay from a spatial throughput point of view.

The relaying problem we are interested in can be explained as follows. Assuming the slotted Aloha protocol is used in the network with Poisson-distributed

nodes, the idle nodes can become a relaying resource to be shared by all transmitting nodes. So we need to study whether an optimal transmitting probability exists or not for channel-aware and/or interferer-aware relay selection methods since its value significantly affects the network capacity. The candidate relays can be selected from the circular area between a TX-RX pair whose diameter is the distance between the transmitter and the receiver. Transmission capacity/spatial throughput can be used as a performance metric to evaluate different relay selection methods. There is not much work in this direction, and a recent related work can be found in [91]. However, relays in that work are modeled by an independent homogeneous PPP, which is different from the aforementioned relaying model in which the idle transmitters form a relaying point process.

There are two possible relay selection methods that are briefly introduced as follows. **(i) Channel-Aware Relay Selection:** a transmitter only sends information when its channel gains to its receiver or to its relays are higher than some threshold(s). If the channel between the transmitter and the receiver is good then relaying may not be needed. Otherwise, the relay with the best channel gain from the transmitter is selected. The basic idea of this selection is to avoid transmitting during a deep fading period of a channel. Hence, the outage probability is reduced so that the transmission capacity is enhanced. **(ii) Progress-Aware Relay Selection:** Progress means the projection of the distance between the selected relay and the transmitter on the direction from the transmitter to the receiver. A transmitter selects a relay based on the product of the progress and the channel gain. The idea of this selection is to select the farthestmost relay with the best channel gain such that the selected relay is as close to the receiver

as possible. Progress-aware selection can avoid choosing the relay which is very close to the transmitter such that the second-hop transmission is in high risk of outage. So it is expected that progress-aware selection will outperform the channel-aware, especially when channels do not undergo fading.

Bibliography

- [1] C. E. Shannon, “A mathematical theory of communication,” *Bell System Technical Journal*, vol. 27, pp. 379–423, Jul. 1948.
- [2] T. M. Cover and J. A. Thomas, *Elements of Information Theory*, 2nd ed. John Wiley and Sons, Inc., 2005.
- [3] O. Oyman and S. Sandhu, “A shannon-theoretic perspective on fading multihop networks,” in *the Proc. of Conference on Information Sciences and Systems*, Mar. 2006.
- [4] J. G. Andrews, N. Jindal, M. Haenggi, R. Berry, S. Jafar, D. Guo, S. Shakkottai, R. Heath, M. Neely, S. Weber, and A. Yener, “Rethinking information theory for mobile ad hoc networks,” *IEEE Commun. Mag.*, pp. 94–101, Oct. 2008.
- [5] T. Cover and A. E. Gamal, “Capacity theorems for the relay channel,” *IEEE Trans. Inf. Theory*, vol. 25, no. 5, pp. 572–584, Sep. 1979.
- [6] G. Kramer, M. Gastpar, and P. Gupta, “Cooperative strategies and capacity theorems for relay networks,” *IEEE Trans. Inf. Theory*, vol. 51, no. 9, pp. 3037–3063, Sep. 2005.

- [7] S. Toumpis and A. J. Goldsmith, “Capacity regions for wireless ad hoc networks,” *IEEE Trans. Wireless Commun.*, vol. 2, no. 4, pp. 736–748, Jul. 2003.
- [8] P. Gupta and P. R. Kumar, “Towards an information theory of large networks: An achievable rate region,” *IEEE Trans. Inf. Theory*, vol. 49, no. 8, pp. 1877–1894, Aug. 2003.
- [9] S. H. A. Ahmad, A. Jovicic, and P. Viswanath, “On outer bounds to the capacity region of wireless networks,” *IEEE Trans. Inf. Theory*, vol. 52, no. 6, pp. 2770–2776, Jun. 2006.
- [10] R. Urgaonkar and M. Neely, “Capacity region, minimum energy and delay for a mobile ad-hoc network,” in *IEEE 4th International Symposium on Modeling and Optimization in Mobile, Ad Hoc, and Wireless Networks (WiOpt’06)*, Apr. 2006.
- [11] P. Gupta and P. R. Kumar, “The capacity of wireless networks,” *IEEE Trans. Inf. Theory*, vol. 46, no. 2, pp. 388–404, Mar. 2000.
- [12] F. Xue and P. R. Kumar, *Scaling Laws for Ad Hoc Wireless Networks: An Information Theoretic Approach*. Now Publishers: Foundations and Trends in Networking, 2006.
- [13] S. Weber, X. Yang, J. G. Andrews, and G. de Veciana, “Transmission capacity of wireless ad hoc networks with outage constraints,” *IEEE Trans. Inf. Theory*, vol. 51, no. 12, pp. 4091–4102, Dec. 2005.

- [14] F. Baccelli, “Stochastic geometry: A tool for modeling telecommunication networks,” *INRIA-ENS*, available at <http://www.di.ens.fr/mistral/sg/webpage>.
- [15] F. Baccelli, B. Błaszczyszyn, and P. Mühlethaler, “An Aloha protocol for multihop mobile wireless networks,” *IEEE Trans. Inf. Theory*, vol. 52, no. 2, pp. 421–436, Feb. 2006.
- [16] R. K. Ganti and M. Haenggi, “Interference and outage in clustered wireless ad hoc networks,” *IEEE Trans. Inf. Theory*, vol. 55, no. 9, pp. 4067–4086, 2009.
- [17] F. Baccelli and B. Błaszczyszyn, *Stochastic Geometry and Wireless Networks—Volume I: Theory*. Now Publishers: Foundations and Trends in Networking, 2010.
- [18] M. Haenggi, J. G. Andrews, F. Baccelli, O. Dousse, and M. Franceschetti, “Stochastic geometry and random graphs for the analysis and design of wireless networks,” *IEEE J. Sel. Areas Commun.*, vol. 27, pp. 1029–1046, Sep. 2009.
- [19] S. Yi, Y. Pei, and S. Kalyanaraman, “On the capacity improvement of ad hoc wireless networks using directional antennas,” in *ACM/IEEE MobiHoc*, Jun. 2003.
- [20] B. Liu, Z. Liu, and D. Towsley, “On the capacity of hybrid wireless networks,” in *Proc. IEEE INFOCOM*, Jun. 2003.

- [21] U. C. Kozat and L. Tassiulas, “Throughput capacity of random ad hoc networks with infrastructure support,” in *Proc. IEEE International Conf. on Mobile Computing and Networking (MobiCom’03)*, Sep. 2003.
- [22] S. R. Kulkarni and P. Viswanath, “A deterministic approach to throughput scaling in wireless networks,” *IEEE Trans. Inf. Theory*, vol. 50, no. 6, pp. 1041–1049, Jun. 2004.
- [23] S. Toumpis, “Capacity bounds for three classes of wireless networks: Asymmetric, cluster, and hybrid,” in *ACM/IEEE MobiHoc*, May 2004.
- [24] A. Zemlianov and G. de Veciana, “Capacity of ad hoc wireless network with infrastructure support,” *IEEE J. Sel. Areas Commun.*, vol. 23, no. 3, pp. 657–667, Mar. 2005.
- [25] J. Gomez and A. T. Campbell, “Variable-range transmission power control in wireless ad hoc networks,” *IEEE Trans. Mobile Comput.*, vol. 6, no. 1, Jan. 2007.
- [26] M. Grossglauser and D. N. C. Tse, “Mobility increases the capacity of ad-hoc wireless networks,” *IEEE/ACM Trans. Netw.*, vol. 10, no. 4, pp. 477–486, Aug. 2002.
- [27] M. Gastpar and M. Vetterlj, “On the capacity of wireless networks: The relay case,” in *Proc. IEEE INFOCOM*, Jun. 2002.
- [28] S. N. Diggavi, M. Grossglauser, and D. N. C. Tse, “Even one-dimensional mobility increases the capacity of wireless networks,” *IEEE Trans. Inf. Theory*, vol. 51, no. 11, pp. 3947–3954, Nov. 2005.

- [29] A. Behzad and I. Rubin, "High transmission power increases the capacity of ad hoc wireless networks," *IEEE Trans. Wireless Commun.*, vol. 5, no. 1, pp. 156–165, Jan. 2006.
- [30] B. Tavit, "Broadcast capacity of wireless networks," *IEEE Commun. Lett.*, vol. 10, no. 2, pp. 68–69, Feb. 2006.
- [31] M. Franceschetti, O. Dousse, D. N. C. Tse, and P. Thiran, "Closing the gap in the capacity of wireless networks via percolation theory," *IEEE Trans. Inf. Theory*, vol. 53, no. 3, pp. 1009–1018, Mar. 2007.
- [32] A. Jovicic, P. Viswanath, and S. R. Kulkarni, "Upper bounds to transport capacity of wireless networks," *IEEE Trans. Inf. Theory*, vol. 50, no. 11, pp. 3136–3141, Nov. 2004.
- [33] F. Xue, L.-L. Xie, and P. R. Kumar, "The transport capacity of wireless networks over fading channels," *IEEE Trans. Inf. Theory*, vol. 51, no. 3, pp. 834–847, Mar. 2005.
- [34] R. Knopp and P. Humblet, "Information capacity and power control in single-cell multiuser communication," in *IEEE International Conference on Communications*, Jun. 1995, pp. 331–335.
- [35] L. Li and A. J. Goldsmith, "Capacity and optimal resource allocation for fading broadcast channels-Part i: Ergodic capacity," *IEEE Trans. Inf. Theory*, vol. 47, no. 3, pp. 1083–1102, Mar. 2001.

- [36] X. Li, E. K. P. Chong, and N. B. Shroff, “Opportunistic transmission scheduling with resource-sharing constraints in wireless networks,” *IEEE J. Sel. Areas Commun.*, vol. 19, no. 10, pp. 2053–2064, Oct. 2001.
- [37] —, “A framework for opportunistic scheduling in wireless networks,” *Computer Networks, Elsevier*, vol. 41, no. 3, pp. 451–474, Mar. 2003.
- [38] W. Choi and J. G. Andrews, “The capacity gain from intercell scheduling in multi-antenna systems,” *IEEE Trans. Wireless Commun.*, vol. 7, no. 2, pp. 714–725, Feb. 2008.
- [39] J.-W. Cho, J. Mo, and S. Chong, “Opportunistic transmission scheduling with resource-sharing constraints in wireless networks,” *IEEE Trans. Wireless Commun.*, vol. 8, no. 3, pp. 1520–1531, Mar. 2009.
- [40] S. Weber, J. G. Andrews, and N. Jindal, “An overview of the transmission capacity of wireless networks,” *IEEE Trans. Commun.*, vol. 56, no. 12, p. 3593V3604, Dec. 2010.
- [41] S. Biswas and R. Morris, “Opportunistic routing in multi-hop wireless networks,” in *ACM SIGCOMM*, Aug. 2005, pp. 133–144.
- [42] S. Jain and S. Das, “Exploiting path diversity in the link layer in wireless ad hoc networks,” in *IEEE WoWMoM*, Jun. 2005, pp. 22–30.
- [43] C. Westphal, “Opportunistic routing in dynamic ad hoc networks: The OPRAH protocol,” in *Proc. IEEE MASS*, Oct. 2006, pp. 570–573.

- [44] F. Baccelli, B. Błaszczyszyn, and P. Mühlethaler, “On the performance of time-space opportunistic routing in multihop mobile ad hoc networks,” in *IEEE 6th International Symposium on Modeling and Optimization in Mobile, Ad Hoc, and Wireless Networks (WiOpt’08)*, Apr. 2008, pp. 307–316.
- [45] H. Liu, B. Zhang, H. T. Mouftah, X. Shen, and J. Ma, “Opportunistic routing for wireless ad hoc and sensor networks: Present and future directions,” *IEEE Commun. Mag.*, pp. 103–109, Dec. 2009.
- [46] M. Felegyhazi and J.-P. Hubaux, *Game Theory in Wireless Networks: A Tutorial*. EPFL Laboratory for Computer Communications and Applications, Lausanne, Switzerland, Tech. Rep. LCA-REPORT-2006-002, 2006.
- [47] D. Zheng, W. Ge, and J. Zhang, “Distributed opportunistic scheduling for ad-hoc communications: An optimal stopping approach,” in *ACM/IEEE MobiHoc*, Sep. 2007.
- [48] D. Zheng, M.-O. Pun, W. Ge, J. Zhang, and H. V. Poor, “Distributed opportunistic scheduling for ad hoc communications with imperfect channel information,” *IEEE Trans. Wireless Commun.*, vol. 7, no. 12, pp. 5450–5460, Dec. 2008.
- [49] Q. Zhang, Q. Chen, F. Yang, X. Shen, and Z. Niu, “Cooperative and opportunistic transmission for wireless ad hoc networks,” *IEEE Network*, pp. 14–20, Feb. 2007.
- [50] C. Thejaswi, J. Zhang, M.-O. Pun, and H. V. Poor, “Distributed opportunistic scheduling with two-level channel probing,” in *IEEE INFOCOM*,

Apr. 2009.

- [51] S. Weber, J. G. Andrews, and N. Jindal, “The effect of fading, channel inversion, and threshold scheduling on ad hoc networks,” *IEEE Trans. Inf. Theory*, vol. 53, no. 11, pp. 4127–4149, Nov. 2007.
- [52] E. S. Sousa, “Interference modeling in a direct-sequence spread-spectrum packet radio network,” *IEEE Trans. Commun.*, vol. 38, no. 9, pp. 1475–1482, Sep. 1990.
- [53] E. S. Sousa and J. A. Silvester, “Optimum transmission ranges in a direct-sequence spread-spectrum multihop packet radio network,” *IEEE J. Sel. Areas Commun.*, vol. 8, no. 5, pp. 762–771, Jun. 1990.
- [54] S. B. Lowen and M. C. Teich, “Power-law shot noise,” *IEEE Trans. Inf. Theory*, vol. 36, no. 6, pp. 1302–1318, Sep. 1990.
- [55] E. S. Sousa, “Performance of a spread spectrum packet radio network link on a poisson field of interferers,” *IEEE Trans. Inf. Theory*, vol. 38, no. 6, pp. 1743–1754, Nov. 1992.
- [56] J. Ilow and D. Hatzinakos, “Optimum transmission ranges in a direct-sequence spread-spectrum multihop packet radio network,” *IEEE Trans. Signal Process.*, vol. 46, no. 6, pp. 1601–1611, Jun. 1998.
- [57] D. Stoyan, W. Kendall, and J. Mecke, *Stochastic Geometry and Its Applications*, 2nd ed. John Wiley and Sons, Inc., 1996.

- [58] S. Shakkottai, X. Liu, and R. Srikant, “The multicast capacity of large multihop wireless networks,” in *Proc. ACM International Symposium on Mobile Ad Hoc Networking and Computing (Mobihoc’07)*, Sep. 2007.
- [59] U. Niesen, P. Gupta, and D. Shah, “The balanced unicast and multicast capacity regions of large wireless networks,” *IEEE Trans. Inf. Theory*, vol. 56, no. 5, pp. 2249–2271, May 2010.
- [60] X.-Y. Li, “Multicast capacity of wireless ad hoc networks,” *IEEE/ACM Trans. Netw.*, vol. 17, no. 3, pp. 950–961, Jun. 2009.
- [61] A. Keshavarz-Haddad, V. Ribeiro, and R. Riedi, “The multicast capacity of large multihop wireless networks,” in *Proc. Annual International Conf. on Mobile Computing and Networking*, Sep. 2006.
- [62] P. Chaporkar and S. Sarkar, “Wireless multicast: theory and approaches,” *IEEE Trans. Inf. Theory*, vol. 51, no. 6, pp. 1954–1972, Jun. 2005.
- [63] P. Jacquet and G. Rodolakis, “Multicast scaling properties in massively dense ad hoc networks,” in *Proc. International Conf. on Parallel and Distributed Systems*, Jun. 2005.
- [64] A. Keshavarz-Haddad, V. Ribeiro, and R. Riedi, “Broadcast capacity in wireless multihop networks,” in *Proc. ACM International Symposium on Mobile Ad Hoc Networking and Computing (Mobihoc’06)*, Sep. 2006.
- [65] R. Zheng, “Information dissemination in power-constrained wireless network,” in *Proc. IEEE INFOCOM*, Apr. 2006.

- [66] A. Keshavarz-Haddad and R. Riedi, “On the broadcast capacity of multihop wireless networks: Interplay of power, density and interference,” in *Proc. Annual IEEE Communications Society Conf. on Sensor, Mesh and Ad Hoc Communications and Networks (SECON’07)*, Jun. 2007.
- [67] O. Arpacioğlu and Z. J. Haas, “On the scalability and capacity of wireless networks with omnidirectional antennas,” in *Proc. Information Processing in Sensor Networks (IPSN’04)*, Apr. 2004.
- [68] O. Dousse and P. Thiran, “Connectivity vs capacity in dense ad hoc networks,” in *Proc. IEEE INFOCOM*, Apr. 2004.
- [69] J. F. C. Kingman, *Poisson Processes*. Oxford University Press, 1993.
- [70] R. K. Ganti and M. Haenggi, “Spatial and temporal correlation of the interference in Aloha ad hoc networks,” *IEEE Commun. Lett.*, vol. 13, no. 9, pp. 631–633, Sep. 2009.
- [71] J. Li, C. Blake, D. S. J. D. Couto, H. I. Lee, and R. Morris, “Capacity of power constrained ad-hoc networks,” in *Proc. IEEE International Conf. on Mobile Computing and Networking (MobiCom’01)*, Jul. 2001.
- [72] R. Negi and A. Rajeswran, “Capacity of power constrained ad-hoc networks,” in *Proc. IEEE INFOCOM*, Apr. 2004.
- [73] S. Meyn and R. L. Tweedie, *Markov Chains and Stochastic Stability*, 2nd ed. Cambridge University Press, 2009.

- [74] E. N. Gilbert, "Capacity of a burst-noise channel," *Bell Syst. Tech. J.*, vol. 39, no. 9, pp. 1253–1265, Sep. 1960.
- [75] E. O. Elliott, "Estimates of error rates for codes on burst-noise channels," *Bell System Technical Journal*, vol. 42, no. 9, pp. 1977–1997, Sep. 1963.
- [76] H. S. Wang and N. Moayeri, "Finite-state markov channel - a useful model for radio communication channels," *IEEE Trans. Veh. Technol.*, vol. 44, no. 1, pp. 163–171, Feb. 1995.
- [77] S. Weber, J. G. Andrews, X. Yang, and G. de Veciana, "Transmission capacity of wireless ad hoc networks with successive interference cancellation," *IEEE Trans. Inf. Theory*, vol. 53, no. 8, pp. 2799–2814, Aug. 2007.
- [78] S. W. J. G. Andrews and M. Haenggi, "Ad hoc networks: To spread or not to spread?" *IEEE Commun. Mag.*, vol. 45, pp. 84–91, Dec. 2007.
- [79] T. Cover, "Broadcast channels," *IEEE Trans. Inf. Theory*, vol. IT-18, no. 1, pp. 2–14, Jan. 1972.
- [80] J. G. Andrews, "Interference cancellation for cellular systems: A contemporary overview," *IEEE Wireless Commun. Mag.*, vol. 12, no. 2, pp. 19–29, Apr. 2005.
- [81] D. N. C. Tse and P. Viswanath, *Fundamentals of Wireless Communication*. Cambridge University Press, 2005.
- [82] M. Haenggi, "The secrecy graph and some of its properties," in *Proc. IEEE International Symposium on Information Theory (ISIT'09)*, Jun. 2008.

- [83] P. C. Pinto, J. Barros, and M. Z. Win, “Physical-layer security in stochastic wireless networks,” in *Proc. IEEE International Conference on Communication System (ICCS’08)*, Nov. 2008.
- [84] M. Bloch, J. Barros, M. R. D. Rodrigues, and S. W. McLaughlin, “Wireless information-theoretic security,” *IEEE Trans. Inf. Theory*, vol. 54, no. 6, pp. 2515–2534, Jun. 2008.
- [85] P. C. Pinto, J. Barros, and M. Z. Win, “Wireless physical-layer security: the case of colluding eavesdroppers,” in *Proc. IEEE International Symposium on Information Theory (ISIT’09)*, Jun. 2009.
- [86] Y. Liang, H. V. Poor, and L. Yin, “Secrecy throughput of manets with malicious nodes,” in *Proc. IEEE International Symposium on Information Theory (ISIT’09)*, Jun. 2009.
- [87] A. Khisti and G. W. Wornell, “Secure transmission with multiple antennas: the mimome channel,” *IEEE Trans. Inf. Theory*, vol. 56, no. 11, pp. 5515–5532, Nov. 2010.
- [88] X. Zhou, R. K. Ganti, and J. G. Andrews, “Secure wireless network connectivity with multi-antenna transmission,” *IEEE Trans. Wireless Commun.*, vol. 10, no. 2, pp. 425–430, Feb. 2011.
- [89] M. Haenggi, “On routing in random rayleigh fading networks,” *IEEE Trans. Wireless Commun.*, vol. 4, no. 7, pp. 1553–1562, Jul. 2005.

- [90] R. K. Ganti and M. Haenggi, “Analysis of uncoordinated opportunistic two-hop wireless ad hoc systems,” in *Proc. IEEE International Symposium on Information Theory (ISIT’09)*, Jun. 2009.
- [91] M. Kountouris and J. G. Andrews, “Throughput scaling laws for wireless ad hoc networks with relay selection,” in *Proc. IEEE Vehicular Technology Conference*, Apr. 2009.
- [92] Q. Zhang and S. A. Kassam, “Finite-state markov model for Rayleigh fading channels,” *IEEE Trans. Commun.*, vol. 47, no. 11, pp. 1688–1692, Nov. 1999.
- [93] A. Khisti, U. Erez, and G. Wornell, “Fundamental limits and scaling behavior of cooperative multicasting in wireless networks,” *IEEE Trans. Inf. Theory*, vol. 52, no. 6, p. 27622770, Jun. 2006.
- [94] B. Sirkeci-Mergen and M. Gastpar, “On the broadcast capacity of wireless networks,” in *Proc. Information Theory and Application Workshop*, Mar. 2007.
- [95] A. M. Hunter, J. G. Andrews, and S. Weber, “Transmission capacity of wireless ad hoc networks with spatial diversity,” *IEEE Trans. Wireless Commun.*, vol. 7, no. 1, pp. 5058–5071, Dec. 2008.
- [96] Y. Sun, V. O. Li, and K.-C. Leung, “Distributed opportunistic scheduling in multihop wireless ad hoc networks,” in *IEEE International Conference on Communications*, Sep. 2008.

Vita

Chun-Hung Liu received his B.S. and M.S. in Electrical Engineering from National Taiwan University, and he also obtained an M.S. in Mechanical Engineering (specialized in networking control and communication systems) from Massachusetts Institute of Technology. He was a recipient of Taiwan Merit Fellowship awarded by the National Science Council of Taiwan from 2005 to 2009. His past research was in system and control. He was a research member in the laboratory for advanced sensing and system control in the department of Electrical Engineering at National Taiwan University. Afterwards, he joined the d'Arbeloff Laboratory for information system and technology at MIT where his research focused on coding and modulation methods for power saving and reliable data communications in wireless sensor networks. He was a research member in the Wireless Networking and Communication Group (WNCG) at the University of Texas at Austin where his research focused on wireless communications, information theory, and stochastic geometry and random graph for wireless ad hoc networks.

Permanent address: 8106 Pilgrims PL, Austin, Texas 78759

This dissertation was typeset with L^AT_EX[†] by the author.

[†]L^AT_EX is a document preparation system developed by Leslie Lamport as a special version of Donald Knuth's T_EX Program.